

NATO/PfP UNCLASSIFIED

**ALLIED
ENGINEERING
PUBLICATION**

**AEP-41, Volume III
(Edition 1)**



**Unified Electromagnetic Environment Effects
Protection**

VOLUME III

ELECTROMAGNETIC COUPLING

JUNE 2012

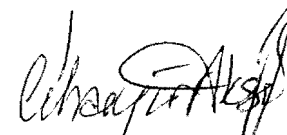
©NATO/OTAN

NATO/PfP UNCLASSIFIED

NORTH ATLANTIC TREATY ORGANIZATION
NATO STANDARDIZATION AGENCY (NSA)
NATO LETTER OF PROMULGATION

6 June 2012

1. AEP-41, Volume III (Edition 1) - "Unified Electromagnetic Environment Effects Protection – Electromagnetic Coupling" is a NATO/PfP UNCLASSIFIED publication.
2. AEP-41, Volume III (Edition 1) is effective on receipt.
3. No part of this publication may be reproduced, stored in a retrieval system, used commercially, adapted, or transmitted in any form or by any means, electronic, mechanical, photocopying, recording or otherwise, without the prior permission of the publisher. With the exception of commercial sales, this does not apply to member nations and Partnership for Peace countries, or NATO commands and bodies.



Cihangir AKSIT, TUR Civ
Director, NATO Standardization Agency

NATION	SPECIFIC RESERVATIONS

RECORD OF CHANGES

Change Date	Date Entered	Effective Date	By Whom Entered

TABLE OF CONTENTS

- 1.0 TABLE OF CONTENTS**
- 2.0 AEP-41, EXECUTIVE SUMMARY**
 - 2.1 Introduction for AEP-41**
 - 2.1.1 Balanced E³ Protection
 - 2.1.2 E³ Protection Needs
 - 2.1.3 Methodology
 - 2.2 Scope for AEP-41**
 - 2.3 Requirements**
- 3.0 AEP-41, VOLUME III, EXECUTIVE SUMMARY**
 - 3.1 Introduction to AEP-41, Volume III**
 - 3.2 Scope for AEP-41, Volume III**
- 4.0 ELECTROMAGNETIC COUPLING**
 - 4.1 Introduction**
 - 4.2 Classification of Electromagnetic Environments and Coupled Stresses**
 - 4.2.1 Introduction
 - 4.2.2 External and Internal Environments
 - 4.3 Coupling to Exterior Equipment**
 - 4.3.1 Introduction
 - 4.3.2 Coupling to Vertical Conductors
 - 4.3.2.1 CW Coupling to Vertical Conductors
 - 4.3.2.2 Pulse Coupling to Vertical Conductors
 - 4.3.3 Coupling to Horizontal Conductors
 - 4.3.3.1 CW Coupling to Horizontal Conductors
 - 4.3.3.2 Pulse Coupling to Horizontal Conductors
 - 4.4 Coupling to Equipment Inside an Enclosure with Apertures**
 - 4.4.1 Introduction
 - 4.4.2 Determination of the Interior Electromagnetic Environment
 - 4.4.2.1 Shielding Effectiveness
 - 4.4.2.2 Numerical Computation of Internal Fields
 - 4.4.2.3 Energy Bounds
 - 4.4.2.4 Fields Inside a Shield with Apertures
 - 4.4.3 Aperture Penetration and Cable Coupling
 - 4.4.3.1 Quasistatic Coupling to Interior Cables
 - 4.4.3.2 Radiative Coupling to Interior Cables in a Non-Resonant Cavity

4.4.3.3

4.4.3.4 Radiative Coupling to Interior Cables in a Resonant Cavity

4.4.3.5 Coupling due to Current Injected on to Shield by Penetration

4.5 Coupling to Equipment Inside a Solid Enclosure

4.5.1 Introduction

4.5.2 Determination of the EM Environment Inside a Closed Shield

4.5.2.1 Barrier Shielding Effectiveness

4.5.2.2 Analytical Determination of Fields Inside a Closed Shield

4.5.3 Internally Generated EMEs and Control of Cavity Q

4.6 Coupling to Printed Circuit Boards and Electronic Components

4.6.1 Background

4.6.2 Coupling to Multiconductor Transmission Lines

4.7 Degradation of Barrier Performance During Equipment Cycle Life

4.7.1 Background

4.7.2 Measurement of the Effective Aperture Area of a Shield

4.7.3 Measurement of Cavity Q

4.7.4 Coupling Measurements

4.8 Spacecraft Charging Effects

4.8.1 Overview of Spacecraft Charging

4.8.2 Significance of Spacecraft Charging Phenomenon

4.9 Unification of Electromagnetic Environments and Effects

4.9.1 Introduction

4.9.2 The QSTAG-1051 Approach to Unification

4.9.2.1 Overview of the QSTAG-1051 Approach

4.9.2.2 Comments on the QSTAG-1051 Approach

4.9.3 Use of Waveform Norms for Unification

4.9.3.1 Overview

4.9.3.2 Comments on the Norms Approach to Unification

4.9.4 Numerical Computation of a Unified, Time Domain Waveform

4.9.4.1 Overview

4.9.4.2 Comments on the Numerical Approach to Unification

4.9.5 Unification of Wideband and Narrowband EMEs

4.9.5.1 Overview

4.9.5.2 Comments on Unification of Wideband and Narrowband EMEs

5.0 UNIFIED EME PROTECTION ALLOCATIONS

5.1 Introduction

5.2 Outline of the Unified EME Allocation Process

6.0 SUMMARY

7.0 CONCLUSIONS

8.0 ANNEXES

8.1 References

8.2 Abbreviations and Acronyms

8.3 Definitions

8.4 An Example of Unified EME Protection Allocation

1.0 TABLE OF CONTENTS

2.0 AEP-41, EXECUTIVE SUMMARY

There is a general consensus for an unified approach to the protection and hardening of all NATO military platforms, systems and equipments (hardware) against Electromagnetic Environmental Effects (E^3) caused by the plethora of Electromagnetic Environments (EMEs) that these platforms, systems and equipments are subjected to during their deployment life. These E^3 can adversely impact the operational capability of this military hardware resulting in their inability to accomplish their mission or even putting the crew's safety at risk. The EMEs are generated by natural, operational and hostile sources. Additionally, today's complex military operational environment is characterized by: multi-national operations, increasingly crowded EM spectrum coupled with a reduction of bandwidth allocated for exclusive military use, military hardware whose mission performance is dependent on electronics, and hardware that is increasingly dependent on more energy sensitive Non-Developmental Items (NDIs) and Commercial-Off-The-Shelf (COTS) electronic components. Traditional hardening against the total battlespace EMEs has been accomplished by considering each EME individually and serially. The Conference of National Armaments Directors (CNAD) recognized the need for a unified E^3 (UE^3) protection policy, and directed the development of an Allied Engineering Publication (AEP)-41 and an associated Standardization Agreement (STANAG) 4567 to describe and define this policy. The proposed UE^3 protection approach can be applied to all six Operational Categories (OCs) of NATO military hardware. These six OCs are:

- OC1 Land Mobile Systems
- OC2 Static Land Systems
- OC3 Space Systems
- OC4 Sea Platforms
- OC5 Air Platforms
- OC6 Command, Control and Information Systems

The CNAD approved the following seven AEP-41 volumes to detail the different functional areas required to achieve, produce and sustain affordable UE^3 protection and survivability:

- a) Volume I, Unified Electromagnetic Environmental Effects (UE^3) Protection, Philosophy and Methodology,
- b) Volume II, Electromagnetic (EM) Environments (EMEs), E^3 , and Operational Categories,
- c) Volume III, Electromagnetic Coupling,
- d) Volume IV, Susceptibility of Platforms, Systems and Equipment to E^3 ,
- e) Volume V, Unified Hardening and Protection Against E^3 ,
- f) Volume VI, Testing and Validation of E^3 Protection, and

g) Volume VII, Hardness and Sustainment Assurance, and Surveillance Test.

The basic philosophy is to provide a User-controlled, performance-based approach to developing cost effective, verifiable, producible, maintainable and sustainable UE³ protection for NATO military hardware. The methodology for implementing UE³ protection to all types of military hardware is based on use of an EM barrier protection concept. In addition, this methodology is inherently accommodating and flexible for future growth and changes, and for sustaining EM hardness against degradations resulting from usage, age, maintenance and repairs, changes and additions, and ambient environments. This AEP uses extensively the EM barrier protection philosophy and methodology documented in QSTAG-1051.

2.1 Introduction for AEP-41

2.1.1 Balanced E³ Protection. This AEP describes an approach for achieving adequate, affordable and balanced UE³ protection and survivability in the battlespace for all classes of NATO military platforms, systems, and equipments (all three defined as hardware) of the six operational categories. The philosophy is a User-controlled approach to developing and verifying balanced E³ protection that is affordable, and can be produced and sustained. Balance is achieved between several factors. First, the protection design is balanced for unified coverage of the EME stresses encountered during operational deployment. Second, a balance is achieved between the protection provided, and cost and operational impact. Thus, the User is afforded the opportunity to balance the level of protection against risk of operational degradation when battlespace EMEs are encountered. The philosophy embodied in AEP-41 does not mandate design solutions; but instead, provides a performance-based methodology that allows the User the flexibility for deriving the final UE³ protection design to meet performance requirements.

2.1.2 E³ Protection Needs. Adequate E³ protection of electronic/electrical military hardware is essential since such hardware must operate during and after exposure to increasingly severe, complex and changing EMEs that can potentially impact crew safety as well as degrade or even destroy mission essential performance capabilities. Potential battlespace EMEs are listed in Table 1. Meeting the EM protection requirement has become more difficult due to the post-cold war policy of deploying NATO coalition forces (even combined with UN forces) consisting of military hardware hardened to different E³ levels and EMEs into many different areas each with its own set of EME threats. In addition to this disparity in E³ hardening, most of the hardware was developed in the cold war. Post-cold war policy of most NATO countries towards this military hardware is to extend the operational life of their deployed hardware by a factor of two or more. This lifetime extension combined with rapidly advancing technology and increasing obsolescence has become the reason for multiple modernization cycles (was one, now eight-to-ten) and the increasing use of

COTS/NDIs and advanced technologies all of which tend to have lower energy upset and damage thresholds. These new impacting factors are in addition to the traditional ones that could degrade E³ survivability such as ambient environments, corrosion, aging, usage, and repeated maintenance and repairs. Thus, the combination of these new and old factors has greatly increased the difficulty of sustaining E³ survivability.

2.1.3 Methodology. The method of achieving UE³ protection and survivability is through the use of EM barrier(s) plus special protective measures to protect Mission and Safety Critical Electronics (MSCEs). An EM protection barrier consists of two elements: one or more EM shields, and/or the necessary electrical and mechanical penetrations through the shields. To maintain the barrier effectiveness, penetration protection devices must be provided for all penetrations in the EM shield. Figure A1 illustrates the EM barrier protection concept applied to a multi-element system. (Note that this concept can be effectively applied to even the cases of military hardware that have effectively no shield.) This protection concept is familiar to digital, circuit, integration and system designers; and, does not require the development of new design practices. The illustrated example employs multiple closed metallic EM topologies to reduce the externally and internally generated EME stresses (conducted and radiated) to residual stress levels consistent with acceptable operation of the protected MSCEs. Choosing the acceptable operational levels and, in turn, the EM barrier performance requirements involves a process of balancing the externally and internally generated EME stresses, the MSCEs immunities, and the margin selected to control risk allocation process, illustrated in Figure 2. The engineering trade studies necessary to achieve this balance are through which is usually iterative and serves basically as a risk management tool. If this concept is properly designed and implemented into military hardware, UE³ protection and survivability can be achieved that is affordable and producible as well as verifiable, maintainable and sustainable throughout the hardware's operational life. Additionally, an integral and essential part of this methodology is testing which is conducted throughout all four of the acquisition life-cycle phases to insure that the EM protection design is: adequate and complete during concept and engineering development, properly implemented during production, and properly maintained and sustained during deployment. Furthermore, the EM barrier protection concept facilitates unified testing by focusing on the barrier rather than individual E³. Since this methodology can create benign internal EME stresses to which the MSCEs must survive, the EM barrier facilitates Diminishing Manufacturing Sources and Material Shortages (DMSMS) and technology insertions, especially COTS/NDIs, and upgrades/enhancements.

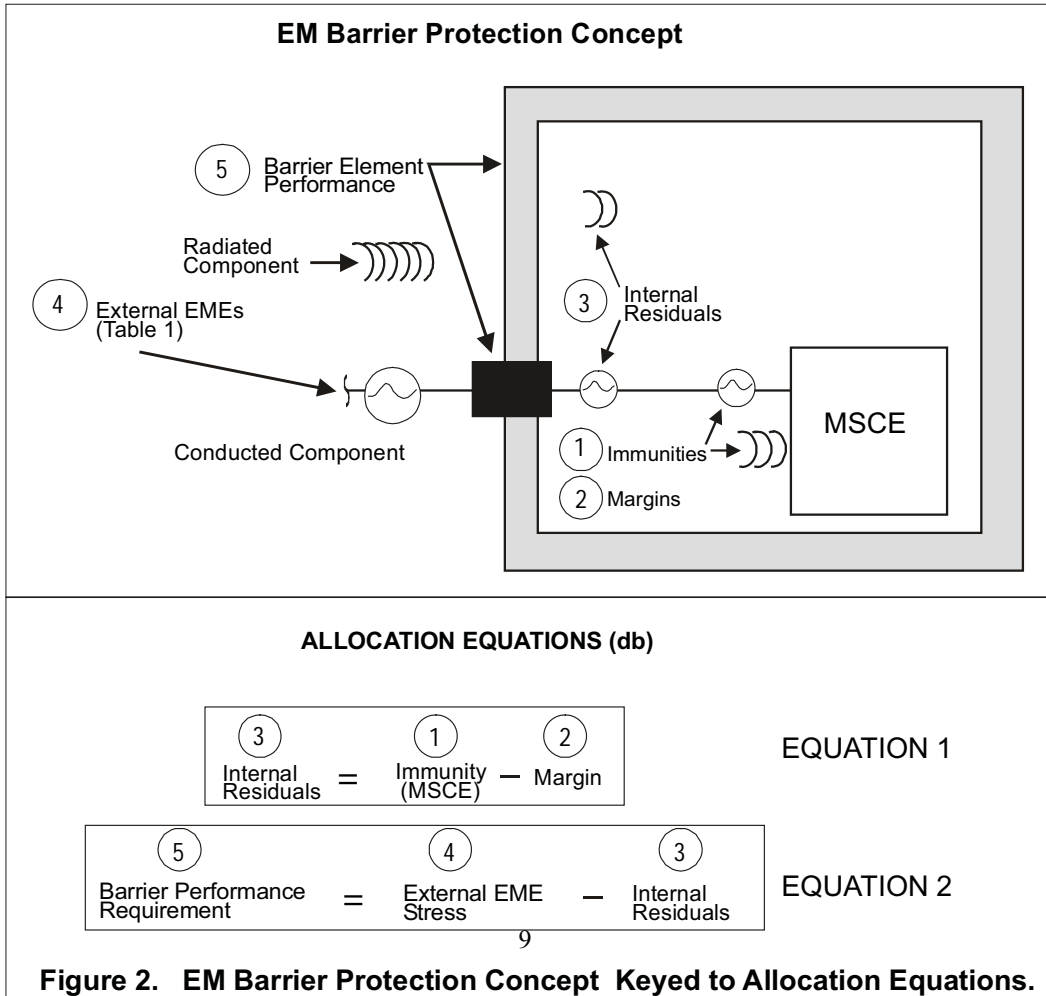
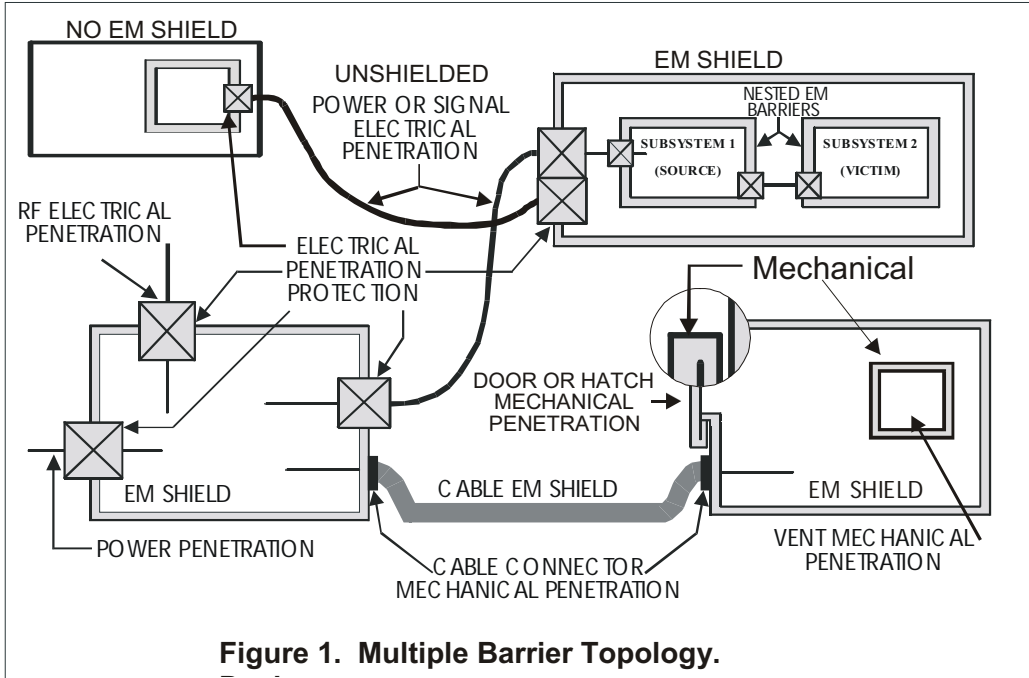
Table 1. Characteristics of Battlespace EMEs.

Externally Generated Electromagnetic Environments			
Environment	Type	Waveform	Propagation *
Near Strike Lightning (NSL)	Natural	Pulse	Radiated and Conducted
Direct Strike Lightning (DSL)	Natural	Pulse	Conducted
High Altitude Electromagnetic Pulse (HEMP) E1, E2, E3	Hostile	Pulse	Radiated and Conducted
Source Region EMP (SREMP)	Hostile	Pulse	Radiated and Conducted
Non-Nuclear EMP (N ² EMP)	Hostile	Pulse	Radiated
Electromagnetic Emissions	Electronic Operation	Pulse, Continuous Wave (CW) and Modulated CW	Radiated and Conducted
High Intensity Radiated Field (HIRF)	Electronic Operation	CW Pulsed, CW and Modulated CW	Radiated
Electronic Counter Measures (ECM)	Hostile	CW and Modulated CW	Radiated
High Power Microwave (HPM)	Hostile	CW Pulsed, CW and Modulated CW, single or multiple Bursts of CW	Radiated
Ultra-Wideband (UWB)	Hostile	Pulse, single or multiple	Radiated and Conducted
Precipitation-Static (P-Static)	Natural	Pulse	Conducted
Electrostatic Discharge (ESD)	Natural	Pulse	Radiated and Conducted
System Generated EMP (SGEMP) External	Hostile	Pulse	Radiated and Conducted
Dispersed EMP (DEMP)	Hostile	Pulse	Radiated and Conducted

*Propagation is the method by which energy arrives from the source to the victim

Internally Generated Electromagnetic Environments			
Environment	Type	Waveform	Propagation *
Electromagnetic Emissions	Electronic Operation	Pulse, CW and Modulated CW	Radiated and Conducted
Electrostatic Discharge (ESD)	Natural	Pulse	Radiated and Conducted
<i>SGEMP - Internal</i> (Box and Cable)	Hostile	Pulse	Radiated and Conducted

*Propagation is the method by which energy arrives from the source to the victim



2.2 Scope for AEP-41

The general scope of this AEP is to document how affordable for all UE³ survivability can be achieved, verified, produced and sustained for all six categories of NATO hardware using the EM barrier protection concept. This scope of work will be accomplished in the following seven volumes.

2.2.1 Volume I. This volume provides the philosophy and methodology for achieving affordable UE³ protection and survivability through the use of the EM barrier protection concept. A discussion of how to apply the EM barrier protection methodology to achieve UE³ survivability that is affordable, verifiable, producible and sustainable in today's and the future battlespace is provided.

2.2.2 Volume II. This volume provides the typical requirements for and defines and discusses the potential battlespace EMEs listed in Table 1 that military hardware must be protected against in order to be E³ survivable in the battlespace. These EMEs interact with military hardware causing E³, which are defined and discussed. Furthermore, military hardware (platforms, systems and equipments) of the six operational categories is discussed.

2.2.3 Volume III. This volume provides detailed discussion of E³ coupling for the various classes of military platforms, systems and equipments defined in Vol. II. Understanding E³ coupling is critical because the EM barrier is basically an E³ management tool to insure that the resultant residual levels from the EME generated stresses are lower than the MSCE immunity levels by a realistic margin. (Margin depends on mission criticality of hardware and permissible risk; therefore, margin is usually 15-20 dB when combined with a life-cycle program.)

2.2.4 Volume IV. This volume discusses E³ susceptibilities common to the six categories of NATO military hardware defined in Vol. II. How these E³ susceptibilities occur, what they are, and how they affect these various hardware classes in the battlespace is discussed.

2.2.5 Volume V. This volume describes how to apply the EM barrier protection concept to achieve UE³ protection and survivability against the E³ susceptibilities described in Vol. IV resulting from the E³ coupling described in Vol. III for the six operational categories of NATO hardware defined in Vol. II. Volume V also discusses why E³ protection must be included early into the design of military hardware in order to be affordable, producible, sustainable as well as accommodating to insertions of DMSMS solutions and COTS/NDIs.

2.2.6 Volume VI. This volume discusses test and validation. A crucial part of achieving, producing and sustaining UE³ survivability is a series of E³ tests that must

be performed during all phases of the hardware's life-cycle and tailored to the requirements of the hardware. The basic test types are: engineering development to support the design activities, acceptance (MSCE equipment immunity (both radiated and conducted) and barrier performance (shielding effectiveness and penetration protection devices), final design validation, production compliance (under Hardness Assurance (HA)), deployment compliance (under Sustainment Assurance (SA)), and Surveillance Test (ST). Both HA and SA includes engineering-type tests and analysis, as necessary, to evaluate and validate that configuration, MSCE, and material changes do not degrade the E³ survivability level of the hardware by increasing risk to unacceptable levels.

2.2.7 Volume VII. This volume discusses hardness and sustainment assurance, and surveillance test. The test and validation aspects of design, engineering development, and hardness assurance are presented in Vol. VI and will be briefly covered in Vol. VII for completeness. Consequently, Vol. VII will focus on sustainment assurance and surveillance test. The objective of a hardness and sustainment assurance program is to establish technical and management activities to ensure that UE³ survivability achieved and verified during the Engineering Development Phase is not only produced, but, is also preserved throughout the hardware's Deployment Phase or its operational life. Also discussed are methods and guidelines on how to accommodate material changes, technology/DMSMS insertions and associated circuit additions, MSCEs upgrades and modernizations without degrading E³ survivability to unacceptable risk levels during deployment. Finally, surveillance tests (and analysis) to periodically validate adequacy of both hardness and sustainment assurance programs are discussed.

2.3 Requirements

Military hardware of the six operational categories must be electro-magnetically compatible as well as survivable to a myriad of changing EMEs in the battlespace; and, this compatibility and survivability must be readily achievable and affordable as well as producible, maintainable and sustainable throughout the hardware's life-cycle. EMC, survivability, and EME requirements are provided in Section 4 of Volume II.

The barrier performance requirements critical to achieving affordable, producible and sustainable UE³ protection for NATO military hardware of the six operational categories are discussed in Section 4.0 of Volumes I, III and V. The E³ performance objectives are established from the mission needs, E³ protection criteria and concepts, and the selected E³ survivability options (may require combinations of UE³ barrier protection with alternate and/or special protective methods to achieve survivability).

The performance objectives consist of: need to protect against specific EMEs, level of protection required, amount of allowable risk associated with the protection and, as

needed, limits on hardware impacts related to E^3 protection. See Volume I, Figure 12 for illustration and paragraph 4.2.2 for discussion. It is important that the E^3 performance objectives be clearly defined early in a program, since they drive performance specifications as well as all subsequent UE^3 protection design and engineering and acceptance test activities, affordability, producibility, sustainability, and flexibility of design.

3.0 AEP-41, VOLUME III, EXECUTIVE SUMMARY

3.1 Introduction to AEP-41, Volume III

Volume I of AEP-41 details the philosophy and methodology for achieving UE^3 protection and survivability of military hardware in all operational environments. The basic philosophy of AEP-41 is the development of an approach to achieve balanced UE^3 protection and preserve that protection throughout the operational life of the hardware. The method defined to achieve balanced UE^3 protection and survivability is based on the use of the EM barrier protection concept whereby EM barriers are used to enclose MSCEs that have inadequate electromagnetic immunity to be able to survive the operational EM environment. The EM barrier usually consists of one or more electromagnetic shields and controlled mechanical and electrical penetrations through the shields. Ideally, the MSCE is totally enclosed inside a solid conductive shield, however, for operational reasons, this is often not possible. Figure 1 illustrates the UE^3 barrier concept.

E^3 can take various paths to reach the MSCE contained within the barrier. Currents are induced on the exterior of the shield by radiated emissions, such as high altitude EMP, RF weapons and High Intensity Radiated Field (HIRF), and by bonding of cables to the shield exterior at entry ports. The dominant leakage path for the energy coupled to the shield is through the apertures that exist in the shield (e.g., waveguide vents, windows, doors, hatches etc.). While there is some direct leakage of the fields through the shield material, the magnitude of these fields is, in general, small and, with the exception of low frequency magnetic fields, can usually be neglected if the shield is metallic. The second major leakage path through the shield is via the electrical conductors that pass through the shield. These conductors carry current to the shield when they are exposed to external electromagnetic fields. Protective devices are normally installed where these external conductors enter the barrier to reduce conducted currents that pass to the interior of the shield. Interior sources (such as ESD, equipment EMI or re-radiation from current carrying cables) also contribute to the interior electromagnetic field.

In the UE^3 barrier concept that has been detailed in Volume I of AEP-41, barrier performance requirements are determined from the external environmental stress and the allowable internal residual fields and currents. These allowable residuals are

determined from the immunities of the MSCE. The two allocation equations given in Figure 2 (see Section 4.0) are used for this purpose.

While the allocation process is simple in principle, procedures are needed for the calculation of the stress transfer function (shielding properties) of the shields, given physical parameters such as size, material properties and aperture dimensions, and for the calculation of currents and Voltages on exterior and interior cables to ensure that the internal residuals (fields, Voltages and currents) are low enough to ensure MSCE survivability. These phenomena are termed **electromagnetic coupling**. The purpose of this volume is to outline the options that are available for making these electromagnetic coupling calculations - not to provide a rigid step-by-step procedure. The procedure adopted by each NATO nation will probably is different in detail depending on the tools and specific experience that each NATO nation has available to complete the process.

3.2 Scope for AEP-41, Volume III

In order to be able to design an effective EM barrier, methods are needed to estimate the coupling of electromagnetic environments to the shield and to the external and internal cables, and the subsequent penetration of this energy through the barriers and to the MSCE. In this Volume of AEP-41, options for making these estimates are outlined that will help the engineer to design and maintain effective UE³ protection. This information is required for the implementation of the procedures outlined in Volume V, "Unified Hardening and Protection Against E³".

In this Volume, we have divided our discussion of electromagnetic coupling into three general topological classes. These topological classes are:

- a) Coupling to Exterior Equipment;
- b) Coupling to Equipment Inside an Enclosure with Apertures, and
- c) Coupling to Equipment Inside a Solid Enclosure.

In practice, barrier topology can be much more complex. Multibarrier and nested barrier designs are often used. Figure 3 provides some typical examples of barrier topologies. These more complex designs can be reduced, however, to zones of the three general topological classes described above.

Unified E³ protection using the barrier protection method would be most straightforward if the MSCE could be enclosed inside a solid, conductive shield. In practice, essentially all systems require access to and communication with the outside world. In spite of this, many in-service systems are well represented by the "MSCE inside a solid enclosure" model. Examples of such systems are often encountered in OC2 "Static Land Systems" and OC3 "Space Systems" and OC6 "Command, Control

and Information Systems". In addition, well-shielded zones in the other OCs can also often be approximated by the "MSCE inside a solid enclosure" model.

For operational reasons, essentially all military systems require apertures in the outer shield in the form of windows, doors and hatches. Such systems are often encountered in OC1 "Land Mobile Systems", OC4 "Sea Platforms", and OC5 "Air Platforms". The allocation process for such platforms and systems is considerably more complex than when the shield is closed. Location of equipment and connecting cables within the outer barrier become important factors, as does cavity loading under resonance conditions.

In certain cases, it is impractical to enclose equipment inside a separate barrier and equipment must be designed to operate in the external electromagnetic environment. Man packed radios and GPS receivers are two such examples. In this case the equipment immunity must be sufficient to withstand the external environment. This is usually achieved by enclosing the electronics in a protective case and/or through circuit design. Coupling of energy to cables and antennas to the equipment remains a concern.

Various options for the calculation of electromagnetic coupling to systems falling into these three general topological classes are presented in the remainder of this volume of AEP-41.

4. ELECTROMAGNETIC COUPLING

4.1 Introduction

The basic philosophy of AEP-41 is the development of an approach to achieve balanced UE³ protection and preserve that protection throughout production and the operational life of the hardware. The method defined to achieve balanced UE³ protection is based on the use of the EM barrier protection concept. In this concept, EM barriers are used to enclose MSCEs that have inadequate electromagnetic immunity to enable them to survive the operational EM environment. The MSCEs may be located within a single compartment or distributed internally and/or externally to the system/platform. These barriers can include such items as:

- Outer EM Shield
- Internal EM Shield
- Cable shields
- Protective devices

As shown in Figure 1, the overall protection concept may involve multiple barrier

design options and shields in order to reduce internal residuals (i.e. fields, Voltages and currents) to a level that is consistent with acceptable operation of the MSCEs. Shield penetrations (electrical and mechanical) must be controlled through the effective use of penetration protection devices, components and/or design. Electrical penetrations are usually controlled with linear protection devices such as filters for Continuous Wave (CW) EMEs and nonlinear terminal protection devices (TPDs) for high intensity pulsed and multi-pulsed EMEs. Mechanical penetrations are usually controlled using conductive gaskets, grids, finger stock, and waveguides. Determination of the barrier performance requirements, involves a process of balancing the externally and internally generated EME stresses, the MSCE immunities, and the margin selected to control risk. The engineering trade studies necessary to achieve this balance are called the **allocation process**, which is usually iterative and serves as a risk management tool. Inclusion of other techniques such as mitigation, operational tactics, software/functional changes, etc, should be considered in the design and engineering evaluation process to enhance E³ survivability and to reduce costs. The proposed barrier protection methodology also simplifies and reduces developmental and verification testing by facilitating unified testing to multiple EMEs, thereby, minimizing test costs and hardware requirements (see AEP-41, Volume VI).

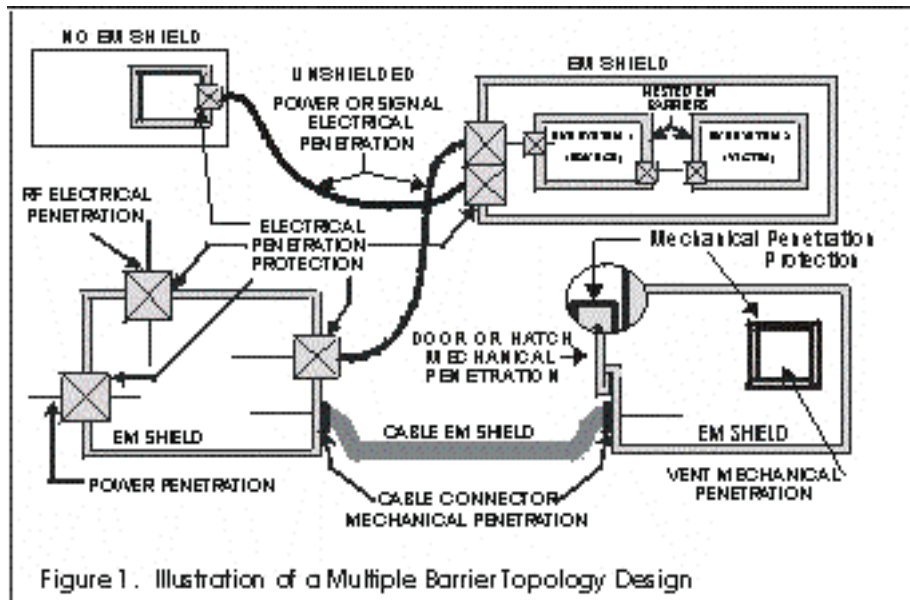
E³ can take various paths that are different to reach the MSCE contained within the barrier. Currents are induced on the exterior of the outer shield by radiated emissions such as HEMP, RF weapons and HIRF. The dominant leakage path for the energy coupled to the shield is through any apertures that exist in the shield (e.g., waveguide vents, windows, doors, hatches, seams, etc.). While there is some direct leakage of the fields through the shield material, if the shield is metallic the magnitude of these fields is in general small and can usually be neglected. The second major leakage path through the shield is via the electrical conductors that pass through the shield. These conductors carry current to the shield when they are exposed to external electromagnetic fields. Protective devices are normally installed where these external conductors enter the shield to reduce conducted currents that pass to the interior of the shield. Interior sources (such as ESD, equipment EMI or re-radiation from current carrying cables) also contribute to the interior electromagnetic field.

Under the UE³ barrier concept that has been detailed in Volume I of AEP-41, barrier performance requirements are determined from the external environmental stress and the allowable internal residual fields and currents, unless there are dominating internal sources. These allowable residuals are determined from the immunities of the MSCE and the selected margins. This process is illustrated in Figure 2.

The general approach is to derive performance requirements for the barriers that assures all of the residual stresses are attenuated below the corresponding MSCE immunities by an amount (margin) chosen by the designer and consistent with mission criticality requirements. A sufficient margin is chosen to cover risk, uncertainties,

affordability, operational degradations, and future additions of MSCEs as well as future COTS insertions.

The allocation process can be viewed as an interactive engineering trade study with the objective of deriving performance requirements for all features of the EM barrier such that these requirements are: balanced to cover all the EMEs; balanced between effectiveness and system performance/cost impact; and adjusted as a function of risk acceptance. The output from the allocation process is used to develop design specifications for UE³ protection and to provide pass/fail criteria for the E³ testing.



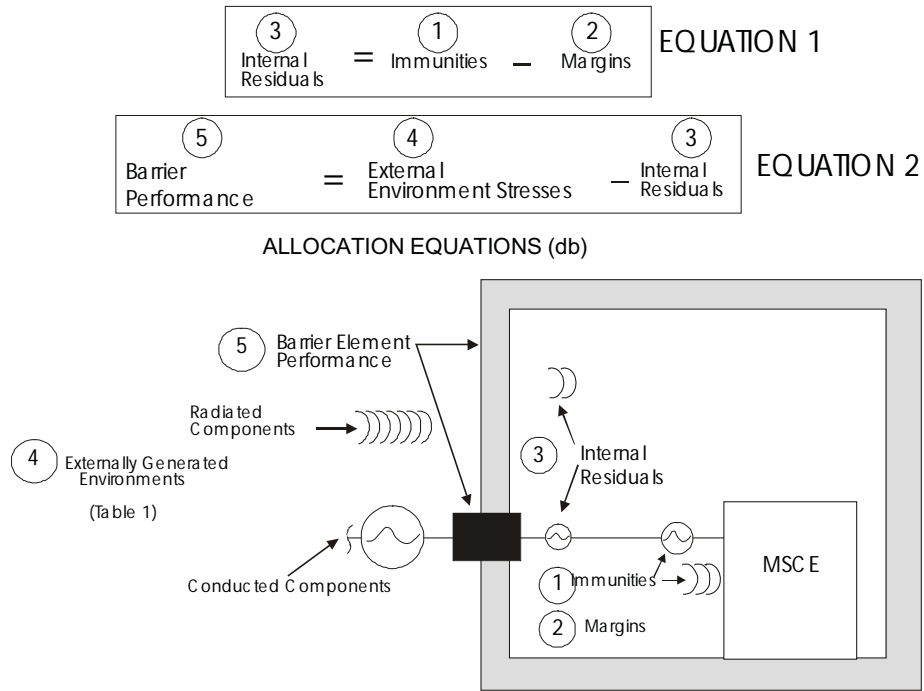


Figure 2. EM Barrier Protection Concept Keyed To Allocation Equations.

In general, the allocation process involves the use of two allocation equations. These equations consist of five terms as shown in the upper part of Figure 2. The terms are numbered in the sequence of occurrence in the allocation process. These equations cover only one feature of the EM response at a time, and must be applied to each of the barrier elements (shield and penetration ports) in the hardware under development. The following definitions are used:

MSCE immunity is the level of EM induced stresses that the MSCEs can tolerate while operating satisfactorily according to the hardware’s operational performance requirements. MSCE immunity against both conducted and radiated EME stresses is required. Ideally, these immunity levels are established using standard test methods. When test data is not available, and the equipment has been built to existing EM standards, such as IEC-61000-4, CE Norms (EMC) and U.S. MIL-STD 461E, then these standards can be used to determine immunity bounds. The existing immunity standards may need to be augmented depending on its hardware’s specific requirements.

Allowed internal residuals are the differences between the MSCE’s immunity level and the margin per the first allocation equation. The **margin allocation** should be affordable; yet, it must be large enough to cover immunity variations, test uncertainties,

future use of MSCEs with lower immunities (including COTS insertion), operational degradations, system upgrades, and risk. The allowed margin for the MSCEs will normally be in the range from 10 to 40 dB. Both conducted and radiated internal residuals are important. In general, the conducted internal residuals will be different for the different types of electrical penetrations. The radiated internal residuals are the residuals from externally generated fields that penetrate the EM shield. In some cases (example ESD), the internally generated EMEs may dominate the residuals resulting from external EME stresses.

The external EME stresses can be conducted and/or radiated, and are generated from external EMEs such as lightning, HPM, UWB, HIRF, HEMP, and forms of ESD. External EMEs stresses are reduced to the internal residuals by the barrier elements such as the EM shield and penetration protection devices.

The internal EME stresses (both radiated and conducted) are usually less than the externally EME stresses. However, if the internally generated EME stresses are greater or are of sufficient magnitude to cause susceptibilities (e.g., ESD radiated fields), they too can effectively be dealt with by the barrier protection concept. Protection against these internally generated stresses can be achieved by: reducing the radiated and conducted emissions; increasing separation distance between victim and source; controlling the absorbing properties of the enclosure and effective aperture area; and providing higher immunity levels for special cases (SREMP and SGEMP). As was the case for externally generated EMEs, shields (nested barrier) and/or protection devices can be added.

Finally, the **barrier performance requirements** are the differences between the external EME stresses and the allowed internal residuals as given by the second allocation equation. Barrier performance requirements for the shield and all penetration protective devices are required. These requirements should be determined for each EME and its corresponding immunity, and then unified.

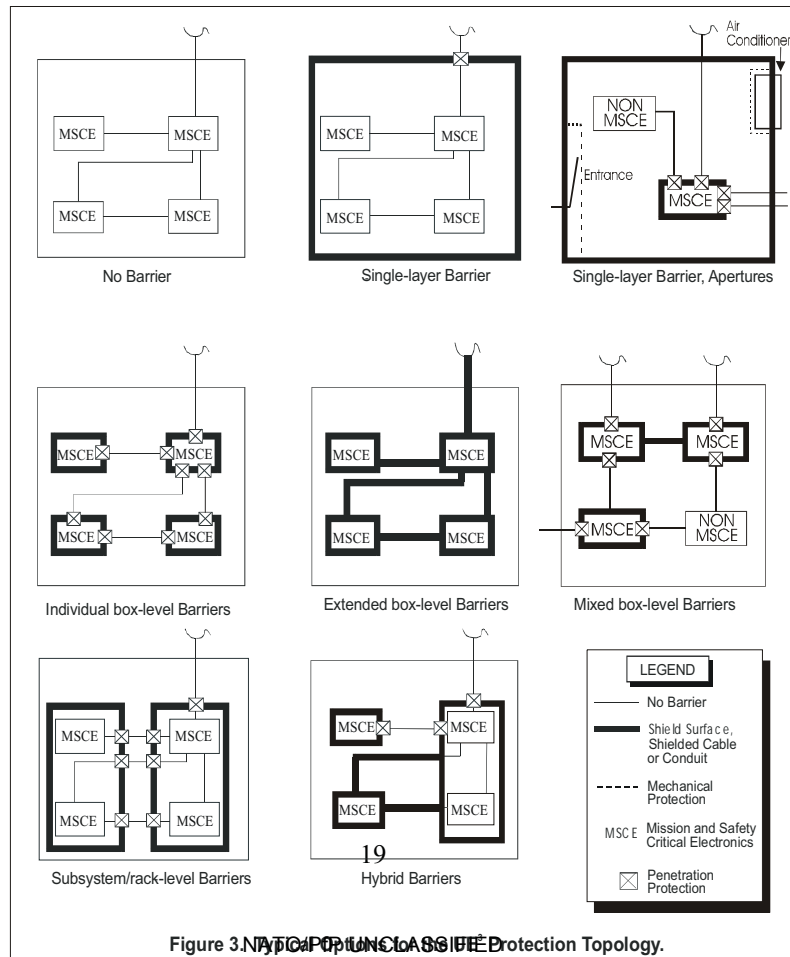
While the allocation procedure given by Equations 1 and 2 in Figure 2 is simple in principle, in practice the procedure can be quite complex. If the barrier elements are linear, barrier performance can be defined in the frequency domain in terms of a **Transfer Function** defined as the ratio of the internal residuals (fields, Voltages or currents) to the external field. For a shield, the transfer function is dependent on physical parameters of the system such as enclosure dimensions, aperture size, and location within the shield and material properties. When the barrier elements are non-linear (e.g. many transient protection devices), it is necessary to carry out the analysis in the time domain. Both cases can be covered by defining a more general **Stress Transfer Function**, which gives the relationship (in the frequency or time domain) of the interior residuals to the external field. A detailed discussion of stress transfer functions is given in AEP-41, Volume V.

To carry out the allocation process, procedures are needed for the calculation of the stress transfer function of the barriers, given physical parameters such as size, material properties and aperture dimensions, and for the calculation of the conducted currents on exterior and interior cables to ensure that the internal residual fields and currents are low enough to ensure MSCE survivability and to provide an adequate safety margin. These phenomena are termed **electromagnetic coupling**. Procedures for making these electromagnetic coupling calculations are outlined in this volume. The volume relies heavily on recent work of Crevier [1] Crevier and Auton [2], Lee[3], Lee and Yang [4] and Warne and Chen[5,6].

In this chapter, we divide our discussion of electromagnetic coupling into three general topological classes. These classes are:

- a) Coupling to Exterior Equipment;
- b) Coupling to Equipment Inside an Enclosure with Apertures, and
- c) Coupling to Equipment Inside a Solid Enclosure.

In practice, barrier topology can be much more complex. Multibarrier and nested barrier designs are often used (Figure 3) to provide added protection to MSCEs against external and internal stresses. These more complex designs can, however, be reduced to zones of the three types described above. With nested barriers, care needs to be taken in defining the "external" EME. Outer barriers will both attenuate



and modify the time behaviour of the incident fields so that fields in interior zones (external environment to the nested zones) can be quite different in magnitude and form from the external EME to the outer barriers.

4.2 Classification of Electromagnetic Environments and Coupled Stresses

4.2.1 Introduction

Volume II of AEP-41 defines and discusses the potential battlespace EMEs. These are also listed in Table 1 of this document. To simplify the discussion of EM coupling, it is useful to divide the external and internal EM environments in to several broad waveform types as has been done in Table 1. These waveform types include:

- a) Pulse: which includes EMP, lightning, ESD etc.,
- b) Continuous Wave: which includes radio transmission and HIRF,
- c) RF pulse or burst CW: which includes HPM and radar emissions, and
- d) Damped sine: which includes response of a resonant structure to external EM excitation.

This section of the report summarises the time and frequency domain characteristics of these waveform types.

4.2.2 External and Internal Environments

a) Pulse Waveforms

The following waveforms are often used as an approximation to pulsed environments such as EMP, ESD, lightning and UWB.

i) Double Exponential Waveform.

The following double exponential form is often [7] used as an approximation to the EMP waveform because of its simplicity in spite of the fact that the first derivative is discontinuous:

$$E(t) = E_0 \kappa (e^{-\beta t} - e^{-\alpha t}) u(t). \quad (1)$$

In this expression, t is time, α is the rate of rise (in sec^{-1}), β is the fall rate (in sec^{-1}), u is the step function and κ is a normalization constant that assures that the peak electric field is E_0 .

If ω is the angular frequency. the spectrum of this pulse is given by:

$$E(\omega) = \int_{-\infty}^{\infty} E(t) e^{i\omega t} dt = \frac{E_0 \kappa(\beta - \alpha)}{(\alpha - i\omega)(\beta - i\omega)}. \quad (2)$$

ii) Inverse Exponential Waveform

While the double exponential pulse (described above) is often used to describe a nuclear EMP because of its simplicity, it is discontinuous at time $t=0$ and has a singularity in its first derivative at this time. This discontinuity results in an overestimation of the high frequency content in the pulse. To overcome this difficulty, the following inverse double exponential waveform has been proposed [8]:

$$E(t) = E_0 \frac{d e^{at}}{1 + e^{\beta(t-t_p)}}, \quad (3)$$

where d is a scaling factor.

The spectrum of this pulse is given by:

$$E(\omega) = E_0 d \frac{\pi e^{(\alpha+i\omega)t_p}}{\beta \sin[(\alpha + i\omega)\frac{\pi}{\beta}]}. \quad (4)$$

iii) Gaussian Waveform

While there is no standard UWB EME waveform, a radiated Gaussian waveform is often used (see AEP-41, Volume II.) to represent this environment. In the time domain, the Gaussian waveform is given by the following analytical expression

$$E(t) = E_0 \exp\left\{-0.693\left[\frac{(t - \tau)}{\sigma}\right]^2\right\}, \quad (5)$$

where σ is the half-width of the pulse, and $\tau=3\sigma$.

The Laplace transform of the Gaussian pulse is given by the equation

$$E(s) = 2.13\sigma E_0 \exp\left[-(3\sigma s + 0.361\{\sigma s\}^2)\right], \quad (6)$$

where $s = j\omega$.

b) Continuous Wave (CW)

Many EM emissions that result from the operation of electronics inside or outside the barrier can be described as "continuous wave or CW. In the time domain, CW emissions can be represented as

$$E(t) = E_0 \exp\{i\omega_0 t\}. \quad (7)$$

The spectrum of a CW signal is given by

$$E(\omega) = 2\pi E_0 \delta(\omega - \omega_0). \quad (8)$$

where δ is the Dirac delta function.

c) RF Pulse or Burst CW

The penetration of RF pulse or burst CW through an aperture and subsequent coupling is of considerable interest because of the potential for threat from High Power Microwaves (HPM) and EM interference from on-board or nearby radars.

A rectangular RF pulse can be represented in the time domain by:

$$E(t) = \begin{cases} E_0 \cos \omega_0 t & |t| \leq a \\ 0 & \text{otherwise} \end{cases} \quad (9)$$

In practice, allowed values of a are restricted as it is not possible to start the pulsed in the middle of a cycle.

The spectrum of this waveform is given by:

$$E(\omega) = \int_{-\infty}^{\infty} E(t) e^{i\omega t} dt = -i E_0 \left[\frac{\sin a(\omega - \omega_0)}{\omega - \omega_0} - \frac{\sin a(\omega + \omega_0)}{\omega + \omega_0} \right]. \quad (10)$$

d) Damped Sine

The response of a resonant structure to an external EM excitation often takes the form of a damped sine wave, which is described by the following equation:

$$E(t) = E_0 \sin \omega_0 t e^{-at} u(t). \quad (11)$$

The spectrum of this waveform is given by:

$$E(\omega) = \int_0^{\infty} E(t) e^{i\omega t} dt = \frac{E_0 \omega_0}{(-a + i\omega)^2 + \omega_0^2}. \quad (12)$$

4.3 Coupling to Exterior Equipment

4.3.1 Introduction

In certain cases, it is impractical to enclose equipment inside a separate barrier and equipment must be designed to operate in the external electromagnetic environment. Man packed radios and Global Positioning System (GPS) receivers are two such examples. In this case the equipment immunity must be sufficient to withstand the external environment. This is usually achieved by enclosing the electronics in a protective case and/or through circuit design. Coupling of energy to external cables and antennas to the equipment remains a concern.

The purpose of this section is to outline options for determining the coupling of fields to external cables and antennas. The material that has been presented has been drawn largely from an unpublished report prepared by Crevier [1]. The method proposed by Crevier (1) is convenient since it is based on the use of a general coupling cross-section equation that is valid for all frequencies (i.e., frequencies above and below resonance) as well as the "bounds" approach. Other excellent treatments of cable coupling, such as the book of Vance [51], are also available. In general, these works require a detailed knowledge of the incident angle of the field and are not valid for all frequencies. They are thus more complicated for the EMC engineer to use.

4.3.2 Coupling to Vertical Conductors

4.3.2.1 CW Coupling to Vertical Conductors [1]

The current driven on vertical conductors by incident CW fields is bounded by:

$$I_0 \leq 2.8 \times 10^{-11} E_0 \left[\frac{f_0 l_m^2}{(((2.1 \times 10^{-8} f_0 l_m - 1)^2 + 1.8 \times 10^{-4})((2.1 \times 10^{-8} f_0 l_m + 1)^2 + 1.8 \times 10^{-4}))^{1/2}} \right], (13)$$

where f_0 is the frequency of the EM field in Hz, l_m is the height of the antenna or conductor in meters and E_0 is the amplitude of the EM field in V/m. If we assume that the system has a 1.5 m whip antenna, the maximum response occurs between 30 MHz and 50 MHz. Care must be taken to distinguish between root mean square (r.m.s.) and peak values of fields. If r.m.s. fields are used, r.m.s. currents are determined; peak fields give peak currents. From equation (13), the maximum current driven on a 1.5 m antenna by a 200 V/m environment is approximately 10 Amps.

4.3.2.2 Pulse Coupling to Vertical Conductors [1]

Bounding current driven on an antenna by a pulse is somewhat more complicated. The current is a mixture of decaying exponentials and damped oscillations, oscillating at the fundamental resonance frequency of the antenna.

Four parameters (norms) quantify the relevant behavior:

1. peak current, I_{peak} ,
2. peak time derivative of the current, I'_{peak} ,
3. integral of the square of the current, $\int (I(t))^2 dt$, called the *action*, and
4. integral of the square of the time derivative of the current, $\int (I'(t))^2 dt$.

Stresses are maximized by assuming an infinite pulse width, $\alpha \gg \beta \approx 0$. In the limit, β tends to 0, the peak current is:

$$I_{peak} \text{ (amps)} \leq 2.7 \times 10^{-3} l_m \left[\frac{\alpha}{\alpha + 3.0 \times 10^8 / l_m} \right] E_0, \quad (14)$$

where α is the pulse rise rate in sec^{-1} . The action is given by:

$$\int_0^{\infty} (I(t))^2 dt \leq 6.3 \times 10^{-8} l_m (I_{peak})^2. \quad (15)$$

The maximum time derivative of the current is:

$$I'_{peak} \leq 8.0 \times 10^5 \left[\frac{\alpha}{\alpha + 3.0 \times 10^8 / l_m} \right]. \quad (16)$$

The integral, $\int_0^{\infty} (I'(t))^2 dt$ can be represented by an integration time, Δt :

$$\int_0^{\infty} (I'(t))^2 dt \equiv \Delta t (I'_{peak})^2, \quad (17)$$

where Δt is given by $\Delta t_s \leq 1.6 \times 10^{-8} I_m$.

The equations given above can be used to compute the peak current, peak current time derivative, and action generated by an EM pulse (such as EMP) incident on a vertical conductor.

4.3.3 Coupling to Horizontal Conductors

4.3.3.1 CW Coupling to Horizontal Conductors [1]

Typical horizontal conductors include power lines and communication lines. Unlike vertical conductors, they are terminated at each end. Incident EM fields with a horizontal electric field aligned with the conductor drive a current bounded by:

$$I_A \leq 8.6 \times 10^4 \left[\frac{(2.1 \times 10^{-8} f_0 z_m)^2 + 2.9 \times 10^{-2}}{(2.1 \times 10^{-8} f_0 z_m - 0.79)^2 + 0.62} \right]^{1/2} \left[\frac{E_0}{f_0} \right], \quad (18)$$

where I_A is the current driven in the conductor in A, f_0 is the frequency of the incident field in Hz, z_m is the height of the conductor above the ground in m, and E_0 is the amplitude of the incident field in V/m. For a given electric field, the current is highest at low frequencies.

4.3.3.2 Pulse Coupling to Horizontal Conductors. [1]

Current driven on horizontal conductors by a pulse is related to the time integral of the total electric field, which is the incident electric field minus the reflected electric field. Four parameters that quantify the relevant behavior are:

1. peak current, I_{peak} ,
2. peak time derivative of the current, I'_{peak} ,
3. integral of the square of the current, $\int (I(t))^2 dt$, called the *action*, and
4. integral of the square of the time derivative of the current, $\int (I'(t))^2 dt$.

In the limit of zero rise time, the peak current is bounded by:

$$I_{peak} \leq 8.0 \times 10^5 \left[\frac{(6.7 \times 10^{-9} \beta z_m + 0.15)}{1 + 6.7 \times 10^{-9} \beta z_m} \right] \left[\frac{E_0}{\beta} \right], \quad (19)$$

where β is the pulse decay rate in sec^{-1} . Action is bounded by:

$$\int_0^{\infty} (I(t))^2 dt \leq 6.3 \times 10^{11} \left[\frac{(6.7 \times 10^{-9} \beta z_m + 0.15)^2}{1 + 6.7 \times 10^{-9} \beta z_m} \right] \left[\frac{E_0}{\beta} \right]. \quad (20)$$

The maximum time derivative of the current is $I'_{peak} \leq 8.0 \times 10^5 E_0$. The integral, $\int_0^{\infty} (I'(t))^2 dt$, can be represented by an integration time, Δt , as:

$$\int_0^{\infty} (I'(t))^2 dt \equiv \Delta t (I'_{peak})^2, \quad (21)$$

where Δt is bounded by

$$\Delta t_s \leq \left[\frac{6.7 \times 10^{-9} \beta z_m + 0.15}{1 + 6.7 \times 10^{-9} \beta z_m} \right] \left[\frac{1}{\beta} \right]. \quad (22)$$

The HEMP environment specified here has a peak field of 54 kV/m, and a decay rate of $4.3 \times 10^7 \text{ sec}^{-1}$. Assume the HEMP field is incident on a line lying on the ground.

Using the specified unclassified HEMP waveform, this model predicts currents of about 1,000 A will be driven on a line located several meters above the ground. However, if a line is several hundred meters or more long, several meters above the ground, and very straight, it is possible to have an "end fire" geometry which would induce a current five to ten times larger than indicated by this model. If good engineering practices are followed, this type of HEMP coupling geometry should rarely be encountered. For each system, a decision must be made on whether it is appropriate to protect against this higher level of HEMP coupling or against the lower levels predicted by this and similar models which neglect the end-fire geometry.

4.4 Coupling to Equipment Inside an Enclosure with Apertures

4.4.1 Introduction

For operational reasons, military systems require apertures in the outer shield in the form of windows, doors and hatches and electrical and data ports. The allocation process for such systems is considerably more complex than when the shield is

closed. Location of equipment and connecting cables within the outer barrier become important factors, as does cavity loading under resonance conditions. In Section 4.4, we deal with some of these issues.

4.4.2 Determination of the EM Environment Inside a Shield with Apertures

4.4.2.1 Shielding Effectiveness

The magnetic and an electric shielding effectiveness are defined in terms of the ratio of the internal fields to the external (incident) fields by the expressions:

$$SE_m(dB) = 20 \log \left[\frac{H_{int}(\omega)}{H_{ext}(\omega)} \right], \quad (23)$$

and

$$SE_e(dB) = 20 \log \left[\frac{E_{int}(\omega)}{E_{ext}(\omega)} \right]. \quad (24)$$

Leakage through a metallic shield with apertures is not, in general, well characterized in terms of shielding effectiveness. At low frequencies (when the wavelength is large compared to the barrier and aperture dimensions), the leakage fields are quasistatic and tend to be concentrated near the apertures in the shield (see Section 4.4.2.4.1). The transition from quasistatic-dominated leakage to radiation-dominated leakage occurs at a distance of about $\lambda/2$, where λ is the wavelength of the incident radiation. The energy associated with these quasistatic fields remains localized around the aperture and flows in and out of the apertures as the exterior field strength changes. The requirements for barrier protection, therefore, depend strongly on whether the MSCE is located close to the apertures in the barrier or not. Barrier requirements can be greatly reduced by defining a minimum **keepout distance** that gives the minimum distance between MSCE and cabling and an aperture. Adoption of this approach can substantially reduce barrier requirements and prevent over specification.

At higher frequencies (when the wavelength is small compared to the aperture dimensions), each aperture acts like a radiating antenna and the radiated fields fall off slowly with distance ($1/r$); hence, these fields can couple to MSCE located well away from the aperture. To characterize barrier quality, it is useful to specify an **effective aperture area** for the barrier. With this approach, the penetration of radiated fields into the barrier through the various apertures is equivalent to penetration through an aperture with a given area, A_{eff} . Techniques for the measurement of the effective aperture area have been defined [9] and can be used to monitor barrier performance during its operational life.

At very high frequencies, when the cavity becomes resonant, the interior field levels depend strongly on the absorbing properties of the shielded cavity as well as on the size of the apertures in the shield. The same shield can appear to have low SE if it is empty and a high SE when filled with equipment and personnel. In order to limit the interior fields, in addition to controlling the effective aperture of the barrier, it is necessary to control the absorbing properties of the shielded enclosure as characterized by the cavity absorption area.

4.4.2.2 Numerical Computation of Internal Fields [10-12]

Electromagnetics is the scientific discipline that deals with electric and magnetic sources and the fields that they produce. Maxwell's equations provide the starting point for the study of electromagnetic problems. Numerical solution of Maxwell's equations is becoming possible even for relatively complex structures because of the dramatic increase in computational power at a modest cost. In this section, an overview of numerical methods that can be used to determine interior fields will be given and references provided. It should be noted that considerable expertise with the various electromagnetic codes is needed to ensure that correct results are obtained.

A common ingredient of essentially all methods for the solution of Maxwell's equations is the establishment of a quantitative relationship between a cause (source or input) and its effect (the response or output). This quantitative relationship is referred to as a field propagator or transfer function. The mathematical form used to describe it determines the computational characteristics of the transfer function.

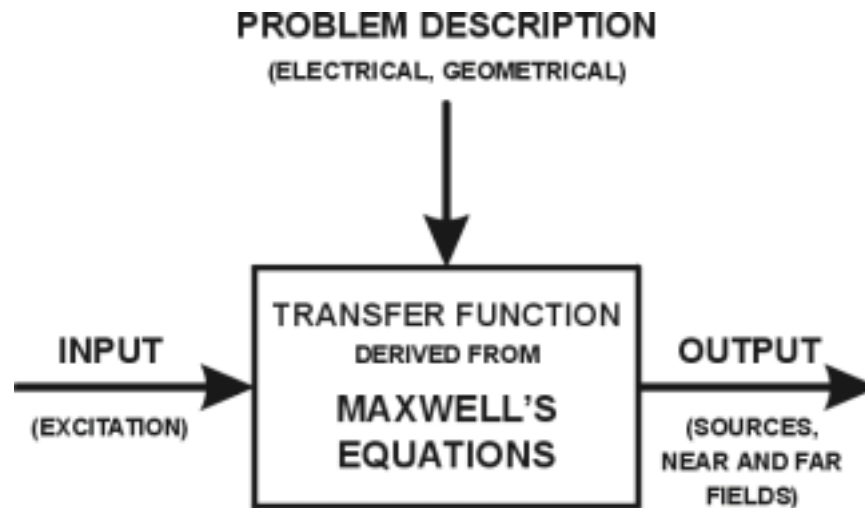


Figure 4. Procedure for the Solution of Maxwell's Equations.

The procedure that is used to solve electromagnetic problems is illustrated in Figure 4. For the determination of interior fields, the input or stress waveform is known and the transfer function is derivable from the problem description. The output or residual fields remain to be determined.

The first step in developing an electromagnetic computer model is the selection of the form of the transfer function. The appropriate transfer function is derived from the particular form of Maxwell's equations that is chosen to solve the problem. The transfer function can take several forms, some of which are discussed below. The nature of the problem to be solved will dictate which forms are most suitable.

1) Integral Equation (IE) Model

The basic starting point for developing an IE model in electromagnetism is the selection of a Green's function appropriate for the problem class of interest. While there are a variety of Green's functions from which to choose, a typical starting point for most IE models is that for an infinite medium. Although the formulation might be accomplished in various ways, one of the more straightforward is based on the scalar Green's function and Green's theorem.

This analytical formulation leads to an integral operator whose kernel can include differential operators as well, which acts on the unknown source or field. Some of the integral equations used in numerical electromagnetism, include the Magnetic Field Integral Equation (MFIE) and Electric Field Integral Equation (EFIE) for perfect conductors for the frequency and time domains.

2) Differential Equation (DE) Model

A differential equation, being based on the defining Maxwell's equations, requires intrinsically less analytical manipulation than does an IE model. Numerical implementation of a DE model, however, can differ significantly from that used for an IE formulation in a number of ways for the following reasons:

- a) The differential operator is a local rather than global one in contrast to the Green's function upon which the integral operator is based. This means that the dimensionality of the calculation is the same as that of the problem rather than one less as the IE model permits if an appropriate Green's function is available.
- b) The differential operator includes a capability to treat medium inhomogeneities, nonlinearities, and time variations in a more straightforward manner than does the integral operator.
- c) The integral operator includes an explicit radiation condition.

3) Network Equation Model

In a network model, electromagnetic field propagation is described in terms of transmission line concepts. In such approach, the modeling space is divided into a number of blocks of shape and dimensions to fit the geometry and frequency requirements. A network of transmission lines, which are interconnected to form a node, is used to replace each block in the modeling space. Transmission lines of adjacent nodes are interconnected to form a mesh describing the entire problem. Voltage and currents on these transmission lines are calculated. These voltages and currents represent the electric and magnetic fields corresponding to the particular problem configuration. Information is available in the time and frequency domain. The user can incorporate different material properties by adjusting the capacitance/inductance of lines representing particular blocks of space.

A variety of numerical methods have been used to solve electromagnetic problems once the appropriate form of the transfer function has been selected. For integral equation formulations, considerable work has been devoted to use of the Method of Moments (MoM). For differential equation formulations, the Finite-Difference Time Domain (FDTD) method and the Finite-Element Method (FEM) have been used. To solve network equations, the Transmission Line Method (TLM) has been used. In the following section, we discuss some of these numerical methods in more detail.

Method of Moments

Harrington [13] was largely responsible for popularizing the MoM in the field of electrical engineering. His pioneering efforts first demonstrated the power and flexibility of this numerical technique for solving problems in electromagnetics.

The MoM is a technique for solving complex integral equations by reducing them to a system of simpler linear equations. To achieve this, MoM methods employ a technique known as the method of weighted residuals. Weighted residual techniques begin by establishing a set of trial solution functions with one or more variable parameters. The residuals are a measure of the difference between the trial solution and the true solution. The variable parameters are determined in a manner that guarantees a "best fit" of the trial functions based on a minimization of the residuals.

The equation to be solved by the MoM is generally a form of the EFIE or the MFIE. Both of these equations can be derived from Maxwell's equations by considering the problem of a field scattered by a perfect conductor (or a lossless dielectric). These equations are of the form,

$$\vec{E} = f_e(\vec{J}) \quad \text{and} \quad \vec{M} = f_m(\vec{J}) \quad ,$$

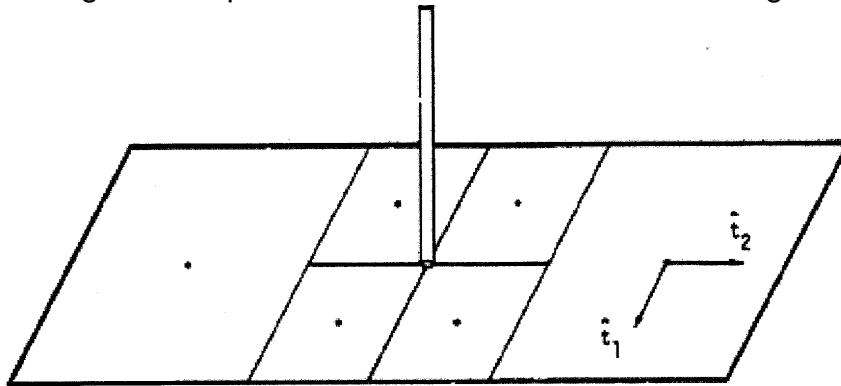
where the terms on the left-hand side of these equations are incident electric and magnetic fields and J is the induced current.

The form of the integral equation used determines which types of problems a MoM technique is best suited to solve. The MFIE is only suitable for calculation EM interaction with closed bodies and hence is not suitable for determining interior fields. EFIE can, however, be used for this purpose.

The MoM does an excellent job in analyzing a wide variety of important three-dimensional electromagnetic radiation problems. Depending on the form of the field integral equation used, moment methods can be applied to configurations of conductors only, homogeneous dielectrics only, or very specific conductor-dielectric geometries. The MoM has been used to solve three major classes of electromagnetic problems: topologies represented by thin wire geometries; topologies represented by surfaces, and; topologies that include apertures.

Since the MoM was first described by Harrington in 1968 [13], it has been very popular for computing interaction of EM waves with simple as well as complex structures [14,15]. The method is useful in situations where a structure, such as a wire antenna, can be easily discretized into a number of small wire segments. Another

implementation of the method also allows discretization of the structure into surface patches and wire segments. As an example, Figure 5 shows a model of a dipole antenna attached to a ground plane. Using the MoM, one can determine various parameters such as the radiation pattern of the antenna and the antenna impedance. Currents on any part of the antenna can be also determined for exposure to an incident waveform. The method requires the discretization of the structure (wire as well as the ground plane) into segments, which are small, compared to the wavelength. One fifth of the wavelength is the minimum recommended for the wire segments and the side dimension of the surface patch. This determines the high frequency limit of the use of the method for given computer resources. Numerical Electromagnetic Code



(NEC) is one of the codes based on the MoM available for computation of EM interaction with structures [16].

Figure 5. Connection of a Wire to a Surface Patch.

Figure 6 shows an example of the use of the MoM in a situation of practical interest. It shows the bridge of a ship with a number of windows. The walls of the bridge are discretized into triangular patches using the criteria described earlier. In this case the moment method allows the determination of electromagnetic fields and currents inside the bridge for an incident plane (or other shapes) wave. Figure 7 shows normalized electric field inside the bridge for various frequencies. The results indicate a strong resonance at some frequencies.

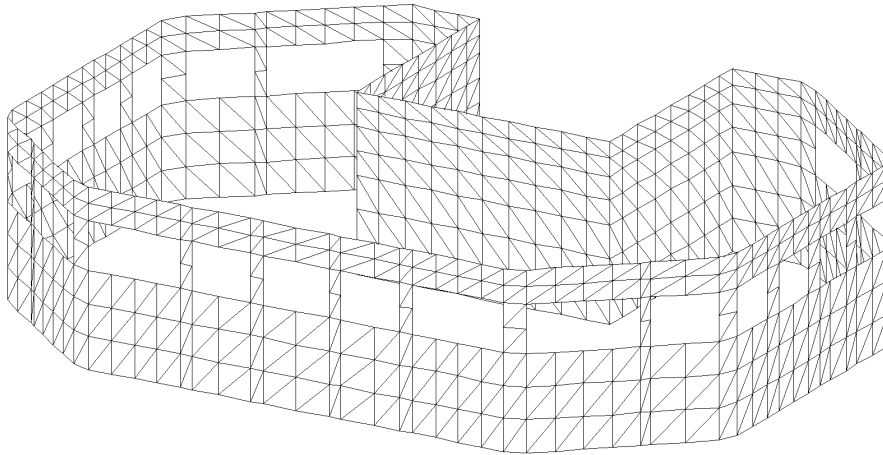


Figure 6. Patch Model of the Bridge of a Ship [17].

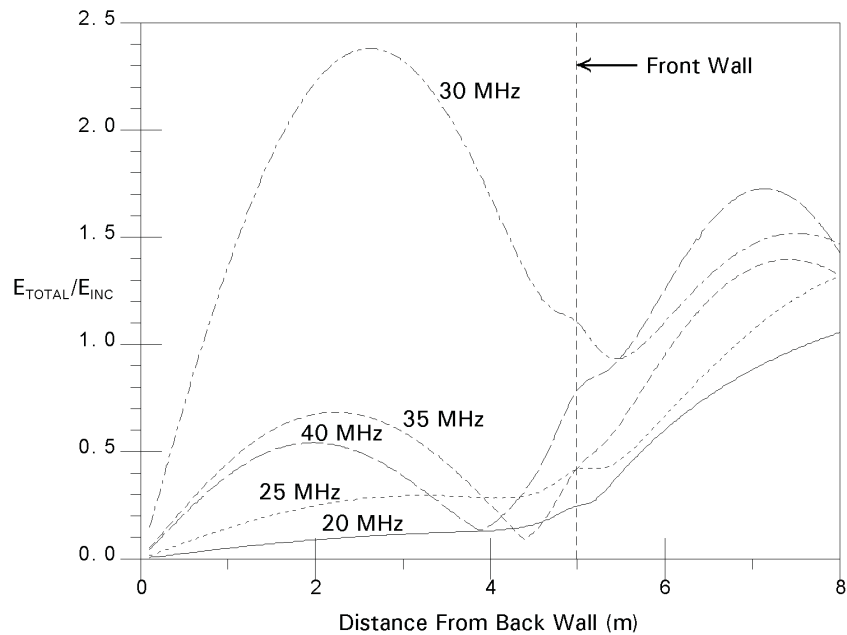


Figure 7. Calculation of Internal Fields Using the Method of Moments [17].

Finite Difference Time Domain Method

The Finite Difference Time Domain (FDTD) method [18] is a direct solution of Maxwell's time dependent curl equations. The method uses simple central-difference approximations to evaluate the space and time derivatives.

The FDTD method is a time stepping procedure. Inputs are time-sampled analog signals. The region being modeled is represented by two interleaved grids of discrete points. One grid contains the points at which the magnetic field is evaluated. The second grid contains the points at which the electric field is evaluated. A first-order central-difference approximation allows the electric field values at time t to be used to find the magnetic field values at time $t+\Delta t$. A similar central-difference approximation can then be applied to find the electric field values at time $t+2\Delta t$ from the magnetic field values at time $t+\Delta t$. By alternately calculating the electric and magnetic fields at each time step, fields are propagated throughout the grid. Time stepping is continued until a steady state solution or the desired response is obtained. At each time step, the equations used to update the field components are fully explicit. No system of linear

equations must be solved. The required computer storage and running time is proportional to the electrical size of the volume being modeled and the grid resolution. Special absorbing elements are used at the outer boundary of the lattice in order to prevent unwanted reflection of signals that reach this boundary. Values of μ, ϵ and σ are assigned to each field component in each cell define the position and electrical properties of the scatterer. These parameters can have different values for different field orientations permitting anisotropic materials to be modeled. Their values can also be adjusted at each time-step depending on conditions making it easy to model nonlinear materials.

Because the basic elements are cubes, curved surfaces on a scatterer must be staircased. For many configurations this does not present a problem. However for configurations with sharp, acute edges, an adequately staircased approximation may require a very small grid size. This can significantly increase the computational size of the problem. Surface conforming FDTD techniques with non-rectangular elements have been introduced to combat this problem.

In the FDTD method, all the electromagnetic phenomena such as induction of surface currents, scattering and multi-scattering, field penetration into cavities are all accounted for in this full wave numerical technique. Additionally, FDTD is very well suited to study EM field penetration into structures with opening as well as EM radiation from sources inside structures with joints and openings. It also facilitates the use of different types of EM sources for excitation purposes. These sources can be a plane wave from a far field source, a point source or a line source. These sources are accounted for by exact modeling of the EM source antenna, or by the use of Equivalence Theory through Huygen's sources. Being a time-domain method the EM excitation used in the FDTD analysis can be any real life waveform such as, EMP, Gaussian pulse, step, a one cycle sine wave (UWB), CW, etc. An FDTD simulation will produce numerous amount of data which can be stored for analysis in both time or frequency domain

Frequency domain results can be obtained by applying a discrete Fourier transform to the time domain results. This requires additional computation, but a wide-band frequency-domain analysis can be obtained by transforming the system's impulse response.

The FDTD data will constitute of individual electric and magnetic field components ($E_x, E_y, E_z, H_x, H_y, H_z$) at each cell location of the computation space. The knowledge of such components together with the physical parameters of a media can produce loss and current information of interest. FDTD in conjunction with plotting software also has the advantage of producing real time animation of the EM interaction with the structure/environment being analyzed.

The only significant disadvantage of this technique is that the problem size can easily get out of hand for some configurations. The fineness of the grid is generally determined by the dimensions of the smallest features that need to be modeled. The volume of the grid must be great enough to encompass the entire object and most of the near field. Large objects with regions that contain small, complex geometries may require large, dense grids. When this is the case, other numerical techniques may be much more efficient than the FDTD or Finite-Volume Time-Domain (FVTD) methods.

Finite Element Methods

Scalar finite element methods are widely used by civil and mechanical engineers to analyze material and structural problems. Electrical engineers use finite element methods to solve complex, nonlinear problems in magnetostatics and electrostatics. Until recently however, very little practical modeling of 3-dimensional electromagnetic radiation problems was performed using this technique. The increasing availability of computer resources coupled with a desire to model more complex electromagnetic problems has resulted in renewed interest in finite element methods for solving EM radiation problems.

The first step in finite-element analysis is to divide the configuration into a number of small homogeneous pieces or elements. The model contains information about the device geometry, material constants, excitations and boundary constraints. The elements can be small where geometric details exist and much larger elsewhere. In each finite element, a simple (often linear) variation of the field quantity is assumed. The corners of the elements are called nodes. The goal of the finite-element analysis is to determine the field quantities at the nodes.

Most finite element methods are variational techniques. Variational methods work by minimizing or maximizing an expression that is known to be stationary about the true solution. Generally, finite-element analysis techniques solve for the unknown field quantities by minimizing an energy functional. The energy functional is an expression describing all the energy associated with the configuration being analyzed.

In order to obtain a unique solution, it is necessary to constrain the values of the field at all boundary nodes. For example, at a metal surface, the tangential electric field at all boundary nodes is set to zero. A weakness of the finite element method is that it is relatively difficult to model open configurations (i.e., configurations where the fields are not known at every point on a closed boundary). Various techniques, such as the use of absorbing boundaries, are used in practice to overcome this deficiency. These techniques work reasonably well for 2-dimensional problems, but so far they are not very effective for 3-dimensional electromagnetic radiation problems.

Finite element methods have the advantage over other EM modeling techniques that the electrical and geometric properties of each element can be defined independently. This permits the problem to be set up with a large number of small elements in regions of complex geometry and fewer, larger elements in relatively open regions. Thus, it is possible to model configurations that have complicated geometries and many arbitrarily shaped dielectric regions in a relatively efficient manner.

Commercial finite element codes [19,20] are available that have graphical user interfaces that determine the optimum placement of node points for a given geometry automatically. These codes have been used to model a wide variety of electromagnetic problems.

Transmission Line Matrix Method

The Transmission Line Matrix (TLM) method is similar to the FDTD method in terms of its capabilities, but its approach is unique. Like FDTD, analysis is performed in the time domain and the entire region of the analysis is gridded. Instead of interleaving E-field and H-field grids, however, a single grid is established and the nodes of this grid are interconnected by virtual transmission lines. Excitations at the source nodes propagate to adjacent nodes through these transmission lines at each time step. The symmetrical condensed node formulation introduced by Johns [21] has become the standard for three-dimensional TLM analysis. Each node is connected to its neighboring nodes by a pair of orthogonally polarized transmission lines. Generally, dielectric loading is accomplished by loading nodes with reactive stubs. These stubs are usually half the length of the mesh spacing and have a characteristic impedance appropriate for the amount of loading desired. Lossy media can be modeled by introducing loss into the transmission line equations or by loading the nodes with lossy stubs. Absorbing boundaries are easily constructed in TLM meshes by terminating each boundary node transmission line with its characteristic impedance.

The advantages of using the TLM method are similar to those of the FDTD method. Complex, nonlinear materials are readily modeled. Impulse responses and the time-domain behavior of systems are determined explicitly. And, like FDTD, this technique is suitable for implementation on massively parallel machines.

The disadvantages of the FDTD method are also shared by this technique. The primary disadvantage being that voluminous problems that must use a fine grid require excessive amounts of computation. Nevertheless, both the TLM and FDTD techniques are very powerful and widely used. For many types of EM problems they represent the only practical methods of analysis. Deciding whether to utilize a TLM or FDTD technique is a largely personal decision. Many engineers find the transmission line analogies of the TLM method to be more intuitive and easier to work with. On the other hand, others prefer the FDTD method because of its simple, direct approach to

the solution of Maxwell's field equations. The TLM method requires significantly more computer memory per node, but it generally does a better job of modeling complex boundary geometries. This is because both E and H are calculated at every boundary node.

A general overview of the TLM method and a two-dimensional TLM code are provided in a book by Hofer [22].

4.4.2.3 Energy Bounds

Lee [3], Lee and Yang [4], Warne and Chen [5,6] and others [2,23] have proposed the use of energy bounds. In this approach, one attempts to determine the maximum energy/power that can couple to an electronic system inside a structure with apertures. This approach recognises that it is virtually impossible to model all of the detail of any real world system and attempts to find a solution (in terms of an upper bound) that is independent of these system details. An upper bound on the energy coupled to MSCE inside the barrier is clearly defined by the energy that can be transmitted through the apertures. This upper bound on the energy that can penetrate the barrier can be compared with estimates of energy required for component damage or upset using a variety of models such as the thermal model of Wunsch and Bell [24] for semiconductor damage.

In the remainder of this section, we summarize the efforts that have been made to define upper bounds on the energy that can be transmitted through an aperture for various incident waveforms of practical interest.

The theory of the calculation of the energy bounds has been given elsewhere [3-6]. To obtain a bound on the energy that can be transmitted through an aperture, use has been made of the following basic relationship for the total energy absorbed and scattered by an aperture. This total energy is related to the total aperture cross-section, σ_t , by the expression:

$$W_{tot} = \frac{1}{2\pi} \int_{-\infty}^{\infty} \frac{|E(\omega)|^2}{\eta_0} \sigma_t(\omega) d\omega, \quad (25)$$

where η_0 is the impedance of free space and $E(\omega)$ is the electric field that is incident on the aperture

a) A Step-Function Bound on EMP Coupling [5]

The step function can be considered as the limiting case of a double exponential pulse where the rise time (α) approaches zero ($\beta \rightarrow \infty$) and the fall time (β) approaches infinity ($\alpha \rightarrow 0$). In this case, the spectrum of the incident field, $\vec{E}(\omega)$, can be written as:

$$\vec{E}(\omega) = \frac{i}{\omega} E_0 \vec{u}_1. \quad (26)$$

By substituting the above expression for $\vec{E}(\omega)$ into equation (25), Warne and Chen [6] have shown that the following upper bound is obtained:

$$W_{tot} \leq 2 \epsilon_0 E_0^2 (\alpha_{m22} - \alpha_{e11}). \quad (27)$$

In this expression, α_m and α_e are the aperture polarizabilities.

An important aspect of this bound is that it does not require any detailed knowledge of the aperture, but only its electrostatic and magnetostatic response, in terms of the components of the polarizability tensors of the aperture. As shown in Table 2, analytical expressions are available for the polarizabilities of a variety of aperture shapes.

Table 2. Aperture Polarizabilities for Various Shapes [25].

Shape	$\alpha_{e,zz}$	$\alpha_{m,xx}$	$\alpha_{m,yy}$
Circle (diameter d)	$\frac{1}{12}d^3$	$\frac{1}{6}d^3$	$\frac{1}{6}d^3$
Ellipse*	$\frac{\pi}{24} \frac{w^2 \ell}{E(m)}$	$\frac{\pi}{24} \frac{\ell^3 m}{K(m) - E(m)}$	$\frac{\pi}{24} \frac{\ell^3 m}{(\ell/w)^2 E(m) - K(m)}$
Narrow Ellipse	$\frac{\pi}{24} w^2 \ell$	$\frac{\pi}{24} \frac{\ell^3}{\ln(4\ell/w) - 1}$	$\frac{\pi}{24} w^2 \ell$
Slot	$\frac{\pi}{16} w^2 \ell$	$\frac{\pi}{24} \frac{\ell^3}{\ln(4\ell/w) - 1}$	$\frac{\pi}{16} w^2 \ell$

*Ellipse eccentricity $e = \sqrt{1 - (w/\ell)^2}$; K and E are complete elliptic integrals of the first and second kind, and $m = e^2$.

b) Generalised Bound on Pulse Waveforms

Recently Morrow-Jones [25] has generalized the step function bound of Warne and Chen and has shown that, without making any assumptions on the character of the scatterer, or restricting the class of EMP waveforms, a bound for the total energy of a pulse of arbitrary shape is given by

$$W_{tot} \leq 2\epsilon_0 \max \left[\left| \omega^2 E(\omega)^2 \right| \right] (\alpha_{m_{22}} - \alpha_{e_{11}}). \quad (28)$$

The similarity of (28) with the Warne-Chen bound (27) should be noted. In this equation, the E_0^2 factor in the Warne-Chen bound has been replaced with

$$\max \left[\left| \omega^2 E(\omega)^2 \right| \right].$$

According to Morrow-Jones [25], the modified factor arises from applying the Holder Inequality. Morrow-Jones shows that this bound is not necessarily smaller than the Warne and Chen case.

Morrow-Jones has evaluated this bound for a number of pulse waveshapes of practical interest. A summary of some of the Morrow-Jones results is given below:

i) Double Exponential Pulse

The spectrum, $E(\omega)$, of the double exponential pulse is given by equation (2) in section 4.2.2 of this report. Using this expression, Morrow-Jones [25] has shown that

$$\max(\omega^2 |E(\omega)|^2) = \kappa^2 \left(\frac{\beta - \alpha}{\beta + \alpha} \right)^2 E_0^2 = \frac{(\alpha/\beta)^{2(\alpha/\beta)/((\alpha/\beta)-1)}}{((\alpha/\beta)+1)^2} E_0^2. \quad (29)$$

ii) Inverse Exponential Pulse

The spectrum, $E(\omega)$, of the inverse exponential pulse is given by equation (4) in Section 4.2.2 of this report. Using this expression, Morrow-Jones [25] has shown that

$$\max(\omega^2 |E(\omega)|^2) = \frac{1.16659 E_0^2 \pi^2 (1 - (\alpha/\beta))^{2(\alpha/\beta)} (\alpha/\beta)(1 - (\alpha/\beta))}{(\alpha/\beta)^{2(\alpha/\beta)} (1 - (\alpha/\beta))^2 [\cosh(4.79871 \sqrt{(\alpha/\beta)(1 - (\alpha/\beta))}) - \cos(2\pi (\alpha/\beta))]} \quad (30)$$

iii) Gamma Distribution Modulated Sine Wave

The pulse shape of a gamma distribution pulse acting as an amplitude modulation for a sine wave can be written as

$$E(t) = E_0 u(t) \kappa'(\alpha t)^n e^{-\alpha t} \cos(\omega_0 t). \quad (31)$$

Morrow-Jones [25] has shown that the spectrum of this pulse is given by

$$E(\omega) = \frac{1}{2} E_0 \kappa' \Gamma(n+1) \left(\frac{1}{(\alpha + i(\omega + \omega_0))^{n+1}} + \frac{1}{(\alpha + i(\omega - \omega_0))^{n+1}} \right). \quad (32)$$

Using this expression, Morrow-Jones [25] has then shown that

$$\max(\omega^2 |E(\omega)|^2) \approx \frac{1}{4} n^{-2n} e^{2n} \Gamma^2(n+1) \left(\frac{\omega_0}{\alpha} \right)^2 E_0^2 \text{ for } \omega \gg \alpha. \quad (33)$$

iv) Gaussian Modulated Sine Wave

The pulse shape of a Gaussian modulated sine wave can be written as

$$E(t) = E_0 e^{-(\alpha t)^2/2} \cos(\omega_0 t). \quad (34)$$

Morrow-Jones [25] has shown that the spectrum of this pulse is given by

$$E(\omega) = \sqrt{\frac{\pi}{2}} \frac{E_0}{\alpha} \left(e^{-(\omega+\omega_0)^2/(2\alpha^2)} + e^{-(\omega-\omega_0)^2/(2\alpha^2)} \right). \quad (35)$$

Using this expression in equation (25), Morrow-Jones [25] has then shown that

$$\begin{aligned} \max(\omega^2 |E(\omega)|^2) &\approx \frac{2\pi}{e} \text{ for } \omega_0 \ll \alpha, \text{ and} \\ \max(\omega^2 |E(\omega)|^2) &\approx \frac{\pi}{2} \left(\frac{\omega_0}{\alpha} \right)^2 \text{ for } \omega_0 \gg \alpha. \end{aligned} \quad (36)$$

c) Other Energy Bounds

The advantage of the Warne-Chen [5] and Morrow-Jones [25] bounds, given in (a) and (b) above, is that they do not require a detailed knowledge of the aperture other than the aperture polarizabilities. By making assumptions regarding the frequency behaviour of the aperture cross-section, a number of authors have derived bounds for the coupling for various pulse shapes. Calculation of these bounds has been based on the following methodology.

In terms of the scattering amplitude, the total energy, W_{tot} , can be written as:

$$W_{tot} = \frac{2c^2}{\eta_0} \int_{-\infty}^{\infty} |E(\omega)|^2 \text{Re}(S(\omega)) d\omega, \quad (37)$$

where the scattering amplitude, $S(\omega)$, is related to the aperture cross-section by the relationship

$$\sigma_i(\omega) = 4\pi c^2 \text{Re}(S(\omega)). \quad (38)$$

General analytical expressions for the cross-section of even the simplest aperture shapes are not available. At low frequencies [26], the cross-section is of the general form $\sigma_i(\omega) \cong \omega^4$ and is also directly related to the electric and magnetic polarizabilities of the aperture. Bethe [26] and Bouwkamp [27] have given analytical expressions for the cross-section of a small, circular aperture. At high frequencies, the aperture cross-section approaches the geometric area of the aperture and is independent of frequency and polarization. The shape of the cross-section when the wavelength of the incident wave is comparable to the size of the aperture is not well understood. Crevier and Auton [2] have proposed a general expression for the aperture cross-section that is valid over all frequencies. An approximate, piece-wise linear expression has also been given by Lee and Yang [4] for the cross-section of a narrow slot.

i) A Bound on EMP Coupling for a "One-Minus-an-Exponential" Pulse [2]

The Warne and Chen [5] bound for the energy that can be transmitted through an aperture by a "step-function" pulse has been presented earlier (equation (27)). This pulse might be expected to overestimate the energy transmitted through an aperture for a pulse with a finite rise time. Crevier and Auton [2] have investigated the effect of finite rise time on the energy that can be radiated through an aperture. To do this, they have assumed a "one-minus-an-exponential" waveform given by the equation

$$E(t) = E_0(1 - e^{-\alpha t})u(t). \quad (39)$$

The Fourier transform of equation (39) is given by

$$|E(\omega)|^2 = \frac{E_0^2 \alpha^2}{\omega^2(\omega^2 + \alpha^2)}. \quad (40)$$

In their work, Crevier and Auton [2] assumed that the aperture cross-section had the following general form as a function of frequency

$$\sigma(\omega) = \frac{\sigma_\infty \omega^4}{[(\omega - \omega_0)^2 + \sigma_0^2][(\omega + \omega_0)^2 + \sigma_0^2]}. \quad (41)$$

Using these results in (25) gave the following bound on the maximum energy that could be radiated through the aperture

$$W_{tot} = \frac{E_0^2 \sigma_\infty}{4\eta\sigma_0} \left[\frac{(\omega_0^2 + \sigma_0^2 + \alpha^2)\alpha^2}{(\omega_0^2 - \sigma_0^2 + \alpha^2)^2 + 4\sigma_0^2\omega_0^2} - \frac{2\sigma_0\alpha^3}{(\omega_0^2 + \sigma_0^2 - \alpha^2)^2 + 4\alpha^2\omega_0^2} \right]. \quad (42)$$

The three constants, ω_0 , σ_0 and σ_∞ , were determined [2] by equating this bound for $\alpha \rightarrow \infty$ to the Warne-Chen limit and ensuring that the aperture cross-section coincides with the effective area of a circular aperture at low frequencies (see [2]).

ii) A Bound on Coupling for a Rectangular RF Pulse [23]

The penetration of rectangular RF pulse through an aperture and subsequent coupling is of considerable interest because of the potential for threat from High Power Microwaves (HPM) and EM interference from on-board or nearby radars.

The following expression has been derived by Louie and Gardner [23] for the bound on the energy that can be transmitted through an aperture:

$$W_{tot} = \frac{\sigma_i(\omega_0) E_0^2}{2\eta_0} \left[2a + \frac{\sin(2a\omega_0)}{\omega_0} \right] = W_0 \left[1 + \frac{\sin(2a\omega_0)}{2a\omega_0} \right]. \quad (43)$$

Equation (43) has a clear physical interpretation. The term outside the first pair of brackets in (43) is the average power that would be transmitted through the aperture by a CW signal at frequency, ω_0 , and having amplitude, E_0 . The first term within the brackets, $2a$, is the pulse length and, when multiplied by the average power, gives a first order approximation to the total energy transmitted through the aperture. The second term represents a correction to the first term to account for the distribution of frequencies in a finite duration pulse. If the pulse is long, the correction becomes negligible.

iii) Bounds for Other Pulse Shapes

Several authors have developed general bounds for other pulse shapes in terms of scattering amplitude however these have not been reduced to a readily useable form. These include: a bound on EMP coupling for a double exponential pulse that has been developed by Warne and Chen [6]; a bound on coupling for an inverse exponential pulse that has been developed by Louie and Gardner [23]; and a bound on coupling for a damped-sine pulse [23]:

4.4.2.4 Fields Inside a Shield with Apertures

In this section, methods for determining the fields inside the barrier are discussed. The nature of the penetration of EM fields inside the barrier depends on frequency. At low frequencies (when the wavelength is large compared to the barrier and aperture dimensions), the leakage fields are quasistatic and tend to be concentrated near the apertures in the shield (see Section 4.4.2.1). At higher frequencies, each aperture acts like a radiating antenna and the radiated fields fall off slowly with distance ($1/r$). At very high frequencies, when the wavelength of the incident field becomes small compared with the barrier dimensions, the cavity inside the barrier becomes resonant and the barrier offers little if any shielding. In the following sections, each of these situations is discussed and approximate expressions are given for the calculation of the EM fields.

4.4.2.4.1 Quasistatic Leakage of Magnetic and Electric Fields Through an Aperture

a) CW Quasistatic Magnetic and Electric Field Leakage [1,28]

Quasistatic leakage fields have characteristics that are similar to the fields near a low impedance antenna. The magnetic fields are important in the coupling process. The approximate quasistatic magnetic field strength directly over a circular aperture is given by the expression:

$$H_{MSCE} \leq 1.4 \times 10^{-4} \frac{d_m^3}{\left[\left(h_m + d_m / (9 + (6h_m / d_m))^2 \right)^2 + 0.129 d_m^2 \right]^{3/2}} E_0, \quad (44)$$

where H_{MSCE} is the magnetic field, in A/m, a distance h_m meters from a circular aperture of diameter d_m meters, and E_0 is the incident electric field amplitude in V/m. The penetrating magnetic field decreases proportional to $1/h^3$ at large distances.

The electric field at the same location is given by:

$$E_{MSCE} \leq 1.1 \times 10^{-9} \frac{d_m^3}{\left[\left(h_m + d_m / (9 + (6h_m / d_m))^2 \right)^2 + 0.129 d_m^2 \right]^{3/2}} f_0 E_0, \quad (45)$$

where E_0 is the incident electric field, in V/m, and f_0 , is the frequency of the incident radiation in Hz. The ratio of electric to magnetic field strength is a function of distance from the aperture and is well below 377 Ohms at frequencies and distances of interest.

From the above equations, one can determine the minimum aperture size at a given keepout distance that limits leakage stresses to an acceptable level for each frequency band of interest.

Equipment immunity is typically expressed in terms of magnetic fields only for frequencies below 1 MHz, where direct diffusion through the shield may be more important than aperture leakage. More typically, equipment immunity is expressed in terms of incident plane-wave electric fields. RS103 in MIL-STD-461E [MIL-STD-461E, 1998] applies to electric fields with frequencies in the range 10 kHz to 40 GHz. Typical interference immunity levels range from 20 V/m and 50 V/m, to include those using COTS/NDIs.

b) Pulse Quasistatic Magnetic and Electric Field Leakage [1,28].

Quasistatic aperture leakage of a transient field with a double exponential pulse waveform produces a non-uniform field with a source impedance well below 377 Ohms. The approximate magnetic field strength is:

$$H_{MSCE} \leq 1.4 \times 10^{-4} \frac{d_m^3}{\left[\left(h_m + d_m / (9 + (6h_m / d_m))^2 \right)^2 + 0.129 d_m^2 \right]^{3/2}} E_0, \quad (46)$$

where H_{MSCE} is the magnetic field in A/m.

The corresponding electric field is:

$$E_{MSCE} \leq 4.8 \times 10^{-10} \frac{d_m^3}{\left[\left(h_m + d_m / (9 + (6h_m / d_m))^2 \right)^2 + 0.129 d_m^2 \right]^{3/2}} \alpha E_0, \quad (47)$$

where E_0 is the peak electric field of the pulse in V/m and α is the pulse rise time in sec^{-1} .

4.4.2.4.2 Radiated Aperture Leakage into a Non-Resonant Cavity [1].

Radiated leakage transports EM energy to greater distances than does quasistatic leakage. Radiating fields fall off more slowly with distance (as $1/r$) from an aperture than quasistatic fields and dominate beyond a distance of $\lambda/2\pi$ from the aperture.

a) CW Radiated Field Leakage into Non-resonant Cavities

If the aperture effective area is σ_{eff} , then the power, P_t , transmitted into the cavity is:

$$P_t = \sigma_{eff} S_i, \quad (48)$$

where S_i is the power density of the incident wave.

The power density within the enclosure at a distance, r_{eff} , from the aperture is given by

$$S_c = \frac{P_t}{r_{eff}^2} = \frac{\sigma_{eff} E_0^2}{\eta r_{eff}^2}. \quad (49)$$

Crevier has shown that the effective area for an aperture is bounded [1] as a function of frequency by:

$$\sigma_{eff} \leq 0.83 d_m^2 \times \left[\frac{(2.1 \times 10^{-8} f_0 d_m)^4}{((2.1 \times 10^{-8} f_0 d_m - 2.85)^2 + 0.42) ((2.1 \times 10^{-8} f_0 d_m + 2.85)^2 + 0.42)} \right], \quad (50)$$

where d_m is the diameter of an equivalent circular aperture in m, and f_0 is the frequency in Hz. This expression is valid for all frequencies (i.e., both above and below resonance).

The maximum field strength that equipment will be exposed to within the cavity is then given by

$$E_{MSCE} = 2.8 \times 10^{-1} \left[\frac{1}{h_m^2 + (d_m/2)^2} \right]^{1/2} \sigma_{eff}^{1/2} E_0, \quad (51)$$

where h_m is the keepout distance in m, and E_0 is the amplitude of the incident electric field in V/m. In many cases, equipment immunity levels are measured in terms of electric field strengths at a given frequency. Equipment tested for Radiated Susceptibility using RS 103 in MIL-STD- 461E must withstand an electric field strength of 20 V/m to 50 V/m. Radiating electric fields leaking through apertures are related to the maximum absorbed power of a circuit by:

$$E_{MSCE} = 2.6 \times 10^{-7} f_0 (P_{MSCE})^{1/2} \quad (52)$$

It should be noted that equation (52) gives the radiated electric field and maximum coupled power to a circuit in a non-resonant cavity. That is, a cavity where CW fields do not have significant reflections back and forth across the cavity. Calculation of the radiated fields for all CW environments determines the largest allowable aperture for a fixed keepout distance, based upon CW radiated aperture leakage coupling to equipment.

b) Pulse Radiated Field Leakage into a Non-Resonant Cavity [1]

This subsection determines the largest allowable aperture size for a given keepout distance based upon radiated aperture leakage of pulse sources coupling to internal equipment. In carrying out this analysis, a double exponential pulse (Equation (1)) is assumed.

EM pulses are broadband and consist of a distribution of frequencies. When a pulse impinges upon a barrier, the incident fields penetrate the shielding through apertures. As discussed earlier, most of the interaction energy remains near an aperture (the quasistatic field); however, some of the energy propagates far into the enclosure (the radiating field).

Radiating aperture leakage acts like a high pass filter, where lower frequencies are removed, but higher frequencies are passed. The cutoff frequency of the aperture, f_c , is inversely proportional to the equivalent aperture diameter, $f_c = 6.8 \times 10^7 / d_m$. For apertures smaller than 10 cm, this implies a cutoff frequency greater than 600 MHz. Pulses with rise rates, $\alpha \leq 10^9 \text{ sec}^{-1}$, such as HEMP and lightning, have most of their energy below about 100 MHz, and consequently penetrate most inadvertent apertures poorly.

For a double exponential pulse, the maximum radiant energy penetrating an aperture is bounded by:

$$W_{in} = 3.0 \times 10^{-12} d_m^3 E_0^2 \left[\frac{(3.3 \times 10^{-9} \alpha d_m)^2}{(3.3 \times 10^{-9} \alpha d_m)^2 + 8.54} \right], \quad (53)$$

where d_m is the diameter of the aperture in m, E_0 is the peak amplitude of the incident electric field in V/m, and α is the pulse rise rate in sec^{-1} .

4.4.2.4.3 Radiated Aperture Leakage into a Resonant Cavity.

In this section of the report, we examine the use of a power conservation approach to estimate the interior fields in a resonant cavity. This discussion largely follows the recent work of Hill et al [29] and Lee and Yang [4].

Consider a plane wave incident on a structure (cavity) with apertures. Initially we assume that the cavity is lossless except for energy re-radiated back through the aperture. This implies that the cavity walls are perfectly conducting and that there is no other absorption of energy within the cavity. In this case, steady state fields are achieved when the power, P_t , being transmitted into the cavity is balanced by the power, P_r , being re-radiated out of the cavity, that is when:

$$P_t = P_r. \quad (54)$$

If the total transmission cross-section of the aperture is σ_t , then the power, P_t , transmitted into the cavity is:

$$P_t = \sigma_t S_i, \quad (55)$$

where S_i is the power density of the incident wave.

A relationship similar to (55) can be written for the power re-radiated from the cavity. In many cases, it is necessary to express the fields inside the cavity as a superposition of plane waves and the cross-section that needs to be used is $\overline{\sigma_r}$, an average over this superposition. In general, the power leaking out of the cavity is given by:

$$P_r = \overline{\sigma_r} S_c^{ap}, \quad (56)$$

where S_c^{ap} is the power density of the field incident on the interior side of the aperture. At high frequency, the excitation of many modes in the cavity creates a complex, three-dimensional interference pattern (modal structure) with regions of high and low field intensity. The modal structure is complex and dependent on frequency and the structure and contents of the enclosure and is thus extremely hard to predict. The statistical

distribution [30] of the fields in the enclosure is, however, uniform and it is useful to define the average power density in the cavity, S_c , given by:

$$S_c = \frac{E^2}{\eta_0} = cW. \quad (57)$$

where c is the speed of light and W is the average energy density in the cavity.

The probability that the power density, S_{meas} , measured at a given point near the aperture will exceed specified power density bound, S_{bound} , is given [30] by the following equation

$$Pr ob(S_{meas} > S_{bound}) = \exp\left[\frac{-S_{bound}}{S_c}\right]. \quad (58)$$

At high frequencies, the superposition can be considered as consisting of plane waves of all incident angles and polarizations, but only plane waves that propagate toward the aperture contribute [29] to the leakage.

The re-radiated power is:

$$P_r = \langle \sigma_r \rangle \frac{S_c}{2}, \quad (59)$$

where $\langle \sigma_r \rangle$ is the average over all incident angles and polarizations, and S_c is the average power density inside the cavity.

The following relationship between S_c , the power density inside the cavity, and S_i , the power density of the incident wave is then obtained:

$$S_c = \frac{2\sigma_t}{\langle \sigma_r \rangle} S_i. \quad (60)$$

The shielding effectiveness of the cavity can be defined in terms of the ratio of the incident and cavity power densities by the following relationship:

$$SE = 10 \log\left(\frac{S_i}{S_c}\right) = 10 \log\left(\frac{\langle \sigma_r \rangle}{2\sigma_t}\right). \quad (61)$$

This shows that the shielding effectiveness of the cavity is determined solely by the ratio of the two aperture cross-sections. In many cases, σ_t is larger than $\langle\sigma_r\rangle$, and hence the shielding effectiveness is negative indicating that the interior fields are greater than the incident fields.

Using the basic definition of cavity Q together with the steady state power condition, the following expression for cavity Q is obtained:

$$Q = \frac{4\pi V}{\lambda\langle\sigma_r\rangle}. \quad (62)$$

In this expression, V is the cavity volume and λ is the wavelength. This expression shows that the average transmission cross-section, $\langle\sigma_r\rangle$, for re-radiation determines the cavity Q , and that the cavity Q increases as the aperture size decreases.

The above discussion assumes, however, that the cavity is lossless. In a practical situation, there will also be wall losses and absorption by systems inside the body that need to be taken into account if interior fields are going to be determined accurately. To control the interior fields when the barrier is resonant, it is necessary to control the absorption of power inside the cavity. Lee and Yang [4] have extended the power conservation approach to address this situation.

Assuming that the field distribution inside the cavity is uniform (ie. high frequency approximation), then the power that can be coupled to the lossy objects is given by:

$$P_a = \sigma_a S_c = \sigma_p S_i. \quad (63)$$

In this expression σ_a is the absorption cross-section that relates the power coupled to the lossy objects from the interior field strength whereas σ_p is the cross-section that relates the power coupled to the wire to the incident field strength. σ_p includes the effects of the aperture.

The total power dissipated in the cavity (including absorption in the interior, the power re-radiated, and other losses such as wall losses) is given by:

$$P_T = P_r + P_a . \quad (64)$$

For conservation of power, the following condition applies:

$$\sigma_T S_c = \sigma_t S_i . \quad (65)$$

Using the power conservation relationship, one can also write:

$$P_a = \sigma_p S_i = \sigma_t \frac{\sigma_a}{\sigma_T} S_i , \quad (66)$$

and thus,

$$\sigma_p = \sigma_t \frac{\sigma_a}{\sigma_T} . \quad (67)$$

As pointed out by Lee and Yang [4], the factor σ_a / σ_T is the fraction of the total power, P_T , being absorbed. If, for simplicity, the only loss mechanisms are absorption by the object and re-radiation through the aperture, then $\sigma_T = \sigma_a + \sigma_r$ and

$$\sigma_p = \sigma_t \left[\frac{\sigma_a}{\sigma_a + \sigma_r} \right] . \quad (68)$$

Certain limiting situations become clear. Consider, for example, the case when the absorption cross-section is large and $\sigma_a \geq \sigma_r$. In this case $\sigma_p \cong \sigma_t$ which indicates that essentially all of the energy being transmitted through the aperture is absorbed in the interior.

4.4.3 Aperture Penetration and Cable Coupling

4.4.3.1 Quasistatic Coupling to Interior Cables

a) CW Quasistatic Coupling to Interior Cables [1]

CW quasistatic coupling to wires or cables running near an aperture is considered first. An incident electric field induces surface currents on the exterior of the shield. An aperture in the shield disrupts the flow of current, and quasistatic fields leak inside the shield near the aperture. These fields induce an electromotive force (emf) on wiring that runs near the aperture. Induced Voltage is strongest for a wire running parallel to the shield and directly over the aperture. For a wire running parallel to a shield at a distance h , and passing directly over a circular aperture of diameter d , quasistatic fields induce a peak emf on the wire:

$$V_{\max} = 2.2 \times 10^{-9} \left[d_m^3 / (h_m^2 + (d_m / 2)^2)^{1/2} \right] [f_0 E_0], \quad (69)$$

where in this expression, V_{\max} is the peak induced emf in Volts, d_m is the diameter of the aperture in m, h_m is the keepout distance in m, f_0 is the frequency of the radiation in Hz, and E_0 is the incident electric field amplitude in V/m.

The power coupled to a load by the induced emf can also be estimated. In principal, a highly resonant antenna could absorb essentially all the power leaking through the aperture. However, to absorb an excessive amount of power, the circuit or cable must be attached to a reactive load that is tuned to the incident frequency and must have an extremely large or small resistance. Such circuits are unlikely to be found inside a shielded enclosure. For purposes of obtaining a reasonable bound on the average absorbed power, inadvertent resonant coupling is not considered and a minimum load resistance of 180 ohms is assumed.

This gives:

$$P_{\max} \leq 2.8 \times 10^{-3} (V_{\max})^2 \quad (70)$$

for the average power coupled to a load by the specified peak emf.

If the load resistance is greater than 180 ohms, a given emf induces less power. If the load impedance is much smaller, cable resistance and inductance become an important factor in limiting current flow, and power coupled to a load is still well represented by the 180 ohm assumption.

If there is the likelihood that multiple apertures will drive a cable, induced Voltages from each aperture may add in phase, creating a greater stress than that determined for a single aperture. If a wire or cable bundle crosses N seams in the EM barrier, total emf could be a factor of N times higher than from a single aperture. Allowances can

be made for multiple apertures by lowering the allowed Voltage by a factor equal to the possible number of aperture crossings. However, assuming worst case coupling at each seam crossing may be overly conservative. Also, it is unlikely that drives from multiple apertures would be in phase at the higher frequencies.

If aperture size is limited to the minimum value determined by this procedure, the shield will protect the equipment from lower frequency CW environments. The protection will likely provide a large safety margin for the lowest frequencies, which are not particularly effective at inducing emfs in cable bundles.

b) Pulse Quasistatic Coupling to Wires inside the Shield. [1]

The equations in this section determine a maximum allowable aperture diameter and minimum effective keepout zone for incident pulse radiation coupling quasistatically through an aperture to a wire. The main characteristics of a pulse are a rapid rise of field strength, followed by field decay. Even if multiple pulses are closely grouped, each pulse can be treated separately when the peak-to-peak separation is much larger than a pulse width. Relevant examples of radiated pulses include nearby lightning strikes, ESD, HEMP, non-nuclear EMP, UWB weapons and HPM.

A double exponential pulse (equation (1)) is used to define a generic pulse shape. Typical unclassified HEMP parameters are $E_0 = 54$ kV/m, $\alpha = 1.2 \times 10^9$ sec⁻¹, and $\beta = 4.3 \times 10^7$ sec⁻¹. Typical lightning parameters are $E_0 = 1.2 \times 10^4/r$ kV/m for a lightning strike r meters away, $\alpha = 6.5 \times 10^5$ sec⁻¹, and $\beta = 1.1 \times 10^4$ sec⁻¹ [MIL-STD-1795A, 1989]. Actual criteria values should be used when available.

Again, an interior wire or cable couples most strongly to the leakage pulse, which has the same time history as the incident pulse, when the wire runs parallel to the shield wall and directly over an aperture. The induced emf has a time history given by the time derivative of the pulse and has a peak amplitude:

$$V_{peak} \leq 9.6 \times 10^{-10} \left[d_m^3 / (h_m^2 + (d_m / 2)^2) \right]^{1/2} \left[\alpha E_0 \right], \quad (71)$$

where d_m is the diameter of the aperture in m, h_m is the keepout distance in m, α is the rise rate of the pulse in sec⁻¹, and E_0 is the peak incident electric field in V/m.

As was done for the CW leakage case, a reasonable bound for the power coupled to a load is made by assuming a minimum load impedance of 180 ohms. This gives:

$$W_{max} (\text{Joules}) \leq 2.8 \times 10^{-3} (V_{peak})^2 / \alpha, \quad (72)$$

For smaller loading, maximum energy is bounded by induction. Furthermore, the energy absorbed from a pulse leaking through an aperture cannot exceed the Warne-Chen bound [6].

$$W_{\max} \leq 3.0 \times 10^{-12} d_m^3 E_0^2$$

Due to the much slower rise time for lightning, a lightning strike would need to be within 30 m to produce leakage energy comparable to HEMP, and within less than 1 m to generate a comparable peak emf. One microjoule is a nominal safe level for damage and one nanojoule is the corresponding level for digital upset.

The minimum aperture diameter at a given keepout zone is determined for each pulse environment. If it is smaller than for the CW cases, it becomes the determining environment. Otherwise, the smaller aperture size required for CW leakage provides additional margin for the pulse cases. The smallest aperture size needed to provide protection from all EM environments is used to set the final specification for the shield.

If a wire is likely to run past several apertures, it might be necessary to make allowances for multiple drives. However, if the rise time of the pulse is short, as it is for a HEMP pulse, it is unlikely that the peak emfs from more than two or three different apertures on a long wire will combine in phase.

4.4.3.2 Radiative Coupling to Interior Cables in a Non-Resonant Cavity [1]

a) CW Radiative Coupling to Wires inside the Shield

The radiating power leaking through an aperture is characterized by an effective area. The effective area for an aperture is bounded as a function of frequency is given by equation (50) in Section 4.4.2.4.2.

Since the absorption cross-section for radiation with frequency, f_0 , is approximately bounded by:

$$\sigma_{\text{eff}} \leq 1.1 \times 10^{16} / f_0^2 \quad (73)$$

The maximum power that can be absorbed by any circuit element is:

$$P_{MEE} \leq 1.9 \times 10^{12} \left[\frac{1}{h_m^2 + (d_m/2)^2} \right] \left[\frac{d_m}{f_0} \right]^2 \times \left[\frac{(2.1 \times 10^{-8} f_0 d_m)^4}{((2.1 \times 10^{-8} f_0 d_m - 2.85)^2 + 0.42) ((2.1 \times 10^{-8} f_0 d_m + 2.85)^2 + 0.42)} \right] E_0^2, \quad (74)$$

where h_m is the keepout distance in m, and E_0 is the amplitude of the incident electric field in V/m. For some sensitive junctions on circuit boards, upset thresholds are around one microwatt, and damage thresholds are typically around one milliwatt.

In many cases, equipment immunity levels are measured in terms of electric field strengths at a given frequency. Equipment tested for radiated susceptibility using RS 103 in MIL-STD- 461E must withstand an electric field strength of 20 V/m to 50 V/m.

Radiating electric fields leaking through apertures are related to the maximum absorbed power of a circuit by:

$$E_{MSCE} = 2.6 \times 10^{-7} f_0 (P_{MSCE})^{1/2} . \quad (75)$$

It should be noted that equation (75) gives the radiated electric field and maximum coupled power to a circuit in a non-resonant cavity, which is a cavity where CW fields do not have significant reflections back and forth. Calculation of the radiated fields for all CW environments determines the largest allowable aperture for a fixed keepout distance, based upon CW radiated aperture leakage coupling to equipment.

b) Pulse Radiative Coupling to Wires in a Non-Resonant Cavity [1]

In carrying out this analysis, a double exponential pulse (1) is assumed. Such a pulse is broadband and the pulses are constructed from a distribution of frequencies. When a pulse impinges upon shielding, fields penetrate the shielding through apertures. Most of the interaction energy remains near an aperture, which is the quasistatic field. Some of the energy propagates far into the enclosure, which is the radiating field.

Radiating aperture leakage acts like a high pass filter, where lower frequencies are removed, but higher frequencies are passed. The cutoff frequency, f_c , is inversely proportional to the equivalent aperture diameter, $f_c = 6.8 \times 10^7 / d_m$, which for apertures smaller than 10 cm implies a cutoff frequency greater than 600 MHz. Pulses with rise rates, $\alpha \leq 10^9 \text{ sec}^{-1}$, such as HEMP and lightning, have most of their energy below about 100 MHz , and consequently penetrate typical inadvertent apertures poorly.

For a double exponential pulse, the maximum radiant energy penetrating an aperture is bounded by:

$$W_{in} = 3.0 \times 10^{-12} d_m^3 E_0^2 \left[\frac{(3.3 \times 10^{-9} \alpha d_m)^2}{(3.3 \times 10^{-9} \alpha d_m)^2 + 8.54} \right] , \quad (76)$$

where d_m is the diameter of the aperture in m, E_0 is the peak amplitude of the incident electric field in V/m, and α is the pulse rise rate in sec^{-1} .

The maximum circuit absorption of radiating pulse energy is bounded by

$$\begin{aligned}
 W_{\text{circ}} (\text{Joules}) \leq & 3.9 \times 10^{-15} \left[\frac{d_m^2}{h_m^2 + (d_m/2)^2} \right] d_m^3 E_0 \\
 & \times \left[(3.3 \times 10^{-9} \alpha d_m) ((3.3 \times 10^{-9} \alpha d_m)^2 + 8.12) + 2.44 \times 10^3 (3.3 \times 10^{-9} \alpha d_m)^6 \right] \\
 & / \left[((3.3 \times 10^{-9} \alpha d_m)^2 + 8.12)(1 + 81(3.3 \times 10^{-9} \alpha d_m)^4) \right] , \tag{77}
 \end{aligned}$$

where h_m is the keepout distance in m.

4.4.3.3 Radiative Coupling to Interior Cables in a Resonant Barrier [31]

a) A Bound on Coupling to a Wire Inside a Lossless Barrier

Consider a plane wave incident on a barrier with apertures. Inside the cavity is a wire or cable that is connected to an electronic component such as an integrated circuit or transistor. An estimate (bound) on the maximum energy that can couple to a wire can be obtained using the power conservation approach that was used in section 4.2.4.3 to obtain the interior field inside a cavity. This estimate (bound) on the maximum energy that can couple to a wire is of interest for the determination of the likelihood of upset or damage.

Assume initially that the cavity is lossless except for the energy that is re-radiated back through the aperture and that is coupled to the wire. In this case, steady state fields are achieved when the power, P_t , being transmitted into the cavity is balanced by the sum of the power, P_r , being re-radiated out of the cavity and the power, P_w , being absorbed by the wire.

That is, when

$$P_t = P_r + P_w . \tag{78}$$

If the total transmission cross-section of the aperture is σ_t , then the power, P_t , transmitted into the cavity is:

$$P_t = \sigma_t S_i, \quad (79)$$

where S_i is the power density of the incident wave.

Relationships similar to (79) can be written for the power re-radiated from the cavity and the power absorbed by the wire. In these cases, it is necessary to recognise that the field inside the cavity is a superposition of plane waves and the cross-section that needs to be used is $\overline{\sigma}_r$, an average over this superposition. The power reradiating from the cavity is given by:

$$P_r = \overline{\sigma}_r S_c. \quad (80)$$

The power that can be coupled to the wire is given by:

$$(81) \quad P_w = \overline{\sigma}_w S_c = \sigma_p S_i,$$

where $\overline{\sigma}_w$ is the absorption cross-section that relates the power coupled to the wire to the interior power density, S_c , whereas σ_p is the cross-section that relates the power coupled to the wire to the incident power density, S_i . From the power conservation relationship it is then found that

$$\sigma_p = \overline{\sigma}_w \frac{S_c}{S_i} = \sigma_t \frac{\overline{\sigma}_w}{\overline{\sigma}_w + \overline{\sigma}_r}, \quad (82)$$

and the maximum power that can be coupled to the wire can be determined by substitution into Equation (81).

b) A Bound on Coupling to a Wire Inside a Lossy Cavity

In many practical situations, objects (such as humans for example) inside the cavity (structure) may absorb RF energy and provide an additional loss mechanism. The theory presented above can be readily generalised to cover this case.

The absorbed power can be related to the cavity power density, S_c , by the relationship:

$$P_a = \overline{\sigma}_a S_c. \quad (83)$$

For conservation of power, we can write:

$$P_t = P_r + P_w + P_a, \quad (84)$$

which gives

$$\sigma_t S_i = \overline{\sigma}_r S_c + \overline{\sigma}_w S_c + \overline{\sigma}_a S_c. \quad (85)$$

Following the same procedure as above, it is then found that

$$\sigma_p = \overline{\sigma}_w \frac{S_c}{S_i} = \sigma_t \frac{\overline{\sigma}_w}{\overline{\sigma}_w + \overline{\sigma}_r + \overline{\sigma}_a}. \quad (86)$$

Substitution of expressions for the appropriate cross-sections then gives a bound on the power that can be absorbed by the wire inside the cavity.

4.4.3.4 Coupling due to Current Injected on to Shield by Penetrations

Excess currents generated on external wiring, antennas and mechanical penetrations are normally shunted to the shield exterior using protection devices such as spark gaps and metal oxide varistors (MOVs) in order to prevent excess currents from reaching the interior and damaging MSCEs. When these currents reach the shield exterior, the current spreads out over the surface of the shield. In the vicinity of the attachment point these currents can be large. Provided good engineering practices are followed (i.e., attachment points are not too close to the apertures), the limits set on effective aperture area to protect the system from coupling of the EME directly to the shield and for coupling of EMEs to external antennas and cables are normally sufficient to protect the system. Additional measures to protect against currents shunted to the shield are not normally required.

4.5 Coupling to Equipment Inside a Solid Enclosure

4.5.1 Introduction

Unified E³ protection using the E³ barrier protection method is most straightforward when the MSCE can be considered to be inside a closed shield where any aperture caused by penetrations are removed through proper shield design and the installation of protective devices at all cable and antenna entrances (MSCE inside a closed shield). Barrier performance requirements are determined from the external environmental stress, the equipment immunities and the desired margin as described

earlier (assuming that the residuals > internal sources). Reliance on a solid shield for UE³ protection greatly simplifies the design process as well as test requirements.

Many in-service systems are well represented by the "MSCE inside a closed shield" model. Communication shelters and well-shielded fixed installations are obvious examples. In addition, however, completely shielded interior zones inside systems with apertures, such as an aircraft, also fall into this category. Direct leakage of the fields through the shield material is in general small and can usually be neglected if the shield is metallic. In many of the modern systems, the new carbon composite and conductive plastic materials that are being used have much lower conductivity and direct leakage of fields through the barrier is of considerable concern. The methods outlined in this section are particularly applicable to these situations.

4.5.2 Determination of the EM Environment Inside a Closed Shield

In this section, we outline options for determining the electromagnetic fields inside the barrier zones of the system.

4.5.2.1 Barrier Shielding Effectiveness [1]

The shielding effectiveness (or transfer function) of a barrier is normally defined in terms of a magnetic and an electric shielding effectiveness which are defined in terms of the ratio of the internal fields to the external (incident) fields by the expressions:

$$SE_m = -20 \log \left[\frac{H_{int}}{H_{ext}} \right], \quad (87)$$

and

$$SE_e = -20 \log \left[\frac{E_{int}}{E_{ext}} \right]. \quad (88)$$

Shielding effectiveness (SE) is usually measured using an insertion loss method whereby the ratio of a received signal with and without the shield present is used to define shielding effectiveness. Almost all of the methods used to measure shielding effectiveness, such as IEEE 299 (1995), are variations of MIL-STD-285, (1956).

4.5.2.2 Analytical Determination of Fields Inside a Closed Shield [8,32]

4.5.2.2.1 Introduction

Penetration of external electromagnetic fields into solid enclosures occurs because the wall material has finite conductivity. The mechanism by which fields penetrate into the interior is termed *diffusion*. At low frequencies, diffusion is known to be an effective mechanism for the penetration of magnetic fields into the interior. By contrast, the shield generally provides good shielding of the electric fields at all frequencies.

Figure 8 illustrates a transient electromagnetic field, H^{ext} , incident on a closed metallic shell with conductivity σ , permeability μ , wall thickness d , enclosure diameter a , enclosure Volume V and enclosure surface S .

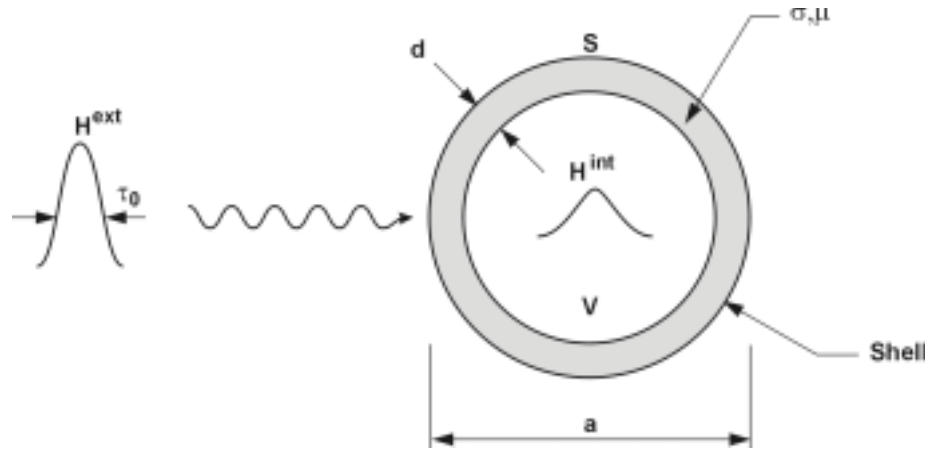


Figure 8. An External EM Field Incident on a Solid Enclosure.

The main features of the interior time domain electromagnetic field, $H^{int}(t)$, are related to the following time parameters:

- i) τ_0 , the pulse width of the incident wave,
- ii) $\tau_a = a/c$, the time to transit the enclosure,
- iii) $\tau_d = \mu\sigma d^2$, the diffusion time for the enclosure wall, and
- iv) $\tau_f = \mu_0\sigma dV/S$, the fall time of the interior pulse.

The main features of the interior frequency domain electromagnetic field, $H^{int}(\omega)$, are related to the following length parameters:

- i) d , the wall thickness,
- ii) $\delta = (2/\omega\sigma\mu)^{1/2}$, the skin depth, and
- iii) $\lambda_0 = \chi\tau_0$, the characteristic wavelength of the incident pulse.

4.5.2.2.2 Shield Design in the Frequency Domain

At low frequencies, when the wall thickness is less than the skin depth, the walls of the shield form a short-circuited loop around the enclosed volume. Currents induced in this loop by the external field oppose the incident field and result in the shielding provided. The shielding provided is dependent on the geometry of the enclosure. Appropriate transfer functions, $T_H(\omega)$, for two parallel plates, a cylindrical shell and a spherical shell are given in Table 3. The magnetic shielding effectiveness, SE_H , of the enclosure is given by the expression:

$$SE_H = 20 \log T_H(\omega) = 20 \log \frac{H^{int}(\omega)}{H^{ext}(\omega)}. \quad (89)$$

Normalised graphs showing the shielding effectiveness of spherical enclosures for a wide variety of shield parameters and frequencies are given in [32].

Table 3. Transfer Function for Solid Enclosures of Various Shapes [32].

Shape of Solid Enclosure	Transfer Function	$T_H(\omega) = \frac{H_i(\omega)}{H_o(\omega)}$
Two Parallel Plates	$\frac{1}{\cosh \gamma d + \frac{1}{2} k \sinh \gamma}$	where $k = \frac{\gamma r}{\mu_r}$ $\gamma = (j\omega\mu\sigma)^{0.5}$
Cylindrical Shell	$\frac{1}{\cosh \gamma d + \frac{1}{2} (k + \frac{1}{k}) \sinh \gamma}$	
Spherical Shell	$\frac{1}{\cosh \gamma d + \frac{1}{3} (k + \frac{2}{k}) \sinh \gamma}$	

4.5.2.2.3 Shield Design in the Time Domain

The time dependent shape of the interior field, $H^{int}(t)$, is different from that of the exterior field. The magnitude of $H^{int}(t)$ is smaller and the rise and fall times are longer.

If we suppose that the incident wave hits the enclosure at time $t=0$, then for $t < \tau_d$, the magnitude of the interior pulse is negligible. The diffusion time, τ_d , is the time required for the pulse to diffuse through the wall of the enclosure. The interior field reaches a maximum for time of the order of τ_d and for $t > \tau_d$, the interior pulse decays through energy dissipation in the walls as the result of induced eddy currents.

Graphical results for the interior field inside enclosures having the three basic shapes given earlier have been given in [32].

4.5.3 Internally Generated EMEs and Control of Cavity Q

In many cases of interest, CW radiation emitted by high frequency sources inside the enclosure bounces (resonates) many times before being absorbed. In this case, the EM field levels will build up within the enclosure until the power absorbed is equal to the power being emitted by interior equipment. These interior fields may build up to unacceptable levels in this situation. In this section of the report, we examine the control of internal EM fields resulting from internal sources through the control of the absorbing properties of the cavity. To do this we make use of a power conservation approach to estimate the interior fields in a resonant cavity following the recent work of Hill et al [29] and Lee and Yang [4].

If there is an internal CW source inside the cavity, steady state fields are achieved when the power, P_t , being transmitted into the cavity from the internal sources is balanced by the power, P_a , being absorbed within the cavity that is when:

$$P_t = P_a. \quad (90)$$

Absorption of power within the cavity results from two major causes: namely through power absorption in the cavity walls as a result of the finite conductivity of the wall materials and by absorption in lossy objects contained within the cavity. For example, in an aircraft, such lossy objects can include people, seats, wiring and so on.

At high frequency, the excitation of many modes in the cavity creates a complex, three-dimensional interference pattern (modal structure) with regions of high and low field intensity. The modal structure is complex and dependent on frequency and the structure and contents of the enclosure and is thus extremely hard to predict. The statistical

distribution [30] of the fields in the enclosure is, however, uniform and it is useful to define the average power density in the cavity, S_c , given by:

$$S_c = \frac{E_{\text{int}}^2}{\eta_0} = cW, \quad (91)$$

where E_{int} is the interior electric field, W is the average energy density of the field inside the cavity and c is the speed of light. The total energy in the cavity is then $W_T = WV$, where V is the volume of the cavity.

The power absorbed inside the cavity is related to the cavity absorption area, σ_a , by the relationship:

$$P_r = \sigma_a S_c. \quad (92)$$

From equations (90) and (92), the average power density, S_c , inside the cavity is related to the transmitted power by the simple relationship

$$S_c = \frac{P_t}{\sigma_a}. \quad (93)$$

Equation (92) shows that the energy density of the interior fields is inversely dependent on the cavity absorption area, σ_a . If interior sources result in interior fields that are too high for the installed MSCE then the problem can be alleviated by increasing the cavity absorption area. This can be accomplished, for example, by adding RF absorbing material to the interior.

The Q of the cavity is related to the cavity absorption area by the expression,

$$Q = \frac{2\pi V}{\lambda \sigma_a}. \quad (94)$$

4.6 Coupling to Printed Circuit Boards and Electronic Components

4.6.1 Background

While the general methodology outlined in Volume I of AEP-41 assumes that the immunity level of the MSCE will normally be known either through measurement or through the application of existing standards and that the allocation procedure outlined in Volume 1 can be used, in certain circumstances it may be necessary to calculate the immunity level of printed circuit boards or electronic components. This can occur, for example, during the periodic upgrades that are expected to occur during system life. With systems/platforms being kept in the field two to four times longer than previously, migration to COTS and new technologies can be expected to occur. These upgrades must be adequately E³ hardened and EMI tested. The lower bound of their immunity must be determined.

The changing nature of the electromagnetic environment (see Volume II) is also expected to result in periodic assessment of system hardening and the need for upgrades. The evolution of RF weapon technology is particularly uncertain. High frequency threats such as HPM and UWB are capable of direct coupling to printed circuit boards and electronics components because the wavelengths are short. Protection against these environments is of growing concern.

4.6.2 Coupling to Multiconductor Transmission Lines [33,34]

In the remainder of this section, a brief description of coupling to printed circuit boards and electronic components is presented.

Electromagnetic fields incident on a printed circuit board (PCB) can induce undesired signals at the endpoints of PCB traces that can cause damage or upset in the electronic components that terminate the networks. The traditional method of modeling the PCB traces is as a multiconductor transmission line (MTL). With this model (Figure 9), there are a set of (n + 1) partial differential equations representing a line consisting of n conductors and a reference conductor for the line voltages. The line is considered to be a uniform line in that the (n + 1) conductors are parallel to each other. The cross-sectional dimensions and properties of the conductors and any inhomogeneous surrounding medium are assumed to be constant along the line.

Coupling to the transmission line can be described by the Telegrapher's equations

$$\frac{d}{dz} \begin{bmatrix} V(s, z) \\ I(s, z) \end{bmatrix} = Z(s) \begin{bmatrix} V(s, z) \\ I(s, z) \end{bmatrix} + F(s, z) \quad . \quad (95)$$

where

$$Z(s) = \begin{bmatrix} 0 & -a(s) \\ -b(s) & 0 \end{bmatrix} \quad \text{and} \quad a(s) = R + sL, \quad b(s) = G + sC. \quad (96)$$

In these equations, R, L, G, and C are the per-unit-length resistance, inductance, conductance and capacitance matrices, respectively. The coefficients $V(z,s)$ and $I(z,s)$ represent the voltage and current vectors as a function of position, z, and complex frequency, s, in the Laplace domain.

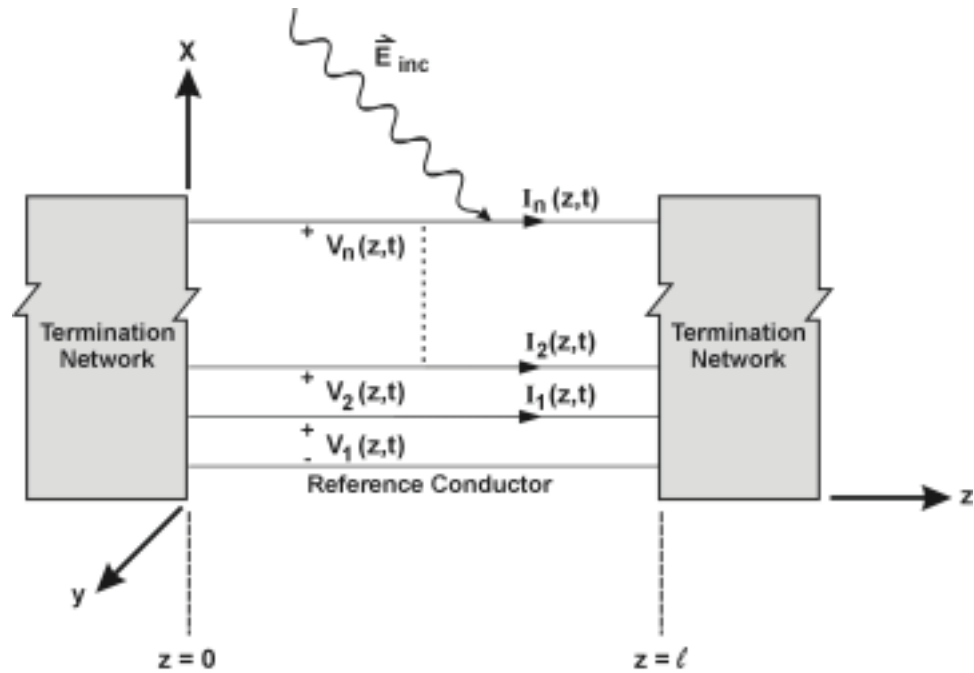


Figure 9. A Multiconductor Transmission Line with EM Field Illumination.

The effects of the incident field appear as the forcing function, $F(s,z)$, on the right-hand side of the Telegrapher's equations. These forcing functions can be expressed as:

$$F(s,z) = \begin{bmatrix} V_F(s,z) \\ I_F(s,z) \end{bmatrix}, \quad (97)$$

where $F(s,z)$ and $I(s,z)$ are integrals [34] involving the incident electromagnetic field and transmission line geometrical parameters.

To be useful for the analysis of complex circuits, it is important that the Telegrapher's equations be cast into a form so that the line voltages and currents are obtained in a time-domain form suitable for use in conventional circuit simulator such as SPICE.

A SPICE model suitable for field coupling to lossless transmission lines was proposed developed by Paul [33]. The SPICE model presented in Paul's paper models the line as a $2n$ -port independent of the terminations, and the terminal constraints (which may be nonlinear) are incorporated by connection at the $2n$ terminals of the SPICE overall model of the line. This allows nonlinear terminations to be incorporated in contrast to other methods, which rely on superposition for computing the time-domain response.

In recent work by Erdin et al [34], an efficient time domain model for incident field coupling for lossy transmission lines has been developed. Their model is based on a closed-form matrix-rational approach of the exponential matrix describing the Telegrapher's equations and a semi-analytical rational approximation of the forcing functions. This method has the advantage that the calculated Voltages and currents can easily be included in SPICE-type simulators, that lossy transmission lines can be treated and that the method is numerically efficient. Figure 10 shows the results of calculations carried out by these authors on a microstrip structure exposed to an external incident field that is connected to a complimentary metal oxide semiconductor (CMOS) inverter circuit. In addition to external fields, the circuit is driven by a Voltage source having a rectangular waveform with an amplitude of 5 Volts, switching transition time of 0.1 ns and duty cycle of 2 ns. The objective of this example was to illustrate the effect of incident fields on the circuit operation. For this purpose, (a) the circuit is initially analyzed with no external field disruption, (b) with the effect of external fields, using the proposed SPICE model. Both results are plotted in Figure 10.

The theoretical treatments developed by both Paul [33] and Erdin et al [34] assume a uniform transmission line. Solutions for non-uniform transmission lines have been presented by Baum et al [35] and Nitsch [36].

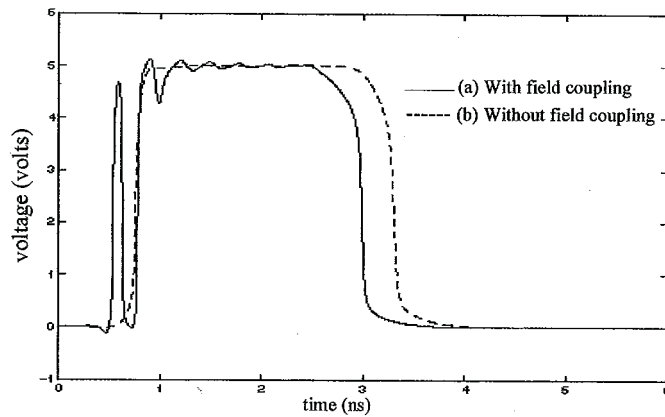


Figure 10. Output of an Inverter Circuit With and Without Field Coupling [34].

4.7 Degradation of Barrier Performance During Equipment Cycle Life

4.7.1 Background

After a system has been constructed and tested to verify that the shield and other barrier elements meet the design requirements, the system is often presumed to be immune to the EM environment. However, because the system is not routinely exposed to the EM environment, there is no indication of the real state of the EM protection following initial production tests. Experience has shown that the protection can be seriously degraded during equipment cycle life unless a deliberate effort is made to recheck and maintain the protection.

Surveillance of the EM protection requires the periodic revalidation of the protection. The purpose of the surveillance is to ensure that the EM protection remains intact and effective throughout the life of the system. Although rugged construction and attention to human factors contribute to the durability of the protection, some testing is usually required to ensure that the EM barrier has not been compromised. The testing may entail repeating the validation test or some subset of the validation test.

Visual inspection of the EM barrier is also an effective method for maintaining EM hardness. Visual inspection can often detect compromise to the barriers such as:

- Power cords and antenna leads through doors and vents.
- Doors propped open for ventilation or entrance/egress convenience.
- New equipment penetrations that have not been properly bonded to shield.
- Filters or surge arrestors that have been disconnected and bypassed.
- New monitor systems or sensors that require wiring to pass through the shield.
- Shield corrosion tears in the shield; hole cut or drilled to accommodate new or existing systems.

- Vault access panels removed (more or less permanently).

Surveillance tests need to be conducted periodically to measure leakage through the cable shield and waveguide bonds and to check the integrity of the shield, doors, and vents. The frequency of the tests will depend on the durability and ruggedness of the barrier, the cost and disruption of the tests, and the history of compliance that builds up during the life of the system. The experience gained from past tests should be used to determine future testing frequencies and to select test points.

In this section, some methods for determining the degradation of barrier performance during equipment cycle life are discussed. The subject is treated more extensively in Volume VII of AEP-41.

4.7.2 Measurement of Effective Aperture Area of a Shield

At higher frequencies, each aperture in a shield acts like a radiating antenna and the radiated fields fall off slowly with distance ($1/r$); hence, these fields can couple to MSCE located well away from the aperture. To characterize the quality of the shield, it is useful to specify an **effective aperture area**. With this approach, the penetration of radiated fields through the various apertures is equivalent to penetration through an equivalent aperture with an area, σ_a .

Measurement of the effective aperture area of a shield can be used to monitor barrier degradation. An increase in effective area indicates degradation in barrier performance and that installed equipment may be susceptible to the external EME. The effective aperture of a barrier should be measured during production and then checked regularly during system life.

A techniques for the measurement of the effective aperture, called the Single Equivalent Aperture Measurement (SEAM) method has been developed by Crevier [9]. The technique has the advantage that the measurement method is independent of cavity Q. It should be noted that different measurement methods are recommended for use for high-Q cavities and low-Q cavities.

4.7.3 Measurement of Cavity Q

As seen in earlier sections, at high frequencies, when the cavity resonates, the interior field depends directly on cavity Q which depends strongly on the absorbing properties of the interior monitoring of cavity Q is thus useful as part of the EM surveillance program. Cavity Q of a system can be measured during production and then checked regularly during system life.

Techniques for the measurement of cavity Q have been developed by Hill et al [37].

4.7.4 Coupling Measurements

Measurement of Voltages or currents induced by well-defined exterior fields on either reference or system wiring is an effective way to monitor barrier degradation. As previously, the Voltage or current on a specific reference element should be measured during production and then checked regularly during system life. If an element of the system wiring (as opposed to a specifically installed reference loop for example) is used to monitor barrier degradation, care should be taken that hardware modification hasn't altered the properties of the element.

4.8 Spacecraft Charging Effects

4.8.1 Overview of Spacecraft Charging [38]

Spacecraft charging is the process by which orbiting spacecraft accumulate electric charge from the surrounding natural space plasma. Some of the effects have been attributed to spacecraft charging include the following:

(a) Operational anomalies (i.e., telemetry glitches, logic upsets, component failures, spurious commands) caused by the coupling of electrostatic discharge (ESD) transients into spacecraft electronics.

(b) Physical spacecraft surface damage (i.e., mirrored thermal control surfaces) as a result of arc discharging.

Above approximately 90 km, a portion of the molecules comprising the Earth's atmosphere is ionized by solar radiation, and positively charged ions and free electrons are produced. This collection of electrically charged particles, known as the natural space plasma, exists in all spacecraft orbits around the Earth.

The properties of the natural space plasma are strongly dependent on altitude and latitude. Low inclination, low-earth orbit (LEO) plasma is relatively dense and has low energy whereas geosynchronous-earth orbit (GEO) spacecraft typically encounter high-energy, low-density plasma associated with geomagnetic substorms.

When a spacecraft orbits the Earth, the charged plasma particles hit the spacecraft and cause charge accumulation on exposed surfaces. This phenomenon is known as spacecraft charging. Two main classes of spacecraft charging are defined. These are classified as surface charging (external) and dielectric charging (internal or bulk). Both types can lead to ESD's that impact space missions. Usually, deep dielectric discharges are more damaging because they occur within dielectric materials or well-

insulated conductors inside a spacecraft in close proximity to sensitive electronic circuitry.

a) Surface Charging

Surface charging is produced by interactions between satellite surfaces and space plasma, geomagnetic fields, and solar radiation. These interactions cause unequal negative and positive currents to spacecraft surfaces and produce an accumulation of charge on the exposed surfaces of a spacecraft. Since different geometry and material properties form the spacecraft surface, various areas on the surface are charged to different levels. This differential charging can lead to surface arcing or ESD between satellite surfaces of different potentials. This discharge can result in direct damage to spacecraft components and result in damage or upset in onboard electronics. Differential charging is particularly common in sunlight, since sunlight tends to keep all illuminated surfaces near the plasma potential, while shaded dielectric surfaces can charge to large negative potentials.

b) Deep Dielectric Charging

Deep dielectric or bulk charging, also referred to as internal charging, is the buildup of charge on and within dielectric materials or on insulated floating conductors inside the spacecraft. Energetic electrons, with energies from approximately tens of keV to several MeV, can penetrate the surface of the spacecraft and deposit charges inside. Deep dielectric charging depends on four factors: the environment, the shielding thickness of the spacecraft, and the characteristics and shape of the charged material. When the rate at which the energetic electrons deposit on the surface or embed inside a bulk dielectric is greater than the rate at which the charge leaks out, the electric field begins to increase in magnitude. Once the generated electric field reaches the breakdown threshold of the dielectric, an arc discharge occurs. The effects of arc discharges can be very detrimental to spacecraft and spacecraft systems.

4.8.2 The Significance of Spacecraft Charging Phenomenon

For 25 years, spacecraft charging has been researched, and an abundant case history has been documented [39] of spacecraft failures and anomalies attributed to this phenomenon. Modern electronic systems, which utilize low voltage and low currents and are packed into small areas, are more sensitive to space charging effects than older generation equipments. Additionally, with spacecraft flying at higher inclinations and in polar orbits, charging caused by high-energy particles becomes significant. The increased use of dielectric thermal coatings and composite spacecraft structures not only increases the risk of spacecraft charging, but also results in increased arc discharge damage to surfaces and thermal control coatings. For these reasons,

protection of space assets against spacecraft charging effects is becoming increasingly important.

Design guidelines for assessing and controlling spacecraft charging effects are available [39]. The normal ESD protection procedures of grounding, use of conductive exterior surfaces, shielding and filtering are recommended. MIL-STD-1541 can be used for testing.

4.9 Unification of Electromagnetic Environments and Effects

4.9.1 Introduction

Hardening against the total battlespace electromagnetic environment has traditionally been done by considering each environment (e.g., EMP, ESD, HPM etc) individually and serially. In recent years, there has been an interest in methods for unifying electromagnetic standards and hardening procedures to simplify electromagnetic design and testing [40]. Expected benefits from a unified approach include reductions in costs and time to design, implement and test the required hardening as a result of fewer standards and handbooks and through the avoidance of test redundancies.

Unification is the concept of considering the totality of battlespace EMEs and their E^3 at all points in the hardening program. This approach is particularly well suited to be used when the barrier protection concept (electromagnetic topological decomposition concept) [40] has been adopted. Topological decomposition subdivides a problem into a set of volumes (or localized areas) through which the electromagnetic energy propagates and surfaces through which it penetrates [8] [41].

The prime level of unification occurs at the barrier. Unification involves setting one set of requirements for the EM barrier that addresses all of the electromagnetic effects. Use of the barrier protection concept leads to unification by allowing validation by testing the EM barrier rather than subjecting the system to every EM environment.

It is also possible to consider other levels of unification as well. When applying UE^3 , it may be possible to combine time or frequency EMEs together to simplify analysis and testing, to reduce the number of the associated standards and handbooks and, thereby, reduce cost. In defining the unified environment, it is usual to subdivide the environment into two categories: wideband and narrowband emissions (or impulsive and continuous). It is often the case that a given environment may be specified with some parameters that may vary within some limits. For instance, a narrowband emission may be defined by specifying a range for its carrier frequency or a wideband impulse by a range for its rise time and duration. Ideally, a design method should allow for such a type of specification. The coupling mechanisms of the EME may take many

forms, such as coupling through intentional receptors (antennas), currents induced in cables, coupling through shields and apertures, etc. As described earlier, coupling can be described in terms of stress transfer functions. The stress transfer function may be linear or non-linear.

For many years, overlaying all of the relevant threats and taking the maximum level at each frequency have unified CW threats. This produces a worst-case environment envelope. By contrast, impulsive threats have always tended to be handled separately. Because of the fundamental differences between impulsive and continuous threats, for most practical situations, they need to be handled separately although, ideally, they would be combined. This ideal situation is unlikely to be realized in practice.

In principle, the impulsive EM environments can be unified by adding all individual environments together ($\Sigma e(t)$). This would unquestionably result in a unified environment that would adequately test the system. Unfortunately, the exact definition of some environments is not always known, but rather they are defined by some parameters, which vary within some limits. Using the superposition property of the transform, $\Sigma e(t) \equiv \Sigma E(f)$, the problem can be solved in frequency domain instead. The various environments are not synchronous; therefore taking the maximum of all spectra (or the envelope of the possible spectra if an environment has some varying parameters) instead of adding them defines the spectrum of the unified environment. It would seem that any waveform whose spectrum meets or exceeds this composite spectrum would be adequate to test the system. It can be shown, however, that some aspects of the system such as particular failure modes may dictate the choice of the composite waveform for test purposes. For test purposes, the minimum phase condition [42] is often used for waveform reconstruction. The minimum phase condition guarantees causality, results in early delivery of the electromagnetic energy and probably maximizes some of the commonly used waveform norms such as peak amplitude and peak derivative.

The coupling mechanisms of the EME may take many forms, such as coupling through intentional receptors (antennas), currents induced in cables, coupling through shielding barriers and apertures, etc. The propagated electromagnetic signals reaching sensitive components may upset or permanently damage them. In order to properly estimate the system susceptibility, it is important to understand how this energy interacts with electronic components to cause failure.

Electromagnetic signals can be described in terms of several physically significant parameters. These parameters include the energy and power spectra as well as various waveform norms that define the signal (e.g., the total energy of the signal, its peak value, its duration, and its maximum rate of change). The physical mechanism that causes failure can depend on several of these parameters. Also, for a given

device, the failure mechanism may be different depending on whether upset or damage is considered. The discussion below shows two possible definitions of the threshold curves, one based on a level sensitivity and the other on a power-duration (energy) relationship.

Upset Threshold: The upset threshold is defined as the minimum signal that will cause a system malfunction, but for which no permanent damage or degradation occurs. Upset thresholds are typically level-sensitive, that is an upset will occur anytime a signal exceeds the threshold, given in Volts or amps. This threshold may be frequency-dependent, hence dependent on the transient duration. Many of the EMC design methodologies described in various textbooks are based on level thresholds [43] [44].

Damage Threshold: The damage threshold is defined as the minimum signal that will cause permanent damage or degradation. This is often the result of an elevated temperature causing meltdown due to the energy deposited by the pulse. For instance, many authors [26] have related the power a semiconductor may safely absorb to the pulse duration. For short pulses, the energy is deposited adiabatically and failure is determined solely by the total energy content of the pulse. For longer pulses, some of the heat dissipates to the surrounding medium resulting in more power being tolerated before breakdown. For even longer pulses, a steady-state regime is established and the failure level becomes related to peak power instead of total energy. A good model based on the thermodynamics of semiconductor junction meltdown was developed by Wunsch and Bell [24]. This type of interaction is not usually taken into account by the classical EMC methodologies.

In the remainder of this section, we outline some of the approaches that have been developed for the unification of E^3 protection.

4.9.2 The QSTAG-1051 Approach to Unification [45]

4.9.2.1 Overview of the QSTAG-1051 Approach

In the approach recommended in QSTAG-1051 and discussed in AEP-41, Volume I, barrier performance requirements are derived in terms of attenuation as a function of frequency. Figure 11 illustrates this general approach for the derivation of barrier performance requirements. Figure 12 illustrates the unification of the barrier performance requirements for each barrier to define a single performance requirement that covers all applicable immunities and EMEs. In the QSTAG-1051 approach, the following steps are taken:

Step 1: EME/Immunity Combination. In this step, each EME/immunity combination is first addressed individually as shown in Figure 11. Each individual immunity and

EME is expressed as a frequency dependent magnitude. For transient EMEs and immunities, this requires a Fourier Transform. The magnitudes of narrow-band immunities and EMEs can be used directly.

Step 2: Design Margins. The margin is also expressed as a frequency dependent magnitude that is usually a constant function of frequency, but can be varied as a function of frequency by the designer. The designers can also choose different margins for each EME/immunity combination. For example, one margin can be used for nearby lightning and a different one for EMP.

Step 3: Residual and Performance Requirements. For each immunity, the allowable residual is calculated by subtracting the margin from the immunity. This is done at each frequency, and it results in an allowed residual for each immunity as a function of frequency. After the magnitude of each residual and EME has been expressed as a function of frequency, the performance requirement for each EME/immunity combination can be determined. This is done for all shields and penetration ports. The performance requirement for each combination is the ratio of the EME to the allowed residual. Since the ratio is calculated as a function of frequency, it provides an attenuation requirement as a function of frequency for each EME/immunity combination for each port. When the quantities are expressed in logarithmic terms (e.g., dB as function of frequency), the ratio becomes a difference.

Shield performance requirements are derived using direct application of the procedure shown in Figure 2. This is accomplished for the externally generated EME's radiated components in combination with each MSCE immunity to derive the corresponding internal radiated residuals. Performance requirements are first determined for the individual radiated EME/immunity combinations – both transient and narrow-band. This provides shield attenuation as a function of frequency for each radiated EME/immunity combination.

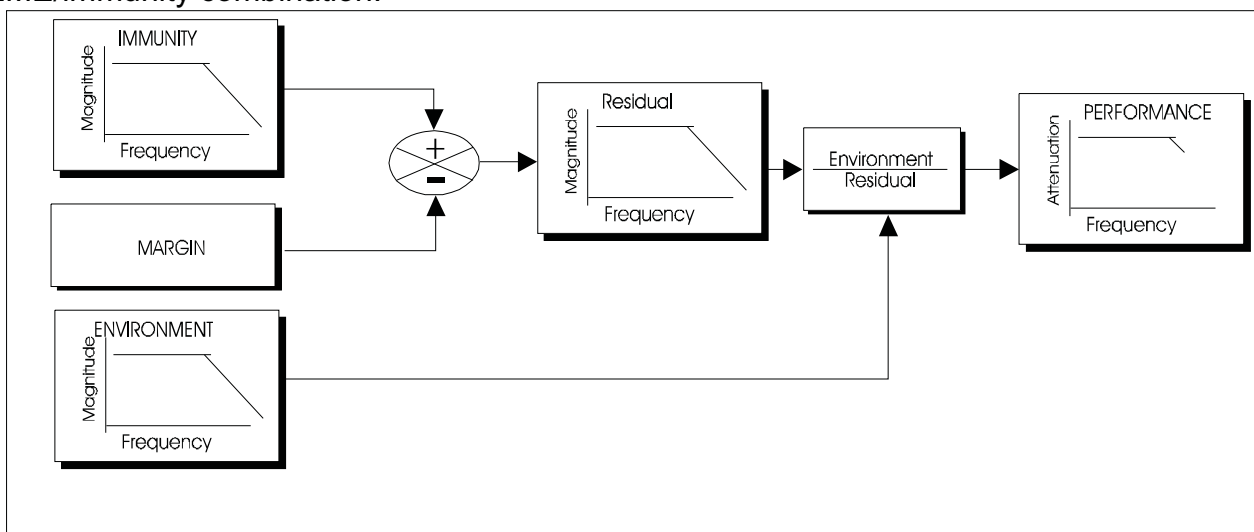


Figure 11. General Approach to Deriving Performance Requirements.

Penetration port (cable and antenna entrances) barrier requirements are derived for the conducted component of the externally generated EMEs using the general procedure shown in Figure 11 adapted to the conducted EME/immunity combinations. To apply this procedure, the conducted penetrations are represented as Thevenin or Norton equivalent circuits. Each equivalent circuit is related to a single penetration port driven by a single conducted EME. The source term is a function of the coupling of each EME to the corresponding penetration. The impedance is a function of the physical configuration of the penetration. Procedures for deriving the equivalent sources from the externally generated EMEs and penetration port physical configurations are described in QSTAG-1051.

Unification is the process of deriving a single set of performance requirements covering the EME/immunity combinations for each enclosure and penetration port. When the performance requirements are met, coverage is provided for the entire constituent EMEs. Therefore, a barrier that meets the performance requirements can be used to provide coverage for all the battlespace EMEs. It is not necessary to provide separate protection for the individual EMEs.

The first step in the unification process is to develop a unified performance requirement for each EME unified across all the immunities that apply to that EME. This procedure is shown in Figure 12. Once the EME specific performance requirements have been obtained, the next step is to unify over all the EMEs. Taking the maximum value at each frequency from the EME specific performance requirements derives the unified performance requirement covering all the EMEs. This results in a unified set of performance requirements that covers all the battlespace EMEs. Barrier protective devices (enclosure and penetration ports) that meet these requirements will provide coverage for all battlespace EMEs considered. It is not necessary to provide individual protective devices for the separate EMEs. This

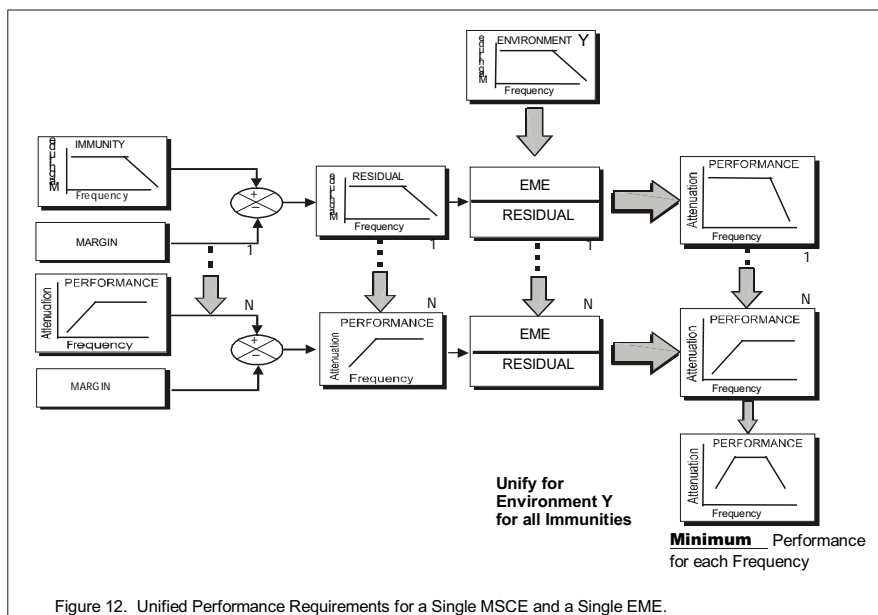


Figure 12. Unified Performance Requirements for a Single MSCE and a Single EME.

procedure is illustrated in Figure 13.

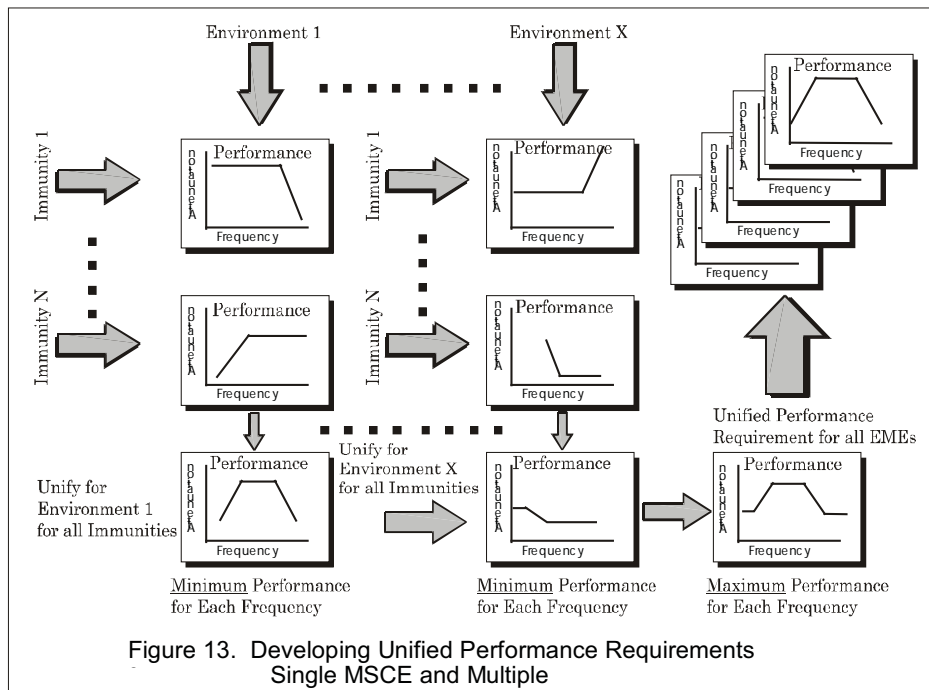


Figure 13. Developing Unified Performance Requirements
Single MSCE and Multiple

4.9.2.2 Comments on the QSTAG-1051 Approach

The UE³ approach detailed in QSTAG-1051 is simple and straightforward and should work well for designing many of the elements of well-shielded systems, such as communications shelters. Certain elements of this approach need to be taken into consideration if it is to be taken into general use.

Some particular points to note are as follows:

- a) The frequency domain approach that has been adopted is only applicable for the design of linear barrier elements such as shields and filters. Non-linear elements, such as terminal protection devices, cannot be specified by this method. Analysis in the time domain must be used in this case.
- b) Care needs to be taken to ensure that there is a proper match between the transient immunities and transient EMEs that are specified. Because only spectral magnitude information is retained in the analysis, details of time behavior are lost. It cannot be assumed that, because an immunity that has been specified for one environment covers the same frequency spectrum as another environment, that it can be used to cover both. Time behavior is important for determining if damage or upset will occur.
- c) Use of the QSTAG-1051 approach to structures with apertures needs to be carried

out with caution. While the QSTAG-1051 procedures for specification of linear barrier elements, such as the outer shield, are correct, the procedures do not specifically recognize that the protection requirements are dependent on position inside the barrier. In particular, failure to recognize that low frequency fields are concentrated in the vicinity of apertures can result in over specification of the barrier. The concept of "keep-out" distance is useful in this case.

d) It should be recognized that the transient behavior of resonant barriers can not be treated by the QSTAG-1051 approach.

4.9.3 Use of Waveform Norms for Unification

4.9.3.1 Overview

Another approach to unification is through the use of waveform norms [46]. Waveform norms provide a quantitative description of the important characteristics of a time domain waveform. These norms can be used to compare different transient stresses. Norm attributes of a waveform are usually written as

$$N = \|f(t)\|. \tag{98}$$

To qualify as a norm attributes, the scalar quantity N must have certain properties [46]. In particular, the norm must be a non-negative real number, must be proportional to the waveform-scaling factor and must obey the right-triangle rule.

There are five waveform norms that have been shown to be significant in comparing waveforms. These are:

$$N_1 = |f(t)|_{\max} \quad \text{Peak Amplitude ,} \tag{99}$$

$$N_2 = \left| \frac{df(t)}{dt} \right|_{\max} \quad \text{Peak Derivative ,} \tag{100}$$

$$N_3 = \left| \int_0^t f(t) dt \right|_{\max} \quad \text{Peak Impulse ,} \tag{101}$$

$$N_4 = \int_0^{\infty} |f(t)| dt \quad \text{Rectified Impulse , and} \tag{102}$$

$$N_5 = \left\{ \int_0^{\infty} [f(t)]^2 dt \right\}^{1/2} \quad \text{Root Action Integral .} \tag{103}$$

These five waveform norms provide a description of the size of the waveform, $f(t)$. The first element, N_1 , is the peak amplitude of the waveform. This quantity is often related to digital circuit upset. N_2 is the peak value of the derivative of the waveform, which describes the maximum rate of change of the waveform, which is related to mutual coupling. N_3 measures the cumulative extent to which the area under a positive (or negative) oscillation is greater than the previous negative (or positive) swing. N_4 measures the total absolute area under the waveform and N_5 gives the area under the square of the waveform, which is related to total energy content. It should be noted that some physical phenomena, such as dielectric breakdown or semiconductor damage, are related to more than one norm. Both dielectric breakdown and semiconductor damage normally depend on a combination of signal amplitude and duration for example.

Waveform norms are useful for defining the properties that a **"substitute waveform"** must have. A substitute waveform is a waveform that can be used as a substitute for a specific threat waveform and that meets certain criteria. If a system or equipment under test is not damaged or upset by the substitute waveform, it is assumed that the system or equipment will also be immune to the original threat waveform. The criteria for a substitute waveform are usually expressed in terms of waveform norms. The general criteria are that the substitute waveform must have waveform norms, N_1 to N_5 , which meet or exceed the corresponding norms of the threat waveform. Sometimes a subset of the 5 norms are taken [40], for example, the peak amplitude, peak derivative and root action integral together with the specification that the absolute value of the amplitude of the frequency spectrum of the substitute waveform exceed that of the threat waveform at all frequencies.

For a substitute threat waveform function, $F_T(t)$, and a substitute waveform, $F_S(t)$, the norm substitution criteria can be expressed by the equations:

$$N_i^S \geq N_i^T \quad i = 1 \text{ to } 5 . \quad (104)$$

The spectral bounding criteria can be written:

$$|f_S(\omega)| \geq |f_T(\omega)| , \quad (105)$$

for all values of ω , where $f_S(\omega)$ and $f_T(\omega)$ are the Fourier transforms of the time domain waveforms, $F_S(t)$ and $F_T(t)$.

Norms can be used in the unification process through the introduction of the concept of

a **"combination waveform"**. A combination waveform is similar to a substitute waveform except that it is used to replace multiple radiated or conducted threats. If a system or equipment under test is not damaged or upset by the combination waveform then it is also considered to be immune to the threat pulses covered by the combination. For multiple transient threat waveforms, $F_{Tj}(t)$, where $j = 1$ to n where n is the number of transient waveforms, the combination waveform, $F_C(t)$, covers all of the threat waveforms if the following norm substitution criteria are met:

$$[N_i^C]_j \geq [N_i^T]_j \quad i = 1 \text{ to } 5, j = 1 \text{ to } n. \quad (106)$$

In this case, the spectral bounding criteria can be written:

$$|f_C(\omega)| \geq |f_{Tj}(\omega)| \quad j = 1 \text{ to } n. \quad (107)$$

The combination process can be applied at various stages during the unification process, specifically for the combination of threat waveforms, for the combination of residuals and the combination of immunities.

4.9.3.2 Comments on the Norms Approach to Unification

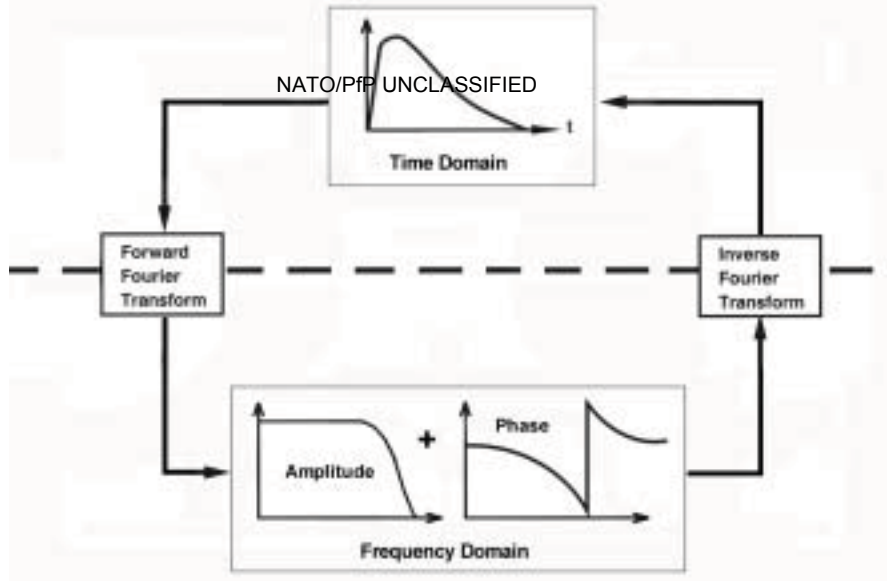
To date, the use of waveform norms has been based on the five waveform norms, N_1 to N_5 , given by equations (99) to (103). As described earlier, the general criteria for the selection of a substitute waveform are that the substitute waveform must have waveform norms, N_1 to N_5 that meet or exceed the corresponding norms for all of the electromagnetic environments being considered. In this method, the assumption is made that, if the equipment is not damaged or upset by the substitute waveform, then the equipment will also be immune to the original EM environments.

While it appears that the selection of the substitute waveform based on norms N_1 to N_5 will optimize the probability of damage, it does not appear that these norms will optimize the probability of upset. The norms that have been chosen will lead to the early delivery of energy and, as near as possible, to adiabatic conditions, which optimize the possibility of device damage. Upset, on the other hand, often depends on the coupled signal having a minimum (threshold) value and its duration. This dependence has been demonstrated in recent studies [47], [48] of the probability of upset of D-type flip-flops.

To ensure that the substitute waveform maximizes the probability of upset, it appears that additional norms need to be added. Additional norms that could be considered include:

$$N_6 = \int_0^{\infty} g_1(t) dt, \quad \text{where } g_1(t) = 1 \quad \text{if } f(t) \geq a_1 \quad (108)$$

$$g_1(t) = 0 \quad \text{if } f(t) < a_1$$



and

$$N_7 = \int_0^{\infty} g_1(t) dx, \quad \text{where } g_1(t) = 1 \quad \text{if } \frac{df(t)}{dt} \geq a_2$$

$$g_1(t) = 0 \quad \text{if } \frac{df(t)}{dt} < a_2. \quad (109)$$

N_6 gives the time that the amplitude of the signal is above a minimum threshold level and N_7 is the time that the time derivative of the signal is above a minimum threshold level. N_7 is related to the coupling of the EM environment to the circuitry and is expected to be especially important.

4.9.4 Numerical Computation of a Unified, Time Domain Waveform [49]

4.9.4.1 Overview

In this method, the generation of the unified time domain waveform is based on frequency domain processing of impulsive environments. The relationship between the time and frequency domain is shown in Figure 14.

The mathematical link between the two domains is the Fourier transform that is an analytical expression. In practice, numerical algorithms have been developed which will numerically transform measured time or frequency data to the other domain. The forward transform translates time data into the frequency domain and the inverse transform translates frequency data into the time domain. Real data is not continuously recorded but is recorded at intervals, which are normally regularly spaced. This interval must be sufficiently small to provide a faithful reproduction. The Nyquist sampling theorem mathematically defines the maximum spacing to be the period of twice the highest frequency present in the data where $t = 1/2f$.

Figure 14. Relationship between the Time and Frequency Domain.

Frequency domain data is always complex with both amplitude and phase components which are mathematically related to the real and imaginary parts of a complex number. Often the phase cannot be measured easily and must be reconstructed. Time domain data is real valued. Frequency data can be directly scaled by the instrumental frequency response. This process is known as convolution that is the mathematical process used in the time domain to achieve the same effect. The frequency domain result can be transformed back to the time domain giving the impulsive response of a given system.

In this method, the initial starting point for the definition of a unified test waveform is the selection of the required threat waveforms and the platform specific transfer function. The threat waveforms can be digitized experimental data or numerically generated using standard mathematical expressions, which represent the specific threats. The platform transfer function could initially be taken from measurements made on previous platforms as a guide to the design of a new platform and then followed with measurements from a prototype. The numerical processing involved in producing a common test waveform is shown in Figure 15.

The key step in this method is the transformation of each specific impulsive threat from the time domain to the frequency domain. This is achieved using the forward Fourier Transform (FT). An optimized algorithm known as the Fast Fourier Transform (FFT) is normally employed for this purpose and is available as a standard routine in most advanced processing languages. The platform transfer function is already in the frequency domain but will normally consist of amplitude only data and the phase must be reconstructed to obtain the true complex data. An established technique known as the minimum phase algorithm [42] is employed to achieve phase reconstruction and can be implemented in as little as six lines of MATLAB script..

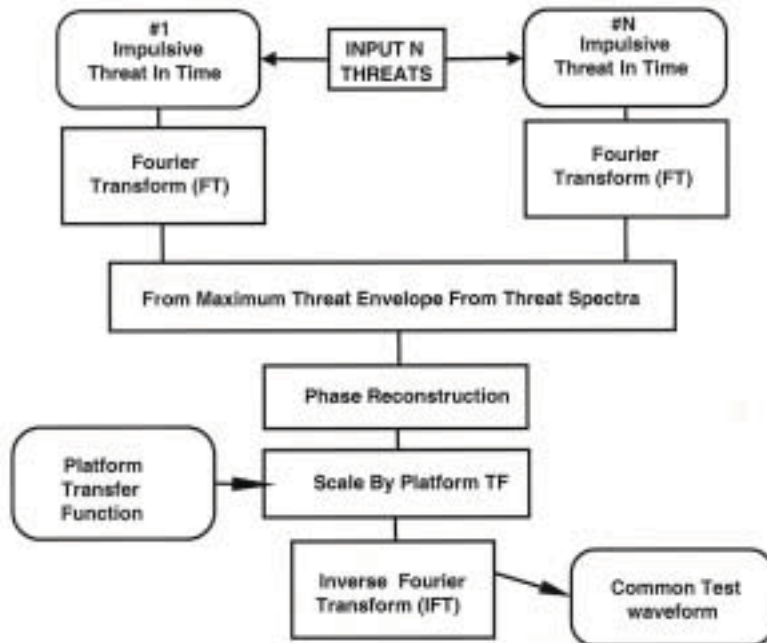


Figure 15. Computation of a Unified Waveform

When all the scaled frequency domain threats have been computed, the maximum envelope of these threats can be found. The maximum envelope spectrum is formed by taking the peak amplitude at each frequency point by searching through the stored threats. Forming a maximum envelope in the frequency domain ensures that over test is minimised. The resulting envelope is the frequency domain equivalent of the required common test waveform. Phase reconstruction and scaling by the platform transfer function is performed next. Finally a time domain common test waveform can be obtained by taking the Inverse Fourier Transform (IFT) of the scaled maximum envelope.

4.9.4.2 Comments on the Numerical Approach to Unification

Numerical computation of a unified, time domain waveform has been extensively used [49] for test purposes. As described earlier, this method is based on the use of the minimum phase condition for waveform reconstruction. The minimum phase condition guarantees causality, results in early delivery of the electromagnetic energy and probably maximizes the commonly used waveform norms such as peak amplitude and peak derivative. While it appears that numerical computation of a substitute waveform based using this method will optimize the probability of damage, for reasons discussed in Section 4.9.3.2 it does not appear that the substitute waveform derived in this manner will optimize the probability of upset.

4.9.5 Unification of Wideband and Narrowband EMEs

4.9.5.1 Overview

An alternative approach to unification has been proposed by Dion et al [50]. In this method, all of the stresses and interactions along a given path may be combined, but a distinction is made between wideband and narrowband electromagnetic quantities (signals or interactions), where narrowband is defined as a quantity demonstrating some resonant features. Wideband quantities are described by a function corresponding to the magnitude of their spectrum, denoted by $H(f)$. In the method proposed, narrowband quantities are described by two discrete values, denoted by $\hat{H}(f_r)$ and $BW_H(f_r)$, corresponding to the peak magnitude and bandwidth at the center (resonance) frequency, f_r . Note that the magnitude, $\hat{H}(f_r)$, represents the peak amplitude in time domain for signals or the maximum coupling (at the center frequency) for interactions. By extension, the magnitude and bandwidth may be described by a function, still denoted by $\hat{H}(f_r)$ and $BW_H(f_r)$, which shows the valid range where such an electromagnetic quantity may occur. Alternatively, the bandwidth may be derived, if not specified, from other parameters such as the resonance factor

(Q), damping coefficient (z) or duration (T), which can be related to one another. Wideband and narrowband signals are combined separately to form two distinct composite signals, which may be further propagated or compared against the predefined failure thresholds.

The following summarizes how a signal, $E(f)$ or $\hat{E}(f_r)$, is propagated [50] through a transfer function $H(f)$ or $\hat{H}(f_r)$ using the following interaction matrix:

Wideband signal / wideband interaction:

$$R(f) = E(f) \cdot H(f) . \quad (110)$$

Wideband signal / narrowband interaction:

$$\hat{R}(f_r) = E(f_r) \cdot \hat{H}(f_r) \cdot 2\pi \cdot BW_H \quad \text{and} \quad BW_R(f_r) = BW_H(f_r) . \quad (111)$$

Narrowband signal / wideband interaction:

$$\hat{R}(f_r) = \hat{E}(f_r) \cdot H(f_r) \quad \text{and} \quad BW_R(f_r) = BW_E(f_r) \quad (112)$$

Narrowband signal / narrowband interaction:

$$\hat{R}(f_r) = \hat{E}(f_r) \cdot \hat{H}(f_r) \cdot \frac{BW_R(f_r)}{BW_E(f_r)} \quad \text{and} \quad BW_R(f_r) = \min(BW_E(f_r), BW_H(f_r)) . \quad (113)$$

In these equations, R represents the response. $R(f)$ denotes a wideband response while $\hat{R}(f_r)$ and $BW_R(f_r)$, represent the magnitude and bandwidth of a narrowband response. This matrix shows that, for narrowband interactions, the response does not depend on the $E \cdot \hat{H}$ and $\hat{E} \cdot \hat{H}$ product alone, but also depends on the bandwidth. Note also that wideband signals may become narrowband as they are propagated.

This interaction matrix is used to model the propagation of electromagnetic signals under various conditions. Simple algorithms for obtaining important time-domain parameters, such as peak value, rise time and duration, were given and these results were then compared against failure threshold curves (level-sensitive or power/duration) to either calculate a failure index or obtain the optimal additional shielding required to harden the system.

One of the main conclusions reached by Dion et al was that it is not sufficient for a unified pulse to have the same spectral amplitude as the sum (or worst case) of all the

threats, but also that some of the time-domain parameters must be respected. In particular, it is important that the duration of the composite pulse must be consistent with the real threats as failures based on a power/duration relationship are very common. The reason for this is that system upset and damage involve complex physical processes and that no single physical parameter, such as total energy or peak value, is sufficient to determine if failure will occur. To ensure that a system is tested properly, it is not sufficient for the unified pulse to have the same spectral amplitude as the sum of all the threats, but also that some of the time-domain parameters be respected, particularly peak value and duration.

4.9.5.2 Comments on Unification of Wideband and Narrowband EMEs.

There has been very limited investigation into this method of unification. Validation of the procedures is needed before the method is considered for use.

5.0 UNIFIED EME PROTECTION ALLOCATIONS

5.1 Introduction

The purpose of the EME protection allocation process is to set protection requirements for each element of the EM barrier (i.e., shields, filters, TPDs, mechanical penetrations, and electrical penetrations). Protection allocations are performance requirements indicating the degree to which individual barrier elements must mitigate incident EM stresses. The objective of this process is to reduce leakage stresses to levels consistent with the allowed residual stresses (immunity levels minus margin). Examples of protection allocations include shielding effectiveness requirements for shields and attenuation requirements for filters. Protection allocations generally do not include detailed design information.

An outline of a general step-by-step process leading to a consistent and comprehensive set of EME protection allocations is included in the remainder of this section. An example of the application of this process is given in Annex 8.6. The material presented in this section is based on the work of Crevier [1].

5.2 Outline of the Unified EME Allocation Process

There are many steps in the EME allocation process, but each step is well defined and straightforward to implement. In the remainder of this section, we outline each of these steps and provide reference to the parts of AEP-41 where the relevant information can be found. The purpose of AEP-41 is to provide options for completing each step in the allocation process - not to provide a rigid step-by-step procedure. The procedure adopted by each NATO nation for the completion of each of these steps will

probably be different in detail depending on the tools and specific experience that each NATO nation has available to complete the process.

Step 1: Determine the External Electromagnetic Environment

Based on the mission requirement, the various EMEs that the hardware is likely to encounter are determined. The various EMEs are defined in detail in AEP-41, Volume II.

Step 2: Determine MSCE immunity.

The MSCE immunities are the levels of EM induced stresses that the MSCEs can tolerate while operating satisfactorily according to the hardware's operational requirements. MSCE immunity against both conducted and radiated EME stresses is required. Ideally, these immunity levels are established using standard test methods. When test data is not available, and the equipment has been built to existing EM standards, such as IEC-61000-4, CE Norms (EMC) and the USA's MIL-STD 461E, then these standards can be used to determine immunity bounds.

Care needs to be taken that the immunity tests chosen are representative of the residual stresses that the MSCE will encounter. It cannot be assumed that, because an immunity that has been specified for one environment covers the same frequency spectrum as another environment, that it can be used to cover both. Time behavior is important for determining if damage or upset will occur. In some cases, it is known that common immunity tests do not reproduce the known stresses very well. As an example, radiated immunity testing emphasizes the use of uniform fields while aperture leakage fields are highly non-uniform.

Step 3: Select Margins and Determine Allowed Residuals

The allowed internal residuals are the differences between the MSCE's immunity level and the selected margin. The margin allocation should be affordable, yet it must be large enough to cover immunity variations, test uncertainties, future use of MSCEs with lower immunities, COTS insertion, operational degradations, and risk. The margin is normally in the range from 15 to 20 dB. Both conducted and radiated internal residuals are important. In some cases (example ESD), the internally generated EMEs may dominate the residuals resulting from external EME stresses.

Step 4: Calculate EME Coupling to External Cables and Antennas

In order to determine the conducted stresses on external cables and antennas, it is necessary to determine how the incident EMEs couple to the system and its attached conductors. Procedures for making these calculations are given in Section 4.5 of this

report. Some of the numerical methods described in Section 4.4.2.2 could also be used. These conducted stresses are needed in order to specify the filters and transient protection devices that are needed to protect the system. Specification of filters and TPDs is discussed in AEP-41, Volume V.

Step 5: Determine Shield Allocations

Given the incident EM environments for the system, the process for determining shield allocations can begin. The process consists of determining the largest aperture size that can be allowed, consistent with the EM environments, equipment immunities and the selected keepout distance and the cavity absorption area. Determination of the shield allocations is an iterative process that involves setting preliminary specifications for the shield and then determining if the shield reduces the residuals to the allowed values.

To determine shield allocations, the following steps are required:

a) Set Preliminary Shield Performance Parameters

In order to quantify shield leakage stresses for multiple EMEs, which consist of CW and pulse environments covering a broad range of frequencies, it is necessary to specify:

- (i) the effective area of apertures in the shield,;
- (ii) the minimum effective distance between apertures and equipment,
and
- (iii) for resonant enclosures, the cavity absorption area, σ_a .

b) Determination of Interior Electric and Magnetic Fields Due to Quasistatic Leakage Through an Aperture

There are two aperture leakage components: quasistatic leakage and radiative leakage. Quasistatic leakage, so called because its strength and special distribution are independent of frequency, is concentrated near the aperture. If equipment or cabling is located near the aperture, leakage fields can couple to the equipment. Specifying an adequate "keep out" distance for the equipment from the aperture minimizes this coupling. Quasistatic leakage needs to be determined (see Section 4.4.2 of this report) for:

- (i) CW environments, and
- (ii) pulse environments.

c) Determination of Quasistatic Coupling to a Wire behind an Aperture

The quasistatic coupling to wires or cables running near to an aperture needs to be calculated so that the conducted currents can be compared to equipment immunity levels. Quasistatic coupling (see Section 4.4.3 of this report) needs to be determined for:

- (i) CW environments, and
- (ii) pulse environments.

d) Determination of Interior Electric and Magnetic Fields Due to Radiative Leakage Through an Aperture (Shield Non-Resonant)

The second component of aperture leakage is the radiated component, which is characterized by an effective area. Below resonance, radiated aperture leakage increases as the fourth power of frequency. Since it falls off more slowly with distance than the quasistatic field, proportional to $1/r$ instead of $1/r^2$, radiated leakage eventually becomes the dominant leakage component. Note that the radiated component dominates at higher frequencies because it becomes stronger, not because the quasistatic component becomes weaker. The calculation of radiative leakage is discussed in Section 4.4.2 of this report. Radiative leakage needs to be determined for:

- (i) CW environments, and
- (ii) pulse environments.

e) Determination of Radiative Coupling to a Wire behind an Aperture

The coupling of radiated fields to interior wiring or cables needs to be calculated so that the conducted currents can be compared to equipment immunity levels. Radiative coupling (see Section 4.4.3 of this report) needs to be determined for:

- (i) CW environments, and
- (ii) pulse environments.

f) Determination of Interior Electric and Magnetic Fields Due to Radiative Leakage Through an Aperture (Shield Resonant)

In many cases of interest, CW radiation entering an enclosure bounces many times before being absorbed. EM field levels build up within the volume until the power absorbed is equal to the power entering the enclosure through apertures. The

coupling of these "cavity filling" fields to these interior fields needs to be calculated. Procedures for making these calculations are given in Section 4.4.3.3 of this report.

g) Determine if Shield Performance is Adequate

In this step, the interior stresses are compared with the allowed residuals to determine if the shield performance is adequate. If the protection offered by the shield is inadequate or if it is over designed, refine the shield performance parameters in step 5a and repeat the calculations.

Step 6: Determination of Barrier Performance Allocations

Once steps 1 - 5 have been completed, barrier performance allocations for all of the barrier elements can be determined using the general procedure outline in AEP-41, Volume 1.

Often, one or two combinations of EME criteria and equipment immunity levels control the EM barrier allocations. In such cases, it may be prudent to perform trade-off analysis of the protection margin, equipment immunity levels and mitigation techniques to allow a lesser quality EM barrier to be used. The User can approve the results of the trade-off study.

For example, assuming a larger separation between the system and certain emitters can lower the RF environment in a certain frequency range. This should be done only if the cost savings associated with a lower quality EM barrier justify the risk and mission impact.

Similarly, equipment immunity levels can be increased to ensure that additional leakage stresses, from an EM barrier of reduced quality, will not reduce the protection margin to an unacceptable level. It may be possible to increase immunity levels, even for COTS equipment, without additional product development. Immunity at one test level does not necessarily imply susceptibility at a somewhat higher test level. Additional immunity testing may reveal that the equipment already has sufficient strength to achieve higher immunity levels.

6. SUMMARY

In order to be able to design an effective EM barrier, methods are needed to estimate the coupling of electromagnetic environments to the shield and to the external and internal cables, and the subsequent penetration of this energy through the barriers and to the MSCE. In AEP-41, Volume III, options for making these estimates are outlined

that will help the engineer to design and maintain effective UE³ protection. This information is required for the implementation of the procedures outlined in Volume V.

Three major topological classes have been considered in our discussion of electromagnetic coupling. These are:

- a) Coupling to Equipment Inside a Solid Enclosure,
- b) Coupling to Equipment Inside an Enclosure with Apertures, and
- c) Coupling to Exterior Equipment.

In practice, barrier topology can be much more complex. Multibarrier and nested barrier designs are often used. These more complex designs can be reduced, however, to zones of the three general topological classes described above. Various options for the calculation of electromagnetic coupling to systems falling into these three general topological classes are presented in this volume of AEP-41.

This volume also outlines the procedures that are available for the unification of electromagnetic environments and effects. A general step-by-step process leading to a consistent and comprehensive set of EME protection allocations is also outlined.

7. CONCLUSIONS

The basic philosophy of AEP-41 is the development of an approach to achieve balanced UE³ protection and maintain it throughout the operational life of the equipment. The method defined to achieve balanced UE³ protection is based on the use of the EM barrier protection concept whereby EM barriers are used to enclose mission and safety critical electronics (MSCE) that have inadequate electromagnetic immunity to enable them to survive the operational EM environment. The MSCEs may be located within a single compartment or distributed internally and/or externally to the system/platform.

Determination of the barrier performance requirements, involves a process of balancing the externally and internally generated EME stresses, the MSCE immunities, and the margin selected to control risk. The engineering trade studies necessary to achieve this balance are called the allocation process, which is usually iterative and serves as a risk management tool. To carry out the allocation process, procedures are needed for the calculation of the stress transfer function of the barriers, given physical parameters such as size, material properties and aperture dimensions, and for the calculation of the conducted currents on exterior and interior cables to ensure that the internal residual fields and currents are low enough to ensure MSCE survivability. These phenomena are termed **electromagnetic coupling**. Procedures for making these electromagnetic coupling calculations are outline in this volume of AEP-41.

AEP-41, Volume IV outlines options for determining the coupling of external and internal electromagnetic fields to antennas, cables, circuit board traces and components. This information is required in order to use the methodology given in AEP-41, Volume I.

8. ANNEXES

8.1 References

1. W.F. Crevier, "Unified EME Protection Allocations", unpublished report written for USANCA. Reproduced with the permission of R.A. Pfeffer, USANCA.
2. W.F. Crevier and J.R. Auton, "An improved limit for the energy radiated through an aperture by a finite rise time pulse", JAYCOR Report SB 92-007, 1992.
3. K.S.H. Lee, "Relations between electric and magnetic polarizabilities and other related quantities", *Radio Science*, 22, 1235 (1987).
4. K.S.H. Lee and F-C. Yang, "Trends and bounds in RF coupling to a wire inside a slotted cavity", *IEEE Trans. on EMC*, 34, 154 (1992).
5. L.K. Warne and K.C. Chen, "A bound on EMP coupling", *IEEE Trans. on EMC*, 32, 217 (1990).
6. L.K. Warne and K.C. Chen, "A bound on aperture coupling from realistic EMP", *IEEE Trans. on EMC*, 36, 149 (1994).
7. "EMP Engineering Design Principles", Bell Laboratories, 1975.
8. K.S.H. Lee (Ed.), EMP Interaction: Principles, Techniques and Reference Data, Hemisphere Publishing Corp., Washington, 1986.
9. W.F. Crevier, "Single Equivalent Aperture Measurement (SEAM): A New Approach to characterizing shielding effectiveness", JAYCOR Report SB93-003, 1993.
10. R. Perez, "Computational Methods in Electromagnetic Compatibility", in *Handbook of Electromagnetic Compatibility*, Academic Press, Inc., San Diego, California 1995.
11. E.K. Miller, "A Selective Survey of Computational Electromagnetics", *IEEE Trans. On Antennas and Propagation*, 36, 1281 (1988).
12. T. Hubing, "Survey of Numerical Electromagnetic Modeling Techniques", Report # TR91-1-001.3, University of Missouri-Rolla, 1991.

13. R.F. Harrington, "Field Computation by Moment Methods", The Macmillan Co., New York, 1968.
14. Moore J., Pizer R., eds., "Moment methods in electromagnetics: techniques and applications", Research Studies Press, 1984.
15. Miller E.K., Medgyesi-Mitschang L., Newman E.H., "Computational electro- magnetics: frequency domain method of moments", IEEE Press, New York, 1992.
16. G.J. Burke and A.J. Poggio, "Numerical Electromagnetic Code (NEC) - Method of Moments", Naval Ocean Systems Center, NOSC Tech. Document 116, 1981.
17. S. Kashyap, unpublished results.
18. A. Taflove and S. Hagness, "Computational Electromagnetics: the finite difference time domain method", Artech House, London, 2000.
19. MSC/EMAS Finite Element Software, MacNeal-Schwendler Corp.
20. MAXWELL Finite Element Software, Ansoft Corp.
21. P.B. Johns, "A Symmetrical Condensed Node for the TLM Method", IEEE Trans. Microwave Theory Tech., MTT-35, 370 (1987).
22. W.J.R. Hoefer, "The Electromagnetic Simulator: A Dynamic Visual Electromagnetic Laboratory Based of the Two-Dimensional TLM Method", Wiley and Sons, England, 1991.
23. C.L. Gardner and A. Louie, "Use of Energy Bounds to Estimate Fields and Coupling Inside a Cavity with Apertures", DREO Report # 1261, 1995.
24. D.C. Wunsch and R.R. Bell, "Determination of threshold failure levels of semiconductor diodes and transistors due to pulse Voltages", IEEE Trans. On Nuclear Science, Vol. NS-15, No. 6, 1968.
25. J. Morrow-Jones, "Bounds on EMP Energy Through an Aperture", JAYCOR Report SB02-008, August 2002.
26. H.A. Bethe, "Theory of diffraction by small holes", Phys. Rev., 66, 163 (1944).
27. C.J. Bouwkamp, "Diffraction Theory", Rep. Prog. Phys., 17, 35 (1954).
28. W. Crevier, J. Morrow-Jones and D. Krueger, "Leakage of HEMP Fields through Shields and the Implication for Hardness Validation", presentation to DTRA, November 2001.
29. D.A. Hill, M.T. Ma, A.R. Ondrejka, B.F. Riddle, M.L. Crawford and R.T. Johnk, "Aperture excitation of electrically large, lossy cavities", IEEE Trans. On EMC, 36, 169 (1994).

30. R. Price, H. Davis and E. Wenaas, "Determination of the Statistical Distribution of Electromagnetic Field Amplitudes in Complex Cavities", Phys. Rev., E-48, 4716 (1993).
31. C.L. Gardner and P.A. Hrubik, "An experimental and analytical study of the use of energy bounds to estimate the coupling to a monopole inside a cavity with an aperture", IEEE Trans. On EMC.
32. EMP Engineering Practices Handbook, NATO File No. 1460-3, November, 1989.
33. C.R. Paul, "A SPICE Model for Multiconductor Transmission Lines Excited by an Incident Electromagnetic Field", IEEE Trans. On EMC, 36, 342 (1994).
34. I. Erdin, A. Dounavis, R. Achar and M. Nakhla, "A SPICE Model for Incident Field Coupling to Lossy Multiconductor Transmission Lines", IEEE Trans. on EMC, 43, 342 (2001).
35. C. Baum, J. Nitsch and R. Sturm, "Nonuniform Multiconductor Transmission Lines", AFWL Interaction Note 516, 1996.
36. J. Nitsch, Exact Analytical Solution for Nonuniform Multiconductor Transmission Lines with the Aid of the Solution of a Corresponding Matrix Riccati Equation", AFWL Interaction Note 534, 1997.
37. D. Hill, J. Adams, M. Ma, A. Ondrejka, B. Riddle, M. Crawford and R. Johnk, NIST Technical Note 1361, 1993.
38. C.K. Purvis, H.B. Garrett, A.C. Whittlesey, and N.J. Stevens, "Design Guidelines for Assessing and Controlling Spacecraft Charging Effects", NASA Technical Paper 2361, 1984.
39. R.D. Leach, and M.B. Alexander, "Failures and Anomalies Attributed to Spacecraft Charging", NASA Reference Publication 1375, 1995.
40. G. Baker, J.P. Castillo and E.F. Vance, "Potential for a Unified Topological Approach to Electromagnetic Effects Protection", IEEE Trans on EMC, 34, No. 3, Aug. 1992.
41. C.E. Baum, "Electromagnetic topology for the analysis and design of complex electromagnetic systems", Proceedings of the NATO Advanced Study Institute on Fast Electrical and Optical Diagnostic Principles and Techniques, 1986.
42. A.V. Oppenheim and R.W. Scafer, "Digital Signal Processing", Prentice-Hall Inc., Englewood Cliffs, 1975.
43. D.R.J. White and M. Mardigian, "EMI Control - Methodology and Procedures", 4th Edition, Interference Control Technologies, 1985.

44. D.R.J. White, "Shielding Design - Methodology and Procedures", 4th edition, Interference Control Technologies, 1985.
45. QSTAG -1051, "A Unified Approach to Electromagnetic Protection", 1998.
46. R.E. Thomas and J.I. Lubell, "EMP Strength Specifications Development Using NORM Attributes", DNA Report DNA-TR-89-271, 1990.
47. R.E. Wallace, S.G. Zaky and K.G. Balmain, "Fast-Transient Susceptibility of a D-Type Flip-Flop", IEEE Trans. On EMC, 37, 75 (1995).
48. C.L. Gardner, S. Kashyap and J.A. Walsh, "A Statistical Approach For The Determination Of The Probability Of Upset Of Digital Circuits", ANTEM Conference Proceedings, Winnipeg, July 2000. pp 373-376.
49. N. Carter, "Integration of EM Environments and/or Immunities", unpublished AEP-41 Working Paper, 2001.
50. M. Dion, C. Gardner and S. Kashyap, "Hardening against a combined electromagnetic threat", AGARD Sensor and Propagation Panel Symposium on "High Power Microwaves", Ottawa, May, 1994.
51. E.F. Vance, "Coupling to Shielded Cables", John Wiley and Sons, 1978.

8.2 Definitions

1. Arc Attachment. The point of contact of the lightning flash with the vehicle so that current can flow onto the vehicle from this point.
2. Charge Transfer. The integral of the current (i) over its entire duration. $\int i dt$. (Coulombs).
3. Final Entry Point. The spot where the lightning flash channel last "enters" the vehicle (usually a trailing edge).
4. Electrically Initiated Device. A single unit, device, or subassembly that uses electrical energy to produce an explosive, pyrotechnic, or mechanical output.
5. Initial Entry Point. The spot where lightning flash channel first "enters" the vehicle (usually an extremity).
6. Internal Environment. Includes the structural current and Voltage changes with associated distribution and the aperture-coupled and diffused electromagnetic fields.
7. Lightning Flash. The total lightning events in which charge is transferred from one charge center to another within a cloud, between clouds, or between a cloud and ground. The event can consist of one or more strokes plus intermediate or continuing currents. Typically, the duration of a flash is 2 seconds or less.

8. Lightning Strike. Any Attachment of the lightning flash to a vehicle or ground facility.
9. Lightning Stroke (Return Stroke). A lightning current surge that occurs when the lightning leader makes contact with the ground or other region of opposite charge,
10. Multiple Burst. A randomly spaced series of bursts of short-duration, low-amplitude current pulses and arch pulse or pulses characterized by rapidly changing currents. These bursts may result from lightning leader progression or branching and may be accompanied by or super imposed upon a stroke or continuing current. The multiple bursts appear to be most intense at time of initial leader attachment to a vehicle.
11. Multiple Stroke. Two or more lightning return strokes occurring during a single lightning flash.
12. Swept "Flash" (Or "Strike") Points. Spots where the flash channel reattaches between the initial and final point, usually associated with the entry part of the flash channel.
13. Action Integral. A critical factor in the production of lightning damage related to the energy deposited or absorbed in a system. The actual energy deposited without knowledge of the resistance of the system.
14. Direct Effects. Any physical damage to an element's structure due to the direct attachment of the lightning channel or the flow of current through the vehicle's structures, either when the vehicle is on the ground or in flight. This includes thermal and shock wave effects on the exterior skins, coatings, or other exposed components such as windshields, nozzles, umbilical, fuel and oxidizer lines, edges, control surfaces, and engines. Damage to electrical or avionics systems or individual equipment due to direct attachment of the lightning flash to an exposed part of such a system is also termed a direct effect.
15. Indirect Effects. Voltage and/or current transients produced in vehicle electrical wiring due to lightning currents in the elements that can upset an/or damage components within electrical /electronic systems. These transients occur due to one or more coupling mechanisms, i.e., changing magnetic or electric fields and structural Voltage rises due to lightning currents in structural resistance. Thus, Voltage induced in a sensor wire harness by changing magnetic fields accompanying lightning currents in unbiblical cable shields are also called indirect effects.
16. Multipaction. An RF effect that occurs strictly in a high vacuum where RF field accelerates free electrons resulting in collisions with surfaces creating secondary

electrons that are accelerated resulting in more electrons and ultimately a major discharge and possible equipment damage.

17. Compromising Emanations. Unintentional intelligence-bearing signals that, if intercepted and analyzed, disclose the national security information transmitted, received, handled, or otherwise processed by any classified information processing system.

18. EMC. Electromagnetic Compatibility. The capability of electrical and electronic systems, equipment and devices to operate in their intended electromagnetic environment within a defined margin of safety, and at design levels of performance. This must be achieved without suffering or causing unacceptable degradation as a result of electromagnetic interference.

19. EMH. Electromagnetic Hazards. This term describes the electromagnetic environment generated by all electromagnetic sources, both frequency and time domain.

20. E³. Electromagnetic Environmental Effects. E³ is the impact of the electromagnetic environment upon the operational capability of platform, system, and equipment. It encompasses all electromagnetic disciplines, including electromagnetic compatibility, electromagnetic interference, electromagnetic vulnerability, electromagnetic pulse, electronic countermeasures, hazards of electromagnetic radiation to ordnance and volatile materials, RF weapons and natural phenomena effects of lightning and p-static.

21. EME. Electromagnetic Environment. The EME is the resulting product of the power and time distribution, within various frequency ranges, and includes the radiated and conducted electromagnetic emission levels that may be encountered. It is the totality of electromagnetic phenomena existing at a given location.

22. EMI. Electromagnetic Interference. EMI is any electromagnetic disturbance, whether intentional or not which interrupts, obstructs or otherwise degrades or limits the effective performance of electronic or electrical equipment. This is normally used to describe the threat posed by the platform's own systems, mutually interfering with one another.

23. HIRF. High Intensity Radiated Fields. This term covers the inadvertent threat posed by ground based and airborne transmitters such as radar, radio and TV transmitters. This threat is the one that is known to have caused the loss and flight control disruption of military aircraft, primarily from ground based HF transmitters.

24. RFW. RF Weapons. This term covers the deliberate use of EM energy in an attempt to disrupt a platform's mission. The use of an exo-atmospheric nuclear burst to generate NEMP could be considered as the first RFW with a continent wide effect. However, in the context of this report RFW covers all non-nuclear EM weapon concepts. RFW are currently being researched and although certain threat waveforms have been identified as being practical, new waveshapes may be used in the future.
25. Platform. A platform is a structure into which systems and equipments are to be installed e.g. ship, aircraft, building, tank, etc.
26. System. A set of equipment/modules interconnected to provide a function e.g. avionic system on an aircraft, a truck, a missile, etc.
27. Subsystem. A set of equipment/modules interconnected to provide a function, e.g. radio, cabling and antenna; fire extinguish amplifier, cabling and sensors; anti-tank missile launcher and display; etc.
28. Equipment. Normally a single electrical/electronic box, line replaceable unit or shop repairable unit. Can also be several modules that form the equipment and are not located in the same box e.g. radio, missile, flat-panel display.
29. Module. A piece of equipment that is reliant on the equipment for functionality e.g. power supply, motherboard, hard disk drive, etc.
30. Circuit. Connecting electronic components together to accomplish a function.
31. Component. Lowest assembly level or integration level consisting of two or more piece-parts, e.g., hybrids, microprocessors, analog-to-digital converter, etc.
32. Piece-part. The smallest element from which components, modules and equipments are built e.g. integrated circuit, resistor, capacitor, transistor, etc.
33. Hardware. A generic term for platform, system, subsystem and equipments
34. Aperture. An electromagnetic transparent opening
35. Upset. An impairment to a platform or system operation, either permanent or momentary (e.g., a change of digital or analog state), that may or may not require manual re-set.
36. Cable Bundle. A group of wires and/or cables bound or routed together that connect two pieces of equipments.

37. Electromagnetic Barrier. The topologically closed surface created to prevent or limit EMEs (radiated and conducted) from entering the enclosed space. The EM barrier consists of a shield and penetration port devices.
38. Electromagnetic Stress. A Voltage, current, charge, or EME that acts on equipment can caused EM stress. If the EM stress exceeds the vulnerability threshold of the equipment, mission impacting damage or upset may occur.
39. Electromagnetic Shield. A continuous metallic housing (enclosure) that substantially reduces the coupling of electric and magnetic fields into the protective volume.
40. Penetration Protection Device. The protective measure used to prevent or limit EM energy from entering the protective volume at a POE or penetration port. Common penetration port or POE protection devices include waveguides below cutoff EM closure plates and metal grids for aperture POEs, and filters and linear/non-linear devices on penetrating conductors.
41. Penetration Port of Point-of-Entry. (POE). A location on the EM barrier where the shield is penetrated and EM energy may enter the protected volume.

8.3 ABBREVIATIONS and ACRONYMS

A	ampere
Abb	abbreviation
ac	alternate current
AEP	Allied Engineering Publication
ANSI	American National Standards Institute
ARP	Aerospace Recommended Practices
CNAD	Combined National Armaments Directors
COTS	Commercial-Off-the-Shelf
CE	Conducted Emissions
CS	Conducted Susceptibility
CW	Continuous Wave
dB	decibel
DC	direct current
DEMP	dispersed electromagnetic pulse
DMS	diminishing manufacturing sources
DMSMS	Diminishing Manufacturing Sources and Material Shortages
DNA	Defense Nuclear Agency
DSL	direct strike lightning
E	environment

EED	Electro-Explosive Device
EID	Electrically Initiated Device
EM	electromagnetic
EMC	electromagnetic compatibility
EME	electromagnetic environment
EMI	electromagnetic interference
EMP	electromagnetic pulse
EMRADHAZ	Electromagnetic Radiation Hazard
EMV	electromagnetic vulnerability
ESD	Electrostatic Discharge
E3	Electromagnetic Environmental Effects
EUT	Equipment Under Test
FM	frequency modulated
GHz	gigaHertz
GZ	Ground Zero
HA	hardness assurance
HAMS	Hardness Assurance Maintenance Surveillance
HEMP	high-altitude electromagnetic pulse
HERF	Hazards of Electromagnetic Radiation to Fuel
HERO	Hazards of Electromagnetic Radiation to Ordnance
HERP	Hazards of Electromagnetic Radiation to Personnel
HIRF	High Intensity Radiated Field
HPM	high power microwave
Hz	Hertz
kHz	kiloHertz
km	kilometer
kV/m	kilovolt per meter
IEC	International Electro-Technical Commission
IEMP	internal electromagnetic pulse
kV	kilovolt
LF	low frequency
LRU	line replaceable unit
MHD	Magneto-Hydrodynamics
MOV	Metal Oxide Varistor
MHz	megaHertz
MIL-STD	Military Standard
MNFS	Maximum No-Fire Stimulus
MSCE	Mission and Safety Critical Electronics
MTS	Modernization Through Spares
NATO	North Atlantic Treaty Organization
NDI	non-developmental item
N2EMP	non-nuclear electromagnetic pulse
NSL	near strike lightning

OC	Operational Category
P	power
PARA.	paragraph
P-Static	Precipitation Static
PEL	Permissible Exposure Limit
PED	Personal Electronic Device
POE	point of entry
PNR	prompt nuclear radiation
QA	quality assurance
QC	quality control
QSTAG	Quadripartite Standardization Agreement
RE	Radiated Emissions
RADHAZ	Radiated Hazards
RF	Radio Frequency
r.m.s.	root mean square
RS	Radiated Susceptibility
SA	sustainment assurance
SAE	Standard of Automobile Engineers
SGEMP	system generated electromagnetic pulse
SREMP	source region electromagnetic pulse
ST	surveillance test
STA	stress transfer function
STANAG	Standard NATO Agreement
SUT	system under test
ms	millisecond
μ s	microsecond
UE3	Unified Electromagnetic Environmental Effects
UWB	Ultra-Wideband
USA	United States of America
V/m	volts per meter
VOL.	volume
W	watt

8.4 An Example of Unified EME Protection Allocations for Operational Class OC1, "Land Mobile Systems"

8.4.1 Introduction

Figure A1 illustrates a typical example of an OC1 system. The system consists of a communications van connected to a communications shelter by a long line. Both the van and shelter are imperfectly shielded. Both also have antennas that penetrate the shield. The specific set of EM environments we have chosen to use for this example is for illustrative purposes only. Many other environments (see AEP-41, Volume 2) could

also have been considered. The output of the EME protection allocation process is a set of requirements for an EM barrier consistent with the specified EM environment and system immunities.

The basic shielding parameter of concern is the size of the largest inadvertent aperture in the shield. This is generally expressed in terms of equivalent aperture size, which can be related to dB of shielding effectiveness, which such an aperture would achieve. Ancillary shield requirements include the minimum separation between protected equipment and possible apertures in the shield, expressed as a keepout distance, and the electromagnetic absorption properties of the protected volume, expressed in terms of a cavity absorption area.

Electrical penetrations in the shield will typically be protected with a combination of nonlinear surge arrestors and filters. The EME protection allocation for electrical penetrations consists of a limit on the leakage stresses, termed residuals, for a specified input stress. Different levels are given for pulse and CW stresses. Residual levels are selected to be consistent with equipment immunity, the selected safety margin and what can be achieved with realistic protection devices.

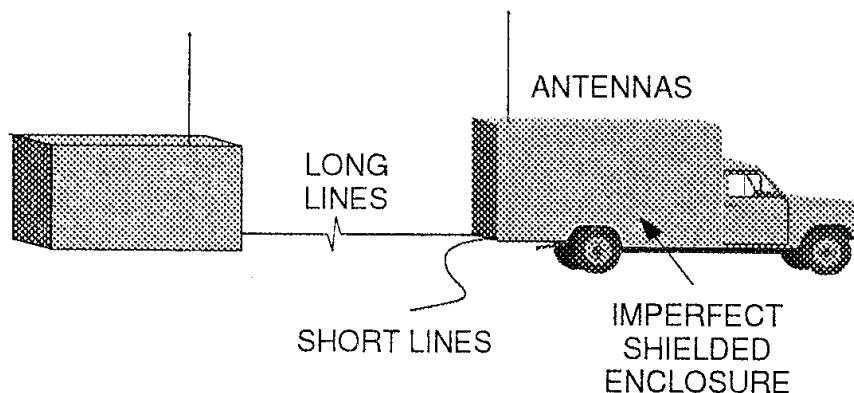


Figure A1. An Example of a Typical Land Mobile System.

8.4.2 The External EM Environment

The EM environments described in Table A1 are specified for purposes of this example only; they are not intended to be recommendations for any specific system. Actual OC1 systems may experience some or all of these environments. Possible additional EMEs, not specifically considered in this example, include ESD, radiated lightning, and various types of RF weapons. If surface or near surface nuclear bursts are concerns, the system may also have SREMP requirements. When specified, these additional EM environments are treated in a manner similar to those considered here.

Table A1. Environments Chosen for OC1 Example.

Environment	Type	Waveform	Propagation
Nearby Lightning	Natural	Pulse	Radiated and Conducted
HIRF	Electronic Operation	CW	Radiated
HEMP	Hostile	Pulse	Radiated

Lightning. Table A2 defines the criteria for a nearby lightning stroke. The current waveform for each of the three components of a strike is represented by a double exponential equation.

Table A2. Characteristics of Nearby Lightning.

Current Component	Description	$i(t) = I_0 (\epsilon^{-\alpha t} - \epsilon^{-\beta t})$ t is time in seconds (s)		
		I_0 (Amperes)	α (s^{-1})	β (s^{-1})
A	Severe stroke	218,810	11,354	647,265
B	Intermediate current	11,300	700	2,000
C	Continuing current	400 for 0.5 s	Not applicable	Not applicable
D	Restrike	109,405	22,708	1,294,530
D/2	Multiple stroke	54,703	22,708	1,294,530
H	Multiple burst	10,572	187,191	19,105,100

HIRF Environment. RF emissions arise from a variety of sources, such as radars and radio transmitters. RF environment criteria are developed by considering emitters a system will be exposed to and defining a minimum distance from the emitter to the system.

Table A3 gives peak and average r.m.s. field values for the HIRF fields.

Table A3. HIRF Environment for OC1.

Frequency Range (MHz)	Electric Field (V/m - rms)	
	Peak	Average
0.01 - 2	25	25
2 - 250	50	50
250 - 1000	1500	50
1000 - 10000	2500	50
10000 - 40000	1500	50
40000 - 45000	-	-

HEMP Environment: Three HEMP components are described in AEP-41, Volume II: early, intermediate and late time HEMP. Intermediate and late time HEMP are important only for systems connected to conductors more than a few kilometers long. In our OC1 example, it is assumed that all conductors are less than 1 km long and that only early time HEMP is considered. For the purposes of this example, it is assumed that the HEMP has a double exponential waveform of the type described in Section 4.2.2 with parameters $E_0 = 54$ kV/m, $\alpha = 1.2 \times 10^9$ s⁻¹, $\beta = 4.3 \times 10^7$ s⁻¹, and $\kappa = 1.174$. For these parameters, the rise time is 1.8 ns. For an actual system, the classified HEMP waveform given in AEP-4 would be used.

8.4.3 MSCE Immunities

It is assumed that all of the equipment to be installed in the land mobile system being discussed in this example has been qualified to meet the requirements of U.S. MIL-STD-461E (1999). Specific MIL-STD-461E requirements relevant to this example include the following:

RS 103, Electric Fields, 10 kHz to 18GHz: The purpose of this requirement is to ensure that the installed equipment will operate without degradation in the HIRF environment which results primarily from antenna transmissions located both on and off the platform. RS 105 limits for Army systems are given in Table A4.

Table A4. RS 103 Limits for Land Systems.

Frequency Range	RS 103 Limits (Volts/m)
10 kHz - 2 MHz	20
2 MHz - 30 MHz	50
30 MHz - 1 GHz	50
1 GHz - 18 GHz	50

CS 114, Bulk Cable Injection, 10 kHz to 400 MHz: The purpose of this requirement is simulate current which will be developed on system cabling when the cabling is exposed to the electromagnetic fields generated by antenna transmissions both on and off the platform. CS 114 limits for Army systems are in Figure A2. The appropriate curve is shown in Table A5.

Table A5. CS 114 Limits for Land Systems.

Frequency Range	CS 114 Limit Curve
10 kHz - 2 MHz	3
2 MHz - 30 MHz	4
30 MHz - 1 GHz	4
1 GHz - 18 GHz	4

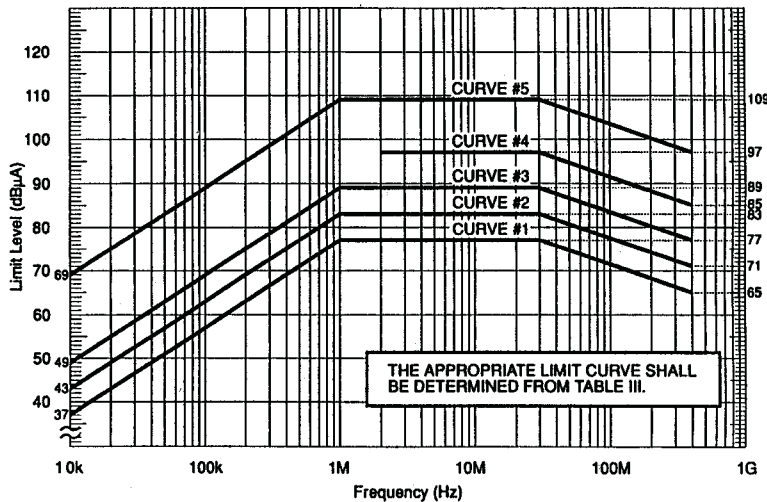


Figure A2. CS 114 Limits.

CS 115, Bulk Cable Impulse Injection, 2/30 ns: The purpose of this requirement is to protect equipment from fast rise and fall time transients that may result from platform switching operations and external transient environments such as lightning and electromagnetic pulse. The measurement waveform is shown in Figure A3.

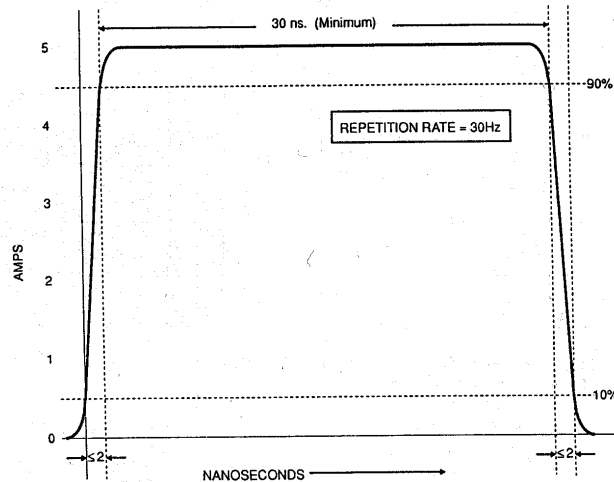


Figure A3. The CS 115 Test Waveform.

8.4.4 Margins and Allowed Residuals

Margin: For the purpose of this example, a constant margin of 10 dB is chosen.

Allowed Residual: The allowed residual is determined from the equipment immunities, given in Section 8.6.3, and the selected margin using the following equation.

Allowed Residual = Immunity - Margin

8.4.5 EME Coupling to External Cables and Antennas

In order to determine the conducted stresses on external cables and antennas, it is necessary to determine how the incident EMEs couple to the system and its attached conductors. Procedures for making these calculations, based on the bounds approach of Crevier (1), are given in Section 4.3 of this volume.

8.4.5.1 Coupling to Vertical Conductors

a) CW Coupling to the Whip Antenna

The current driven on vertical conductors by incident CW fields is bounded by equation (13) given in Section 4.3.2.1 of this volume. If we assume, for this example, that the system has a 1.5 m long whip antenna, then maximum coupling occurs at

approximately 31.75 MHz. From Table A2, it is seen that the RF environment in this frequency range is 50 V/m. Substitution of these parameters into this equation gives a maximum current for the specified HIRF environment of approximately 2.75 A.

b) Pulse Coupling to the Whip Antenna

Bounding the current driven onto the antenna by a pulse is more complicated than CW coupling. The coupled current is a mixture of decaying exponentials and damped oscillations oscillating at the fundamental resonant frequency of the antenna. Several waveform norms are used to characterize this behavior. These include: peak current; peak time derivative of the current; and, action integral. Bounds on these quantities are given in Section 4.3.2.2 of this volume.

Because of its large amplitude and fast rise time, maximum current is expected to be coupled onto the whip antenna by the HEMP environment. Taking a peak field of 54 kV/m and a rise rate of $1.2 \times 10^9 \text{ s}^{-1}$, then, from equations (14), (15) and (16), we obtain a peak current of 200 A, an action of $6 \times 10^{-3} \text{ A}^2\text{-s}$, and a peak time derivative of the current of $4 \times 10^{10} \text{ A/s}$.

8.4.5.2 Coupling to Horizontal Conductors

Typical horizontal conductors include power lines and communication cables that connect the land mobile system (Figure A1). Unlike vertical conductors, horizontal conductors are terminated at each end.

a) CW Coupling to Horizontal Conductors

The maximum current induced on a horizontal conductor by an incident EM field is bounded by equation 18 in Section 4.3.3. Based on the specified HIRF environment, the lowest frequency that is horizontally polarized is 32 MHz, with a field strength of 50 V/m. Assuming that the horizontal conductors are lying on the ground ($z_m = 0$), the induced current is less than 25 mA. With this model, the induced current increases as the height of the line is increased. Once the line is about half a wavelength high, the current is near its peak and it does not increase significantly with a further increase in height. The peak current for a wire well off the ground is about 0.2 A.

b) Pulse Coupling to Horizontal Conductors

Bounding the current driven onto a horizontal conductor by a pulse is more complicated than CW coupling. Several waveform norms are used to characterize this behavior. These include: peak current; peak time derivative of the current; and, action integral. Bounds on these quantities are given by equations (19) - (22) in Section 4.3.3 of this volume.

The HEMP environment specified here has a peak field of 54 kV/m, and a decay rate of $4.3 \times 10^7 \text{ sec}^{-1}$. Assuming that the HEMP field is incident on a line lying on the ground, then the peak current is found to be about 200 A and the action integral to be about $10^{-3} \text{ A}^2\text{-s}$. This model predicts currents of about 1,000 A will be driven on a line located several meters above the ground. However, if a line is several hundred meters or more long, several meters above the ground, and very straight, it is possible to have an "end fire" geometry which would induce a current five to ten times larger than indicated by this model. If good engineering practices are followed, this type of HEMP coupling geometry should rarely be encountered. For each system, a decision must be made on whether it is appropriate to protect against this higher level of HEMP coupling or against the lower levels predicted by this and similar models which neglect the end-fire geometry.

8.4.6 Shield Allocations

The shield allocation process consists of determining the largest aperture size that can be allowed, consistent with the EM environments, equipment immunities, the selected keepout distance and the selected cavity absorption area. Determination of the shield allocations is an iterative process that involves setting preliminary specifications for the shield and then determining if the shield reduces the residuals to the allowed values.

8.4.6.1 Preliminary Shield Specifications

The preliminary shield specifications given in Table A6 have been chosen for the purpose of this calculation.

Table A6. Preliminary Shield Specifications.

Parameter	Preliminary Allocation	Description
Maximum Effective Aperture Size (Diameter)	3 cm	Maximum diameter of aperture in the shield
Minimum Keepout Distance	10 cm	Minimum distance between apertures and electronic equipment or wiring connected to the equipment
Cavity Absorption Area	2 m^2	Coupling cross-section for EM radiation inside the shield

8.4.6.2 Determination of Interior Electric and Magnetic Fields Due to Quasistatic Leakage Through an Aperture

a) CW Quasistatic Magnetic Field Leakage

The quasistatic leakage of CW magnetic fields through an aperture is given by equation (44) in Section 4.4.2.4.1. This model is valid up to about 400 MHz. From this expression, it is seen that quasistatic magnetic field leakage is independent of frequency. Maximum field leakage will thus occur for the largest field value below this frequency range, which is seen to be 1500 V/m peak from Table A2. Using an effective aperture size of 3 cm and a keepout distance of 10 cm, the peak quasistatic magnetic field is determined to be about 4×10^{-3} A/m.

b) CW Quasistatic Electric Field Leakage

Quasistatic electric field leakage through an aperture is given by equation (45). Electric field leakage increases linearly with frequency. Using the same preliminary shield specifications as above, the peak electric field is determined to be 2.5 V/m.

c) Comparison with Allowed Residuals

Relating quasistatic leakage stresses to equipment immunity levels is not completely straightforward. Radiated immunity tests emphasize the use of uniform fields whereas aperture leakage fields are non-uniform. Also, radiated immunity testing above 1 MHz defines the electric field but does not specify the magnetic field. The quasistatic fields calculated in this example are small compared to the immunity levels based on the RS 103 requirement of MIL-STD-461E, which is 50 V/m (Table A4).

8.4.6.3 Determination of Quasistatic Coupling to a Wire behind an Aperture

The quasistatic coupling to wires or cables running near to an aperture needs to be calculated so that the conducted currents can be compared to equipment immunity levels.

a) Coupling of CW Fields to a Wire behind an Aperture

The peak emf induced on a wire running parallel to a shield at a given keepout distance and passing directly over the aperture is given by equation (69) in Section 4.4.3.1 of this volume. Maximum coupling occurs at high frequencies but the model starts to break down above 400 MHz because the fields no longer oscillate in phase along the illuminated section of the wire. Using the preliminary shield specifications and the HIRF environment at 400 MHz (Table A2), the peak-coupled emf is determined to be about 0.4 V. The CS 114 requirement of MIL-STD-461E calls for an equivalent peak emf of 2.5 V, which is 6 times higher than the value expected.

b) Pulse Quasistatic Coupling to Wires inside the Shield

The peak Voltage induced by quasistatic coupling of HEMP fields on a wire located behind an aperture is given by equation (71) in Section 4.4.3.1 of this volume. Using the HEMP environment specified in Section 8.5.2 (54 kV/m peak and a rise rate of $1.2 \times 10^9 \text{ s}^{-1}$), a peak-coupled emf is determined to be 20 V/m. Equipment passing the CS 115 requirement of MIL-STD-461E can withstand at least 500 V peak since the test specifies a 5 A peak current driven into a cable terminated with 50Ω at each end.

8.4.6.3 Determination of Interior Electric and Magnetic Fields Due to Radiative Leakage Through an Aperture (Shield Non-Resonant)

a) CW Radiated Field Leakage (Shield Non-Resonant)

The maximum field strength that equipment will be exposed to when it is located behind an aperture and within the shield is given by equation (51) in Section 4.4.2.4.2 of this volume. Radiated aperture leakage tends to dominate above 400 MHz and falls off less quickly with distance from the aperture than quasistatic leakage. Small apertures (0.5 to 10 cm) in an EM barrier resonate in this frequency range and readily pass radiation. A 3 cm aperture (corresponding to the preliminary barrier specifications) resonates at approximately 5 GHz. The HIRF environment (Table A2) has peak fields as high as 2500 V/m. Using this field value and the preliminary shield specifications, it is determined that the peak electric field experienced by the equipment is 700 V/m.

The 700 V/m field at 10 cm from the aperture is much higher than the RS 103 requirement of 50 V/m called for in MIL-STD-461E. In this case, where the immunity level is much less than the leakage stress, the only option is to reduce the leakage stress by changing the preliminary shield specifications - specifically by reducing aperture size and increasing the keepout distance. Alternate approaches might be to do further testing to see if the equipment can meet higher immunity levels or to ask the user to review operational requirements to see if the immunities can be relaxed.

b) Radiative Leakage of Pulse Fields (Shield Non-Resonant)

Pulsed environments, like HEMP, with rise times longer than 1 ns, have most of their energy below about 100 MHz and, consequently, most of the energy that penetrates the aperture is quasistatic and is located near the aperture. There will however be a small radiative component that propagates into the shielded enclosure. The maximum radiated energy that can penetrate the shield is given by equation (53) of Section

4.4.2.4.2 of this volume. Using the HEMP environment of 54 kV/m for the peak electric field and 1.2×10^9 for the rise rate, the maximum energy that penetrates is found to be only 0.4 nJ. The energy that couples to a particular circuit would normally be much less than this. Such low energies are well below the immunity levels. This result applies to resonant cavities as well as nonresonant cavities. It should be noted that, if the specified EM environment includes much faster rise time UWB threats, the radiated energy might be much larger.

8.6.6.3 Radiative Leakage of CW Fields into a Resonant Cavity

In many cases, the shielded volume of OC1 systems will support resonance in the gigaHertz range. In this case, the CW leakage into the shield through the aperture will "pump" the cavity until the field becomes high enough that the transmitted power is balanced by cavity losses (power absorbed inside the cavity and by power retransmitted back out of the aperture). This process is described in Section 4.4.2.4.3 of this volume.

The relationship between the average power density of the incident EM environment to the average power density inside the cavity is given by equation (65) in section 4.4.2.4.3. The power densities are related by the ratio of the aperture transmission cross-section (equation (50)) to the total cross-section, σ_T , for power dissipation in the cavity, which includes absorption of power in the interior, re-radiation of power through the aperture and wall losses. In general, for shielded systems, absorption of power (as characterized by the cavity absorption area, σ_a , as specified in Table A6) is expected to dominate and the average power density in the cavity is given by the relationship

$$S_c \approx \frac{\sigma_{eff}}{\sigma_a} S_i \quad (1)$$

The electric field, E_c , is then given by:

$$E_c \approx \left[\frac{\sigma_{eff}}{\sigma_a} \right]^{1/2} E_i \quad (2)$$

Maximum power is transmitted into the cavity when the aperture is resonant which is about 4.5 GHz. The effective cross section at 4.5 GHz is (from equation (50)) found to be about $4 \times 10^{-3} \text{ m}^2$. The HIRF environment (Table A2) has a peak field of 2500 $V_{r.m.s.}/m$ at 4.5 GHz. From equation (2) above, the average peak interior fields are thus found to be about 150 V/m. This is a factor of 3 above the 50 V/m limit called for by the RS 103 requirement in MIL-STD-461E. It should be noted that these field levels exist everywhere in the cavity and not just in the vicinity of the aperture. The actual

fields in the cavity will vary strongly with position because of the random location of the peaks and valleys in the cavity modes. Peak field levels can be considerably higher than the average fields. The statistics of the field distribution is discussed in Section 4.4.2.4.3. To ensure that there is a probability of less than 1 part in a million that the field will be exceeded, the field value rises to 550 V/m. These levels are close to those associated with direct CW illumination of equipment within 10 cm of a 3 cm aperture. The difference is that these fields may exist everywhere within the shield as discussed earlier.

Options for reducing the field inside the resonant shield include reducing the effective aperture size and/or increasing the absorption cross-section of the shield. A second iteration of the process is needed to determine if the new shield specifications are adequate to protect the equipment against all of the specified environments.

8.4.6.4 Summary of EM Shield Allocations

In this Annex, an example of how the unified EME protection allocation approach may be applied to a practical system is given. The systematic approach given in section 5 has been followed. The initial estimates of effective aperture size, keepout distance and cavity absorption area were found to provide adequate protection against most of the specified EME. The notable exception involved the high frequency CW environment. The large field strength of the HIRF environment above 1 GHz as well as aperture and shield resonances in this frequency range result in very high internal fields. For the preliminary shield specifications chosen, the interior fields were found to be more than a factor of 10 higher than the RS 103 requirements of MIL-STD-461E call for. To reduce these fields, it is necessary to improve the quality of the shield by reducing the size of the allowed aperture size, increasing the cavity absorption area and/or increasing the keepout distance. If these measures turn out to be too demanding, it is also possible to seek user approval to increase equipment immunity levels, reduce the specified high frequency operational EM environment and/or introduce other special protective measures.